ALMA MATER STUDIORUM · UNIVERSITÀ DI BOLOGNA

Corso di Laurea Magistrale in Matematica

From Khovanov homology to the Rasmussen s-invariant via Lee homology

Tesi di Laurea in Geometria

Relatore:
Prof.ssa
Alessia Cattabriga

Presentata da:
Arianna Charrere

Correlatore:
Prof. ssa
Marithania Silvero

Sessione Unica
Anno Accademico 2024/2025

Alle donne della mia famiglia

Introduction

Take a piece of string, tie it in a knot, and join the ends together. You have created a mathematical object, a closed curve in three-dimensional space, that has fascinated mathematicians for over a century. The question "*Is this knot really knotted, or can it be untangled?*" seems simple, almost childlike. Yet answering it rigorously has led to some of the deepest and most beautiful mathematics of our time, connecting topology with algebra, geometry with physics, and pure theory with practical computation.

Knot theory began not in mathematics but in physics. In the 1860s, Lord Kelvin proposed that atoms might be knotted vortices in the luminiferous ether. Peter Guthrie Tait, inspired by this vision, produced elaborate tables of knots with up to ten crossings. Though Kelvin's vortex atom theory was soon abandoned, Tait's tables survived, and knot theory was born as an independent mathematical discipline.

The fundamental problem, determining when two knots are equivalent, i.e., whether one tied rope can be deformed into an other, proved stubbornly difficult. The breakthrough came in the 1920s when Reidemeister [Rei74] proved that any two diagrams (projection) of the same knot can be connected by a finite sequence of three simple moves. This reduced the equivalence problem to a combinatorial question: can we find knot invariants that distinguish different knots?

For fifty years, the knot exterior, Alexander polynomial [Ale28] and related invariants were the primary tools for distinguishing knots. Then came 1984, when Vaughan Jones [Jon85] discovered a new polynomial invariant through his study of operator algebras. The *Jones polynomial* could distinguish knots that all previous invariants had failed to separate and revealed unexpected connections between knot theory and statistical mechanics, quantum field theory, and representation theory.

The Jones polynomial's success raised a natural question: what deeper structure underlies this polynomial? The answer came in 2000 from Mikhail Khovanov

[Kho00], who showed that the Jones polynomial is the shadow of a richer theory. Khovanov constructed a bigraded homology theory whose graded Euler characteristic is precisely the Jones polynomial making Khovanov homology a strictly stronger knot invariant than the Jones polynomial itself. This categorification transformed knot theory, providing new tools for attacking classical problems. When Lee [Lee05] introduced a deformation of *Khovanov homology* and Rasmussen [Ras10] extracted from it the *s-invariant*, knot theory gained its first purely combinatorial tool for understanding the slice genus. Rasmussen's proof of the *Milnor conjecture*, a forty-year-old problem about torus knots, already proved using Gauge theory.

This thesis provides a comprehensive introduction to Khovanov homology, Lee homology, and the Rasmussen s-invariant, with explicit computations and the proof of the Milnor conjecture. Our presentation is self-contained, requiring only basic knowledge of topology and algebra, and follows primarily the foundational works of Khovanov [Kho00], Bar-Natan [Bar02], Lee [Lee05], and Rasmussen [Ras10].

The thesis makes several personal contributions. We provide detailed worked examples throughout, computing Khovanov and Lee homology explicitly for fundamental knots. We have unified the notation by adopting Bar-Natan's cohomological framework, systematically translating from the homological conventions used in some references. We present the Lee spectral sequence in complete detail with concrete computations for the trefoil. Finally, we provide expanded proofs of key results, filling in technical details often omitted in the literature.

The first chapter establishes the foundations of knot theory: knots, links, diagrams, Reidemeister moves, and basic invariants including crossing number, linking number, genus, and Seifert surfaces. The chapter concludes with torus knots, which play a crucial role in an example of computing Khovanov homology via the Khovanov skein sequence and in the Milnor conjecture.

The second chapter introduces the Jones polynomial via the Kauffman bracket, providing the polynomial invariant that Khovanov homology categorifies. We establish the key properties of the Jones polynomial, and present both the original variable formulation and the quantum variable formulation needed for comparison with Khovanov homology. Detailed examples illustrate the computation techniques, first using the tree resolution method and then using the cube of resolutions. This second approach, organizing resolutions as vertices of a hypercube with edges corresponding to changing individual crossing resolutions, motivates

the structure of Khovanov's chain complex directly.

The third chapter presents Khovanov's categorification of the Jones polynomial. We construct the Khovanov chain complex from the cube of resolutions of a knot diagram, where each vertex of the cube corresponds to a complete resolution of all crossings, and edges correspond to changing a single crossing resolution. To each resolution we assign a graded vector space built from the Frobenius algebra $V = \mathbb{Q}[X]/(X^2)$, with one tensor factor for each circle in the resolution. The differential maps between resolutions differing at a single crossing are defined using multiplication and comultiplication maps on this Frobenius algebra, with signs determined by a fixed order on the crossings. We prove that the resulting homology is a knot invariant by establishing invariance under the three Reidemeister moves, a technical but crucial verification requiring careful analysis of how the chain complex changes under each of the moves.

Complete computations for the unknot, trefoil, and Hopf link in Section 3.3 demonstrate the theory in action, showing how to construct the chain groups, compute all differentials, determine kernels and images, and extract the bigraded homology groups. We verify in examples that the graded Euler characteristic of Khovanov homology recovers the Jones polynomial, confirming that Khovanov homology truly categorifies this classical invariant. The chapter then introduces framed Khovanov homology, an invariant of framed knots, and develops the Khovanov skein sequence, an exact sequence relating the Khovanov homology of three knot diagrams differing at a small neighborhood of a crossing. These tools are applied to compute the Khovanov homology of torus knots $T(2, n)$, an infinite family of knots whose Khovanov homology exhibits a beautiful recursive pattern. The chapter concludes with a discussion of the cobordism interpretation of Khovanov homology, showing how the algebraic structure of the Frobenius algebra corresponds to topological operations of gluing cobordisms, connecting to the framework of topological quantum field theory.

The fourth chapter develops Lee's deformation of Khovanov homology and its applications to the slice genus problem. We show how to modify Khovanov's differential by adding a perturbation map ϕ that raises quantum degree by four, producing the Lee complex. The key insight is that this perturbation dramatically simplifies the homology: unlike Khovanov homology, which can be arbitrarily complex, Lee homology of a knot is always two-dimensional, spanned by two canonical generators regardless of the knot. The construction of these canonical generators, which arise naturally from the algebraic structure of the Lee defor-

mation, is explained in detail. We show that the Lee differential decomposes as $d' = d + \phi$, where d is the original Khovanov differential and ϕ is the new perturbation, and this decomposition is the key to understanding the relationship between the two theories.

The Lee spectral sequence, connecting Khovanov homology at the E^1-page to Lee homology at the E^∞-page, is constructed explicitly in Section 4.2 with all differentials identified. We explain how the spectral sequence arises from filtering the Lee complex by quantum degree: the perturbation ϕ raises quantum degree, so although the Lee differential d' is not homogeneous with respect to quantum grading, it never lowers this grading. This filtration produces a spectral sequence whose successive pages detect interactions between different quantum degree levels. The E^0-page recovers the Khovanov chain complex with its homogeneous differential d, the E^1-page is Khovanov homology, and the sequence converges to Lee homology. Differentials on higher pages measure how the perturbation ϕ connects different parts of the complex. We compute the spectral sequence for the trefoil completely, showing explicitly how the first potential nonzero differential ∂^4 acts and how the sequence stabilizes at E^∞ to yield the two-dimensional Lee homology.

The Rasmussen s-invariant is then defined as a normalized average of the quantum degrees of Lee homology's two canonical generators. Since these generators are well-defined up to normalization, and their quantum degrees are determined by the spectral sequence structure, the s-invariant is a well-defined integer invariant of the knot. We establish the crucial property that s provides a lower bound for the four-ball genus: for any knot K, we have $2g_*(K) \geq |s(K)|$, where $g_*(K)$ denotes the minimum genus of a smoothly embedded surface in the four-ball B^4 whose boundary is K. This inequality, which follows from a deep topological argument relating the spectral sequence filtration to geometric properties of surfaces in four-dimensional space, is the key to Rasmussen's proof of the Milnor conjecture.

The appendix provides background on graded vector spaces, chain complexes, Frobenius algebras and their connection to topological quantum field theory, and spectral sequences for filtered complexes.

Our exposition follows primarily Bar-Natan [Bar02] for Khovanov homology, Lee [Lee05] for Lee homology, and Rasmussen [Ras10] for the s-invariant and Milnor conjecture. The introductory chapter draws on standard references in knot theory [Lic97; Cro04; Kaw96; Mur08], while additional sources are cited through-

out the text as they become relevant.

Contents

Chapter 1

Knots and Links

The notion of knots is something that everyone has in mind, however the mathematical definition differs a bit on the one we have in mind.

Knot theory is a branch of low-dimensional topology that studies the properties of knots, links, and their invariants under ambient isotopy. Originating in the nineteenth century with the work of Gauss and later developed systematically by Tait, knot theory has grown into a rich mathematical discipline with deep connections to three-manifold topology, quantum algebra, and mathematical physics. The aim of this introductory chapter is to lay the rigorous foundations that will be used throughout the thesis. We follow the exposition of Murasugi [Mur08] and Kawauchi [Kaw96], to which the reader is referred for further details and proofs.

1.1 Basic definitions

Let us define a knot and its multiple counterpart starting by our experience. Intuitively, a knot is a rope tied in such a way that when you pull the two strands it cannot become a string; however, since the rope is not "closed" it can always be unknotted. For this reason, the idea in topology, is that a knot is a tied "rope" in $\mathbb{R}^3$ whose ends are glued at the infinity. See Figure 1.1. Now that we have this in mind, let us define it in a more rigorous way:

Definition 1.1 (Knot). A *knot* is a smooth (or piecewise-linear) embedding

$$K : S^1 \hookrightarrow S^3.$$

The image $K(S^1) \subset S^3$ is also called a knot and is denoted by the same letter when no confusion arises.

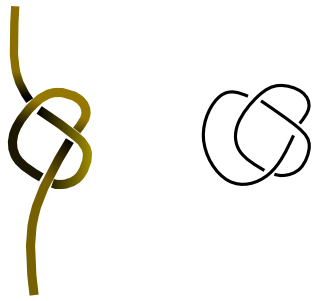

Figure 1.1

Definition 1.2 (Link). A *link* L with m components is a smooth embedding $L : \bigsqcup_m S^1 \hookrightarrow S^3$. Under the identification of a link with its image, a link can be viewed as a closed subset of S^3 homeomorphic to a disjoint union of circles $L = \{L_1, L_2, ..., L_m\}$. Each knot L_i is called the i-th component of L.

A knot is therefore a link with a single component.

Example 1.3 (The unknot and the trefoil)**.** The simplest knot is the *unknot* (or *trivial knot*) ◯, represented by the standard embedding of S^1 so that S^1 bounds a disk $D^2 \subset S^3$. The *trefoil knot* 3_1 is the simplest non-trivial knot; it appears naturally as the intersection of the complex curve $z^2 + w^3 = 0$ with the unit sphere $S^3 \subset \mathbb{C}^2$ [Mur08, Ch. 1]. See Figure 1.2 for a planar representation of the two knots.

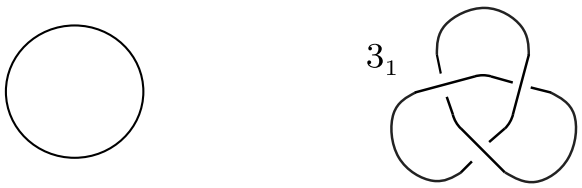

Figure 1.2: *A planar representation of the unknot (on the left) and of the right handed trefoil knot* 3_1 *(on the right).*

Remark 1.4. Since S^3 is homeomorphic to $\mathbb{R}^3 \cup \{\infty\}$ and any 1-dimension submanifold of S^3 can be embedded in S^3 avoiding a point, we can also think of a knot in $\mathbb{R}^3$.

The core challenge in defining knot equivalence lies in the physical intuition of "stretching" or "deforming." If we define deformation too broadly, any knot can be "pulled tight" until the knotted region effectively vanishes into a single point, mathematically reducing every complex knot to a simple, trivial circle.

To prevent this collapse and maintain the topological integrity of the knot, we move from simple continuous deformation to the more robust framework of ambient isotopy.

Definition 1.5 (**Isotopy**). An *isotopy* between two maps $f, g : X \longrightarrow X$ is a map $F : X \times [0,1] \longrightarrow X$ such that:

i. $F(\,\cdot\,, t)$ is a (smooth, PL) isomorphism for all $t \in [0,1]$,
ii. $F(x,0) = f(x)\ \forall x \in X$,
iii. $F(x,1) = g(x)\ \forall x \in X$.

Definition 1.6 (**Ambient isotopy**). Given $Y_1, Y_2 \subseteq X$, an *ambient isotopy* between Y_1 and Y_2 is an isotopy $F : X \times [0,1] \longrightarrow X$ between id_X, the identity on X, and a map $f : X \longrightarrow X$ such that $f(Y_1) = f(Y_2)$.

Remark 1.7. One can easily verify that it is an equivalence relation.

Definition 1.8 (**Equivalent links**). Two links L and L' are said to be *equivalent* if there exist an ambient isotopy $h : S^3 \times [0,1] \longrightarrow S^3$ between them. If L and L' are equivalent, we denote it $L \approx L'$.

In knot theory, we generally adopt the convention of "classification up to equivalence". Because ambient isotopy preserves all fundamental topological properties, we treat the entire equivalence class as a single entity. Consequently, when two links are ambient isotopic, we disregard their specific geometric positioning and formally identify them as the same link.

Definition 1.9 (**Oriented knots and links**). An *oriented knot* K is a knot together with a choice of direction of traversal of S^1. An oriented link $L = \{L_1, ..., L_m\}$ is a link together with a choice of direction for each component of L.

Example 1.10 (The n-component unlink). The n-component unlink, consisting of n disjoint unknotted circles with no crossings between them (see Figure 1.3 for a standard planar representation of it).

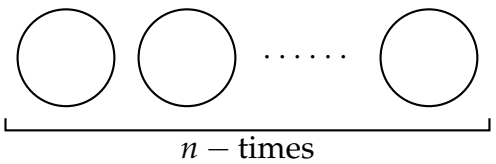

Figure 1.3: *A planar representation of the unoriented n-component unlink.*

Example 1.11 (The Hopf link)**.** The *Hopf link* 2_1^2 is the simplest non-trivial link with two components. Each component bounds a disc, yet the two circles are interlinked. It arises as the fibers of the Hopf fibration $S^3 \to S^2$ [Kaw96, Ch. 7]. See Figure 1.4 for a planar representation of it together with a choice of orientation of each components.

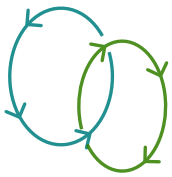

Figure 1.4: *A planar representation of the oriented Hopf link.*

Definition 1.12 (**Equivalent oriented links**)**.** Two oriented links $L = \{L_1, ..., L_m\}$ and $L' = \{L'_1, ..., L'_m\}$ are said to be *equivalent* or *isotopic* if there exists an orientation-preserving homeomorphism $h : S^3 \to S^3$ such that $h(L_i) = L'_i$ for all $i = 1, ..., m$.

One of the central goals of knot theory is to classify knots up to ambient isotopy. This is, however, a surprisingly subtle task. While a single small deformation of a knot leaves it visually unchanged, repeatedly applying small deformations at different locations can produce a knot that appears to be something entirely different. A classical illustration of this phenomenon is the *Perko's pair* (see Figure 1.5): for nearly 100 years, the two knots in this pair were believed to be distinct, until 1974, when American lawyer K.A. Perko demonstrated that they are in fact equivalent by exhibiting an explicit sequence of ambient isotopies transforming one into the other.

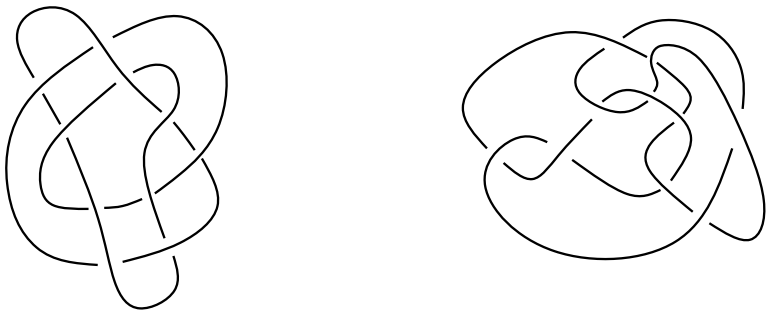

Figure 1.5: *Perko's pair knots.*

With a notion of equivalence in hand, it is natural to ask whether knots can be decomposed into simpler pieces, much as integers factor into primes. To make

this precise, we introduce an operation that combines two knots into a single, more complex one.

Let K_1 and K_2 be two oriented knots in S^3. Consider their disjoint union $K_1 \sqcup K_2$, viewed as a split link in S^3. Since K_1 and K_2 are disjoint, there exists a 2-sphere $S^2 \subset S^3$ separating K_1 from K_2, that is, K_1 lies in one component of $S^3 \setminus S^2$ and K_2 lies in the other (see Figure 1.6).

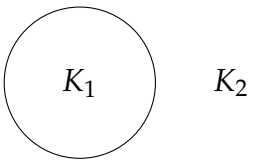

Figure 1.6: *A projection of the disjoint union between K_1 and K_2 and S^2 separating them.*

Definition 1.13 (**Connected sum**). Let K_1 and K_2 be two disjoint oriented knots in S^3, separated by a 2-sphere S^2 as above. Remove a small open arc from each knot compatible with its orientation: $a_1, b_1 \in K_1$ be the endpoints of the small arc of K_1 and let $a_2, b_2 \in K_2$ be the endpoints of the small arc of K_2, where in each case the first endpoint precedes the second with respect to the orientation. The *connected sum* $K_1\#K_2$ is the oriented knot obtained by joining the endpoints a_1 to b_2 and a_2 to b_1 by two new arcs, so that the orientation flows continuously through the new connections, producing a single closed oriented curve. The two new arcs should be chosen so that, together with the arcs $a1b1$ and $a2b2$, constitute the boundary of a strip whose interior is disjoint from $K_1 \cup K_2$, and which meets the separating sphere S^2 in a single simple arc. See Figure 1.7. The resulting knot equivalence class is independent of the choices of arcs.

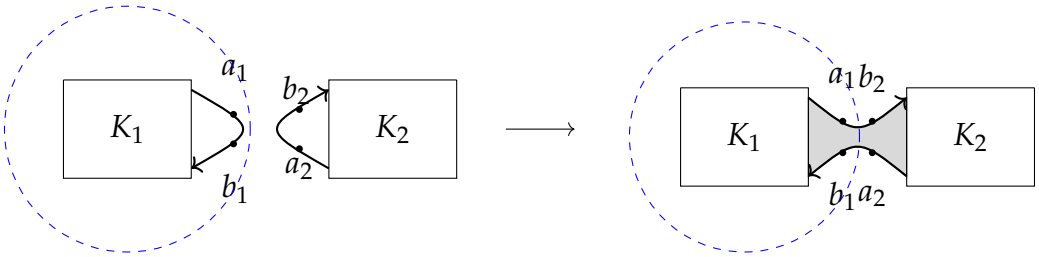

Figure 1.7: *The connected sum operation. Left: Two oriented knots K_1 and K_2 with endpoints labeled according to orientation. Right: The connected sum $K_1\#K_2$ obtained by connecting the endpoints with an embedded strip.*

Remark 1.14. For unoriented knots, the connected sum is not well defined in general. When joining the four endpoints, there are two distinct ways to connect the strands, and the two resulting knots need not be equivalent.

Proposition 1.15. *The connected sum is well-defined on equivalence classes of oriented knots, commutative,* $K_1\#K_2 \approx K_2\#K_1$ *and associative,* $K_1\#(K_2\#K_3) \approx (K_1\#K_2)\#K_3$ *up to equivalence, and admits the unknot* ◯ *as an identity element:* $K\#\bigcirc \approx K$ *for any knot* K*.*

Remark 1.16. By construction, the two knot summands K_1 and K_2 can be separated by a 2-sphere in S^3 that meets $K_1\#K_2$ transversely in exactly the two joining points (see Figure 1.7). This geometric picture makes it natural to discuss decompositions of knots as connected sums of simpler knots, and motivates the notion of a *prime knot* as one that cannot be expressed as a non-trivial connected sum.

Definition 1.17 (**Prime knot**)**.** A non-trivial knot K is said to be *prime* if, whenever $K \approx K_1\#K_2$, either K_1 or K_2 is equivalent to the unknot. A knot that is not prime is called *composite*.

A celebrated theorem due to Schubert (1949) asserts:

Theorem 1.18. *[Sch49] Every non-trivial knot decomposes, up to equivalence, as a connected sum of finitely many prime knots, and this decomposition is unique up to reordering of the factors.*

This result, the analogue of the fundamental theorem of arithmetic for knots, justifies restricting attention to prime knots when undertaking a classification. One might hope that the connected sum endows the set of oriented knots with a group structure, but this is not the case: no non-trivial knot admits an inverse. Consequently, the set of oriented knots equipped with the connected sum forms only a commutative monoid, freely generated by the prime knots. The proof of this statement is deferred to Section 1.2.3, where it will follow naturally from the additivity of the genus under connected sum.

Another natural question arising from knot equivalence is whether a knot can be distinguished from its mirror image. Recalling the identification of S^3 with $R^3 \cup \{\infty\}$, given a knot $K \subset S^3$, its *mirror image* K^* is the knot obtained by composing with an orientation-reversing homeomorphism of S^3, Concretely, one may reflect through a plane in $\mathbb{R}^3$ and extend to all of S^3 by setting $\infty \mapsto \infty$, yielding a well-defined orientation-reversing homeomorphism of S^3.

Definition 1.19 (Amphichiral and chiral knots). A knot K is said to be *amphichiral* (or *achiral*) if $K \approx K^*$, that is, if K and its mirror image are ambient isotopic. A knot that is not amphichiral is called *chiral*.

Example 1.20. The unknot and the figure-eight knot are amphichiral, whereas the trefoil knot is chiral: its left-handed and right-handed versions, depicted in Figure 1.8, are not ambient isotopic. This was first proved by Dehn in 1914 in [Deh14] using the knot group.

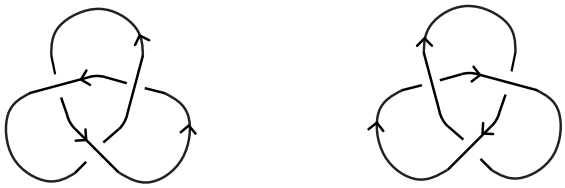

Figure 1.8: *The right-handed trefoil 3_1 (on the left) and its mirror image the left handed trefoil knot 3_1^* (on the right).*

Example 1.21. A further example is provided by the granny knot and the square knot, both of which arise as connected sums of two trefoil knots; the granny knot is the connected sum of two copies of the same-handed trefoil 3_1, while the square knot joins two trefoils of opposite handedness 3_1 and its mirror image 3_1^*. Kinoshita and Terasaka established their non-equivalence in 1957 using the fundamental group of the knot complement [KT57]. See Figure 1.9.

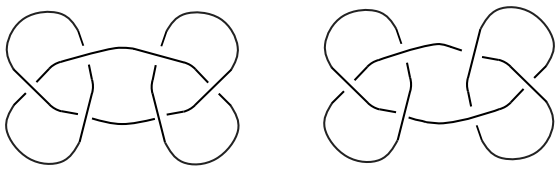

Figure 1.9: *The square knot $3_1\#3_1^*$ (left) and the granny knot $3_1\#3_1$ (right) as the connected sum of two trefoil knots.*

1.1.1 Diagrams and Reidemeister moves

Working directly with embeddings in S^3 is often difficult. A standard tool is to project a knot onto a plane and record the over/under crossing information.

Let $L \subset S^3$ be a link and $\pi : S^3 \setminus \{p\} \to P$ a *projection* from a point $p \notin L$ to a plane P not intersecting L. The projection is *regular* if:

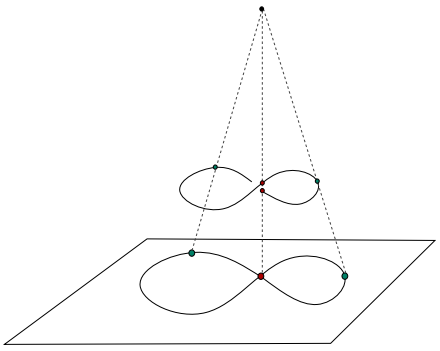

Figure 1.10: *A regular projection of the unknot.*

- the number of point whose preimage has more than one point is finite,
- the preimage of every point has at most two elements (Figure 1.11(b) shows a non-regular projection with a triple point)),
- the preimage of each double point consists of two transverse arcs,
- no cups of the link maps to a double point (Figures 1.11(c) and (d) illustrate non-regular projections where vertices map to double points).

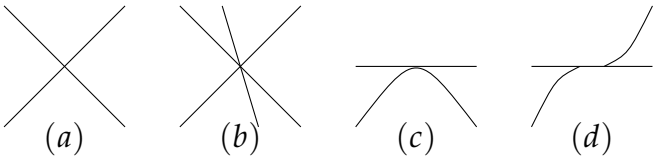

Figure 1.11: (a) *Regular projection with a transverse double point.* (b) *Non-regular projection with a triple point.* (c), (d) *Non-regular projections where cups map to crossings.*

Definition 1.22 (**Diagram**). Let L be a link, a *diagram* D of L is the image of a regular projection together with, at each double point, called a *crossing*, the information of which strand passes over (i.e., is closer to the projection point) and which passes under (i.e., is farther from the projection point). In a diagram, an orientation is recorded by placing an arrow on each arc.

In a standard link diagram, this spatial relationship is visually encoded by introducing a small break in the lower strand. By erasing a short segment of the arc as it approaches the crossing point, we create a clear visual cue that it passes beneath the continuous "over-strand". See Figure 1.12.

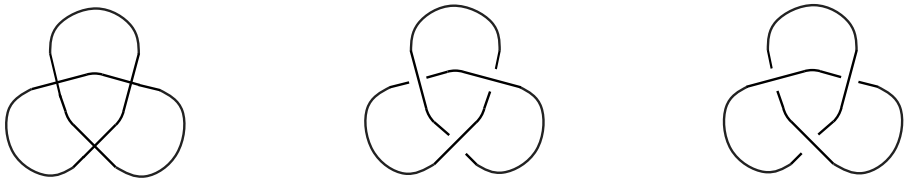

Figure 1.12: *A regular projection of the trefoil knot (on the left). Two diagrams of the trefoil knot with over/under crossing information indicated by breaks in the understrands. In the center the left-handed trefoil knot,* 3_1*, and on the right its mirror image,* 3_1^**, the right-handed trefoil knot.*

Definition 1.23 (**Alternatig diagram**)**.** A knot diagram D is defined as *alternating* if, when traversing the curve from any starting point, the crossings encountered follow a strict, repeating sequence of over-arc followed by under-arc.

Remark 1.24. As Kawauchi discusses in [Kaw96], the alternating property is a diagrammatic one, i.e., strictly depends on the diagram as shown in Figure 1.13. Moreover, not every knot has an alternating diagram.

Definition 1.25 (**Alternating knots**)**.** A knot K is *alternating* if it can be represented with an alternating diagram.

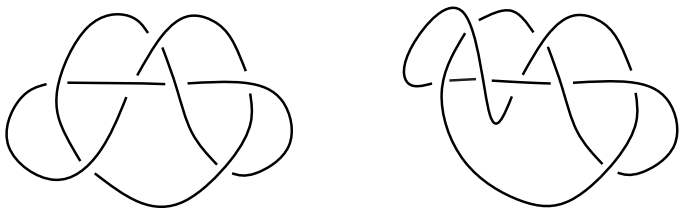

Figure 1.13: *Two diagrams of the* 7_7 *knot, one is an alternating diagram (left) the other one is not (right).*

A natural question arises: when do two diagrams represent the same link? The answer is provided by a classical theorem due to Reidemeister, which reduces the equivalence of diagrams to a finite set of local moves.

Definition 1.26 (**Reidemeister moves**)**.** The three *Reidemeister moves* are local modifications of a link diagram, leaving the diagram unchanged outside a small disk, described as follows:

R1) A link diagram containing a twist and the same diagram obtained by removing the twist.

R2) A link diagram containing two adjacent crossings formed by one strand passing over another and the diagram in which the two strands are separated:

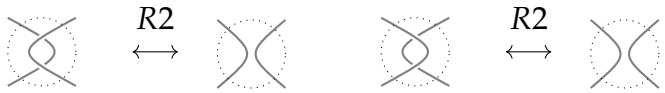

R3) A link diagram containing a crossing with the under-strand on the left the diagram in which the under-strand passes on the right:

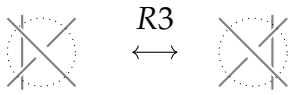

Theorem 1.27 (**Reidemeister, 1927**). *[Rei74] Two link diagrams D and D' represent equivalent links if and only if they are related by a finite sequence of Reidemeister moves and planar isotopies.*

A detailed proof can be found in [BZH14] or in [Lic97].

Remark 1.28. This theorem is fundamental, as it reduces a three-dimensional equivalence problem to a combinatorial one. It allows one to work entirely within the diagrammatic setting: to prove that two links are equivalent it suffices to exhibit a finite sequence of moves.

Definition 1.29 (**Nugatory crossing**). A crossing c in a knot diagram D is called *nugatory* if there exists a simple closed curve in the projection plane that meets D transversely in exactly the single point c, see Figure 1.14.

Definition 1.30 (**Reduced diagram**). A knot diagram D is called *reduced* if it contains no nugatory crossings.

Remark 1.31. Every knot admits a reduced diagram, obtained by repeatedly removing nugatory crossings until none remain.

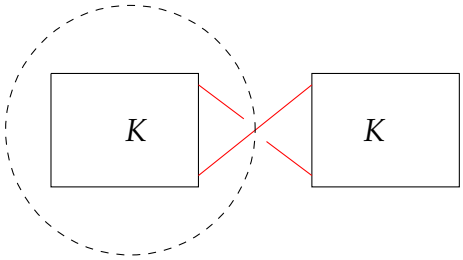

Figure 1.14: *A nugatory crossing (marked in red) enclosed by a simple closed curve (dashed). This crossing can be removed by a sequence of Reidemeister move R1, leaving the knot type unchanged.*

1.2 Invariants

The central problem of knot theory is the classification of knots up to ambient isotopy. In order to distinguish knots, one seeks quantities that are preserved under equivalence, that is, quantities that assign the same value to any two equivalent knots. Such a quantity is called a *knot invariant*.

Definition 1.32 (Knot invariant). A *knot invariant* is a map $\mathcal{I}$ from the set of links to some set S, such that $K \approx K'$ implies $\mathcal{I}(K) = \mathcal{I}(K')$.

In light of Reidemeister's theorem, a diagrammatic quantity is a knot invariant if and only if it is preserved under all three Reidemeister moves and planar isotopies. This observation reduces the verification of invariance to a finite, purely combinatorial check, and is the strategy we shall adopt throughout.

The history of knot invariants reflects a steady progression toward greater sophistication and discriminating power. Among the earliest invariants is the linking number, which measures the pairwise entanglement of the components of an oriented link. Simple as it is, the linking number already fails to distinguish many non-equivalent links, and this limitation drove the development of more refined tools throughout the twentieth century. A major breakthrough came with the introduction of polynomial invariants: the Alexander polynomial, and later the Jones polynomial, revealed deep and unexpected connections between knot theory, algebra, and mathematical physics, demonstrating that subtle combinatorial data encoded in link diagrams could carry remarkably strong topological information. These discoveries in turn inspired a broad range of further constructions, from skein-theoretic and quantum invariants to homological ones, progressively enriching both the technical toolkit and the conceptual landscape of the field.

In what follows, we introduce the invariants that will play a direct role in the constructions developed in this thesis. We begin with elementary numerical invariants (Section 1.2.1), before turning to invariants of a more geometric nature, culminating with the genus of a knot (Section 1.2.3), the Jones polynomial (Chapter 2), Khovanov and Lee homologies (Chapter 3 and Chapter 4) and the s-invariant (Section 4.3).

1.2.1 Numerical invariants

The simplest knot invariants are numerical ones, assigning to each knot or link an integer or rational number that is preserved under ambient isotopy. Despite their elementary nature, such invariants already capture meaningful geometric and combinatorial information, and some of the most fundamental questions about them remain open to this day.

Crossing number

Definition 1.33 (Crossing number). The *crossing number* $c(K)$ of a knot K is the minimum number of crossings over all diagrams of K:

$$c(K) = \min\{\, cr(D) : D \text{ is a diagram of } K \,\},$$

where $cr(D)$ denotes the number of crossings of D.

Theorem 1.34. *[Mur08, Theorem 4.2.1]*
The crossing number $c(K)$ of a knot K is a knot invariant.

While the definition is elementary, computing the crossing number of a given knot is in general a difficult problem. In particular, proving that a diagram realizes the crossing number requires showing that no diagram with fewer crossings exists, which is non-trivial. For alternating knots, this is settled by the Tait Conjecture (Theorem 1.35) which was proven in 1987 by Kauffman [Kau87], Murasugi [Mur87], and Thistlethwaite [Thi87] using Jones polynomial:

Theorem 1.35 (Tait conjecture). *Any reduced alternating diagram of a knot realizes the crossing number, that is, a reduced alternating diagram has the minimum possible number of crossings.*

Example 1.36. We compute the crossing number of the trefoil knot 3_1 and the figure-eight knot 4_1 using Theorem 1.35. Both knots admit reduced alternating

diagrams, as shown in Figure 1.15: the standard diagram of the trefoil has 3 crossings, and the standard diagram of the figure-eight knot has 4 crossings. Since both diagrams are reduced and alternating, the theorem guarantees that these diagrams are minimal, and therefore

$$c(3_1) = 3, \qquad c(4_1) = 4.$$

In particular, since $c(3_1) = 3 > 0$, the trefoil is not equivalent to the unknot. Moreover, since $c(3_1) \neq c(4_1)$, the trefoil and the figure-eight knot are not equivalent to one another. One also verifies directly that no knot has crossing number 1 or 2: any knot diagram with one or two crossings is not reduced, and therefore can be simplified to the unknot.

Figure 1.15: *The reduced alternating diagrams of the right-handed trefoil knot* 3_1 *(on the left) and the figure eight knot* 4_1 *(on the right).*

For some specific types of non-alternating knots (or link) the crossing number has been completely determined; however, in general the problem is considerably harder and remains open.

A similarly elusive problem concerns the behavior of the crossing number under connected sum. One might expect this invariant to be additive, in analogy with the genus, but this remains unproven in general:

Conjecture 1.37. *Let* K_1 *and* K_2 *be two knots, then*

$$c(K_1 \# K_2) = c(K_1) + c(K_2).$$

The conjecture is known to hold when both K_1 and K_2 are alternating, as an immediate consequence of Theorem 1.35: since the connected sum of two reduced alternating diagrams is itself a reduced alternating diagram, additivity follows from the minimality of reduced alternating diagrams.

Linking number

The invariant introduced so far is intrinsic to a single knot (even if it could be defined for links analogously). We now turn to invariants that are sensitive to

additional structure: the orientation of the diagram and, in the case of links, the interaction between distinct components. A key preliminary notion is the sign of a crossing. Given an oriented diagram, each crossing admits one of two possible local configurations, illustrated in Figure 1.16, where case (a) is called a *positive* crossing, and case (b) a *negative* crossing.

Figure 1.16: *The two possible local configuration of a crossing.*

The writhe and the linking numbers are both defined by summing the signs of crossings, and we therefore begin by making precise the notion of sign of a crossing.

Definition 1.38 (**Sign of a crossing**)**.** Let c be a crossing in an oriented diagram. The *sign* of c, denoted $\text{sign}(c)$, is defined to be $+1$ if c is a positive crossing and -1 if c is a negative crossing, according to the local orientation convention illustrated in Figure 1.17.

Figure 1.17: *The sign of the two possible local configuration of a crossing.*

This notion admits a natural globalization to the level of knots. If every crossing in some diagram of a knot can be made positive, the knot itself is said to be *positive*.

Definition 1.39 (**Positive knot**)**.** We say that a knot K is a *positive* knot if it admits a diagram with only positive crossings.

The sign of a crossing can be used to define two closely related numerical quantities. The first, the writhe, is associated to a single oriented diagram and sums the signs of all its crossings.

Definition 1.40 (**Writhe**)**.** The *writhe* $w(D)$ of an oriented knot diagram D is de-

fined as

$$w(D) = \sum_{c \in D} \text{sign}(c).$$

Remark 1.41. The writhe is preserved under Reidemeister moves $R2$ and $R3$, but changes by ± 1 under $R1$. It is not a knot invariant: two diagrams representing the same knot may have different writhes. This sensitivity to $R1$ will play a crucial role in Chapter 2, where the writhe will be used to normalize the Kauffman bracket into the Jones polynomial.

Example 1.42. We compute the writhe of two diagrams of the oriented figure-eight knot 4_1, shown in Figure 1.18. Let D denote the canonical diagram (left), and let D_p denote the same diagram with an additional positive twist (right). For the canonical diagram D, we have two positive and two negative crossings, giving

$$w(D) = (+1) + (+1) + (-1) + (-1) = 0.$$

For the diagram with the added twist D_p, we have three positive and two negative crossings, giving

$$w(D_p) = (+1) + (+1) + (+1) + (-1) + (-1) = 1.$$

Since D and D_p represent the same knot but have different writhes, this confirms that the writhe is not a knot invariant. The two diagrams are related by a single application of Reidemeister move $R1$, which changes the writhe by exactly $+1$, as predicted by the remark above.

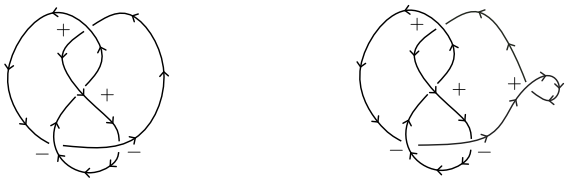

Figure 1.18: *The canonical diagram D of the oriented figure eight knot 4_1 with crossing signs indicated (left), giving $w(D) = 0$. The same diagram with an additional positive twist D_p (right), giving $w(D_p) = 1$. The two diagrams are related by Reidemeister move $R1$.*

The second quantity, the linking number, measures the mutual entanglement of the components of an oriented link. Unlike the writhe, it is a genuine invariant. Given a two-component oriented link $L = \{L_1, L_2\}$, we restrict attention to the crossings at which the two components interact.

Definition 1.43 (Linking number). Let $L = \{L_1, L_2\}$ be a two-component oriented link and D a diagram of L. The *linking number* $lk(L)$ is defined as

$$lk(L) = \frac{1}{2} \sum_{c \in D(L_1, L_2)} \text{sign}(c),$$

where the sum is taken over all crossings c at which L_1 and L_2 cross each other. We ignore the crossing points which are self-intersection between the link components L_i.

Example 1.44. The n-component unlink has linking number 0. The Hopf link has linking number ± 1 depending on the choice of orientations of its components, see Figure 1.19. In particular, the Hopf link is not equivalent to the unlink.

Figure 1.19: *The canonical diagram of the Hopf link with all its possible orientation with crossing sign indicated.*

Proposition 1.45. *The linking number $lk(L)$ is an integer, is independent of the choice of diagram D, and is invariant under ambient isotopy. Moreover, it holds:*

$$lk(L_1, -L_2) = -lk(L_1, L_2),$$

where $-L_i$ is the component L_i with reverse orientation.

Proof. For the proof of invariance under ambient isotopy, we refer the reader to [Mur08]. Regarding the orientation-reversal formula, we remark that reversing the orientation of L_2 changes the sign of every crossing between L_1 and L_2, since the sign convention at each crossing depends on the orientations of both strands. Therefore,

$$lk(L_1, -L_2) = \frac{1}{2} \sum_{c \in C(L_1, L_2)} (-sign(c)) = -\frac{1}{2} \sum_{c \in C(L_1, L_2)} sign(c) = -lk(L_1, L_2).$$

□

This notion can be extended to a link with m components by defining the *total linking number*:

Definition 1.46 (Total linking number). Let $L = \{L_1, ..., L_m\}$ be an m component link, the *total linking number* of L is defined as:

$$lk(L) = \sum_{1 \leq i < j \leq m} lk(L_i, L_j).$$

Example 1.47. We compute the total linking number of the Borromean rings, a classical three-component link denoted $L = \{L_1, L_2, L_3\}$, using the oriented diagram shown in Figure 1.20. The *Borromean rings* have the remarkable property that any two components are unlinked when considered in isolation, yet the three components cannot be separated without cutting. We verify this analytically by computing the pairwise linking numbers. For the components L_1 and L_2, we identify the crossings where these two components interact. Examining the diagram in Figure 1.20, we observe two such crossings: one positive and one negative. Therefore

$$\mathrm{lk}(L_1, L_2) = \frac{1}{2}\big((+1) + (-1)\big) = 0.$$

By the symmetry of the Borromean rings under cyclic permutation of the components, the same computation applies to the other pairs:

$$\mathrm{lk}(L_2, L_3) = 0, \qquad \mathrm{lk}(L_1, L_3) = 0.$$

The total linking number is therefore

$$\mathrm{lk}(L) = \sum_{1 \leq i < j \leq 3} \mathrm{lk}(L_i, L_j) = \mathrm{lk}(L_1, L_2) + \mathrm{lk}(L_2, L_3) + \mathrm{lk}(L_1, L_3) = 0 + 0 + 0 = 0.$$

This calculation confirms that the linking number alone cannot detect the topological complexity of the Borromean rings: despite being a non-trivial link with profound entanglement properties, the total linking number vanishes. This illustrates a fundamental limitation of the linking number as an invariant and motivates the development of more sophisticated invariants.

1.2.2 Topological invariants

The numerical invariants introduced so far are defined combinatorially, directly from the data of a knot diagram. We now turn to invariants of a different nature, arising not from the combinatorics of crossings but from the topology of

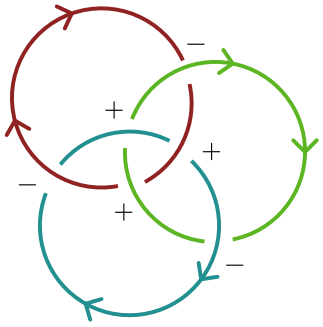

Figure 1.20: *The canonical diagram of the Borromean link with crossing sign indicated.*

surfaces associated to the knot. These invariants are in general harder to compute, but carry geometric information that purely diagrammatic invariants cannot capture.

The central construction in Section 1.2.3 is that of a *Seifert surface*: an oriented compact surface embedded in S^3 whose boundary is precisely the knot. The existence of such a surface for any knot is guaranteed by a classical algorithm due to Seifert. This leads to one of the most fundamental geometric invariants in knot theory, the *genus* of a knot, which measures the minimal topological complexity of any Seifert surface the knot bounds.

The genus is a particularly powerful invariant for several reasons. It is additive under connected sum, a property that we announced in Section 1.1.1 and that will be established here as a consequence of the Seifert surface construction. It will reappear in Chapter 4 through the work of Rasmussen, and the s-invariant arising from Lee homology.

1.2.3 Genus and Seifert surface

Seifert surface

The starting point is the following existence theorem, originally due to Frankl and Pontryagin:

Theorem 1.48. *Given an arbitrary link L, there exist an orientable connected surface S in S^3 such that $\partial S = L$.*

Definition 1.49 (Seifert surface). A *Seifer surface* S of a link L is a an orientable connected surface S such that $\partial S = K$.

Although the theorem was first proved by Frankl and Pontryagin in 1930 [Fra30], we present instead the constructive proof given by Seifert in 1934 [Sei34], which has the considerable advantage of yielding an explicit algorithm, known as the *Seifert algorithm*, for constructing such a surface directly from a knot diagram.

Proof. The proof is constructive and proceeds in three steps, known collectively as the *Seifert algorithm*.

Step 1: Seifert circles.

Let D be an oriented diagram of L. At each crossing of D, we perform a local modification called a *Seifert smoothing*: we replace the crossing by two non-crossing strands, in the only way preserving the orientation of the original diagram, as illustrated in Figure 1.21. The result is a collection of disjoint oriented simple closed curves in the plane, each of these curve is called a *Seifert circle*, and we say that the diagram is smoothed in an *orientation preserving* way.

Figure 1.21: *Resolution of two crossings in an orientation preserving way.*

Step 2: Assembling the surface.

We construct a surface S as follows. To each Seifert circle, we associate a flat oriented disk in S^3, with the height of each disk being the number of circles nesting the corresponding Seifer circle. At each crossing of the original diagram D, we then attach a twisted band connecting the two disks whose boundaries correspond to the strands involved in that crossing. The orientation of each band is chosen consistently with the orientations of the disks and the crossing information of D. See Figure 1.22.

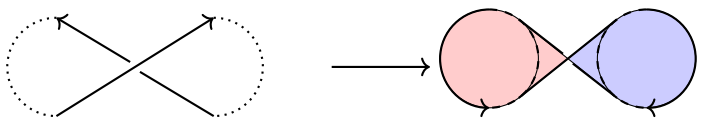

Figure 1.22: *A twisted band connecting two disk whose boundaries correspond to the strands of the crossing.*

Step 3: Verifying the properties.

By construction, the surface S is compact and oriented, since the orientations of the Seifert circles are compatible and the bands are attached consistently. One verifies directly that $\partial S = L$: the boundary of each disk contributes a Seifert circle, and the bands reintroduce precisely the crossings of D, reconstructing L as the boundary. It remains to check that S is connected. This need not hold automatically: the collection of Seifert circles may have several connected components, yielding a disconnected surface. However, one can always restore connectivity by joining distinct components with additional thin tubes, a standard procedure that does not alter the boundary. We refer to [Lic97] for the full details of this verification. □

Example 1.50. We apply the Seifert algorithm to construct a Seifert surface for the figure-eight knot 4_1, illustrated in Figure 1.23.

Step 1: Seifert smoothing.

Starting with the standard oriented diagram of 4_1 (on the left), we apply the Seifert smoothing at each of the four crossings. This replaces each crossing with two non-crossing arcs, preserving the local orientation. The resulting diagram consists of three disjoint oriented circles, shown in the middle of Figure 1.23: one outer circle (cyan), one inner circle (green), and one isolated circle (red).

Step 2: Attaching disks and bands.

We attach an oriented disk to each Seifert circle, positioning them at slightly different heights in S^3 to ensure they are disjoint. At each of the four crossings of the original diagram, we then attach a twisted band connecting the two disks whose boundaries correspond to the Seifert circles joined at that crossing. The orientation of each band is determined by the crossing type and the orientations of the adjacent disks, following the conventions established in Section 1.2.3. The resulting surface S is shown in the right, where the bands connect the three colored disks to form a single connected orientable surface.

We hence obtained a Seifert surface for 4_1.

Remark 1.51. The surface produced by the Seifert algorithm depends in general on the choice of diagram D, and different diagrams of the same knot may yield non-isotopic Seifert surfaces.

Definition 1.52 (Projection surface). A Seifert surface S produced by applying the Seifer algorithm to a diagram D of an oriented link L is called a *projection surface* of L.

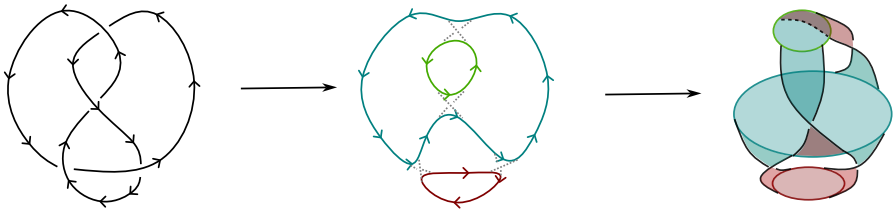

Figure 1.23: *An application of the Seifert algorithm on the canonical diagram of the figure-eight knot* 4_1.

Genus

To extract a knot invariant from this construction, we define the genus as the minimum complexity over all possible surfaces which bounds the knot.

Definition 1.53 (Genus of a knot). Let K be a knot. The *genus* of K, denoted $g(K)$, is defined as

$$g(K) = \min\{g(S) : \ S \ \text{ is a connected, orientable, compact surface s.t. } \ \partial S = K\},$$

where $g(S)$ denotes the genus of the surface S.

Remark 1.54. A knot K has genus 0 if and only if it bounds a disk, which occurs if and only if K is the unknot. The genus is therefore an unknot detector.

Remark 1.55. Computing the genus of a knot is in general a difficult problem. Although the Seifert algorithm guarantees the existence of a Seifert surface for any knot diagram, it does not necessarily produce a surface of minimal genus. Indeed, for some knots, the minimum genus is realized only by Seifert surfaces that cannot be obtained from any diagram via the Seifert algorithm.

In order to compute the genus of the projection surface produced by Seifert's algorithm, it is convenient to encode the combinatorial data of the surface in a graph.

Let D be an oriented knot diagram and S the Seifert surface produced by the Seifert algorithm applied to D. The *Seifert graph* $G(D)$ is the graph defined as follows:

- to each Seifert circle of D we associate a vertex of $G(D)$,
- to each crossing of D we associate an edge connecting the two vertices corresponding to the Seifert circles joined by the band at that crossing.

Remark 1.56. The Seifert graph may have multiple edges between the same pair of vertices, corresponding to multiple crossings connecting the same pair of Seifert circles, and may also have loops, corresponding to crossings where both strands belong to the same Seifert circle.

The Seifert graph encodes precisely the information needed to compute the Euler characteristic of the associated projection surface, and hence its genus. Recall that for a connected oriented compact surface S with one boundary component, the Euler characteristic, $\chi(S)$, and the genus, $g(S)$, are related by

$$\chi(S) = 2 - 2g(S) - 1 = 1 - 2g(S),$$

so that

$$g(S) = \frac{1 - \chi(S)}{2}.$$

We now compute $\chi(S)$ directly from the combinatorial data of the diagram.

Proposition 1.57. *Let D be a knot diagram with n crossings and k Seifert circles. The Seifert surface S produced by applying the Seifert algorithm to D has Euler characteristic*

$$\chi(S) = k - n,$$

and therefore genus

$$g(S) = \frac{1 - k + n}{2}.$$

Example 1.58. We compute the genus of the projection surface for the figure-eight knot 4_1 of its standard diagram. The Seifert algorithm applied to the standard diagram of 4_1, see Example 1.50, produces $k = 3$ Seifert circles and the diagram has $n = 4$ crossings. Its Seifert graph $G(D)$ is shown in Figure 1.24.

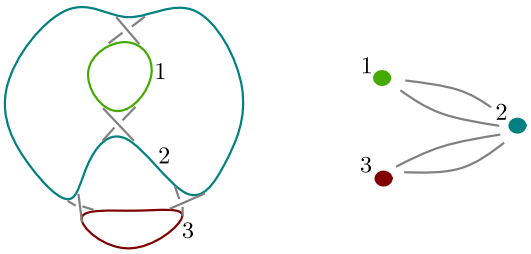

Figure 1.24: *The Seifert graph of the canonical diagram of the figure-eight knot.*

The genus of the resulting projection surface is therefore

$$g(S) = \frac{1 - 3 + 4}{2} = 1.$$

Since one can show that the figure eight knot is not the unknot by Remark 1.54, we have $g(4_1) \geq 1$, and since we have exhibited a Seifert surface of genus 1, we conclude $g(4_1) = 1$.

Remark 1.59. The formula $g(S) = \frac{1-k+n}{2}$ gives the genus of the particular Seifert surface produced by the algorithm applied to the diagram D, which is in general an upper bound for the genus of the knot. To obtain the genus of the knot itself, one must minimize over all Seifert surfaces of K. In practice, one combines this upper bound with a lower bound coming from another invariant, such as the degree of the Alexander polynomial or the Rasmussen s-invariant, to pin down the exact value. We will present on of such bounds in Section 4.3.

Properties

Having established the definition and computation of the genus, we now turn to its fundamental properties. The most important of these is additivity under connected sum, which we announced in Section 1.1.1 and can now establish rigorously.

Theorem 1.60 (Additivity of genus). *Let K_1 and K_2 be two knots. Then*

$$g(K_1 \# K_2) = g(K_1) + g(K_2).$$

Proof. We prove both inequalities separately.

Upper bound.

Let S_1 and S_2 be Seifert surfaces of minimal genus for K_1 and K_2 respectively, so that $g(S_i) = g(K_i)$. The connected sum $K_1 \# K_2$ is formed by removing a small arc from each knot and joining the endpoints. Performing the same operation on S_1 and S_2, removing a small disk from each surface along the identified arc and gluing the resulting boundary circles together, yields a connected oriented compact surface S with boundary $K_1 \# K_2$ (see Figure 1.25). Since the genus is additive under this gluing operation, we obtain $g(S) = g(S_1) + g(S_2) = g(K_1) + g(K_2)$, and therefore

$$g(K_1 \# K_2) \leq g(K_1) + g(K_2).$$

Lower bound.

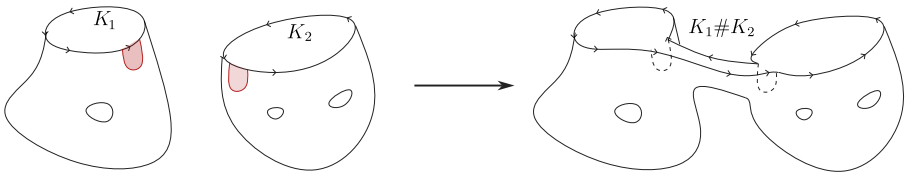

Figure 1.25: *The gluing of two Serfert surface S_1 and S_2, with $\partial S_1 = K_1$ and $\partial S_2 = K_2$. The resulting surface S is such that $\partial S = K_1\#K_2$.*

Let S be a Seifert surface of minimal genus for $K_1\#K_2$. By a standard transversality argument, one can arrange S to intersect the decomposing sphere, the 2-sphere along which the connected sum is performed, in a single simple closed curve, which separates S into two surfaces S_1 and S_2 with boundaries K_1 and K_2 respectively. Since

$g(S) = g(S_1) + g(S_2) \geq g(K_1) + g(K_2)$, we conclude $g(K_1\#K_2) \geq g(K_1) + g(K_2)$.

Combining both inequalities gives the result. □

As announced in Section 1.1, this theorem has an important consequence for the algebraic structure of the set of knots under connected sum.

Corollary 1.61. *No non-trivial knot admits an inverse with respect to the connected sum. Consequently, the set of oriented knots equipped with the connected sum is a commutative monoid, freely generated by the prime knots.*

Proof. Suppose $K\#K' \approx \bigcirc$ for some knots K and K'. Then by additivity of genus,

$$0 = g(\bigcirc) = g(K\#K') = g(K) + g(K').$$

Since genus is non-negative, this forces $g(K) = g(K') = 0$, hence by Remark 1.54 both K and K' must be equivalent to the unknot, which is a contraddiction. □

Beyond additivity, the genus satisfies several other fundamental properties that make it a particularly well-behaved invariant.

Remark 1.62. The Seifert algorithm applied to a reduced alternating diagram always produces a minimal genus Seifert surface, so that for alternating knots the genus can be computed directly from any reduced alternating diagram.

1.3 Torus Knots

Torus knots are among the simplest non-trivial knots from a geometric point of view, yet they exhibit rich structure that makes them an ideal testing ground for knot invariants. In particular, the computation of Khovanov homology for the family $T(2,n)$ of torus knots will serve as a fundamental example in Chapter 3.4, and the genus of torus knots will be a key ingredient in the proof of the Milnor conjecture via the Rasmussen s-invariant in Chapter 4.

Definition 1.63 (Torus knot). Let p, q be coprime integers. The *torus knot* $T(p,q)$ is the knot obtained by embedding a curve on the surface of a standardly embedded torus $\mathbb{T}^2 \subset S^3$ that winds $|p|$ times around the longitude (the circle bounding a disk in the exterior of the torus) and $|q|$ times around the meridian (the circle bounding a disk on the interior of the torus). The signs of p and q record the directionality of the winding: a negative value indicates winding in the opposite direction. When p and q are not coprime, the same construction yields a *torus link* with $\gcd(p,q)$ components.

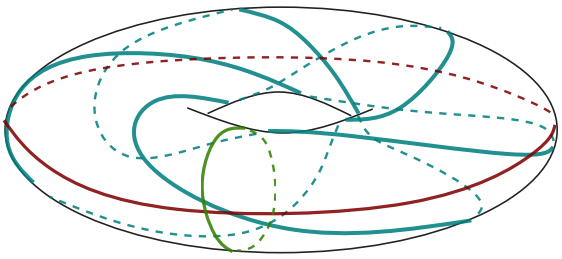

Figure 1.26: *Torus knot $T(3,5)$ embedded on a torus $\mathbb{T}^2$, with the longitude (red) and the meridian (green) indicated.*

Example 1.64. The simplest non-trivial torus knots are (see Figure1.27):

- $T(2,3)$: the right-handed trefoil knot,
- $T(2,5)$: the cinquefoil knot,
- $T(3,4)$: the first torus knot not of the form $T(2,n)$.

More generally, $T(2,1)$ is the unknot, and $T(2,n)$ for odd $n \geq 3$ gives an infinite family of alternating knots,.

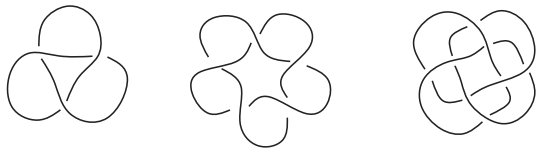

Figure 1.27: *Diagram of the torus knots $T(2,3)$ (left), $T(2,5)$ (center) and $T(3,4)$ (right).*

Proposition 1.65. *Let $T(p,q)$ be a torus knot. If $p \in \{0, \pm 1\}$ or $q \in \{0, \pm 1\}$ then $T(p,q)$ is the unknot.*

Remark 1.66. The torus knot $T(p,q)$ is equivalent to $T(q,p)$, reflecting the symmetry of the torus under the exchange of longitude and meridian. Moreover, changing both signs gives the mirror image: $T(p,-q) = T(p,q)^*$.

Theorem 1.67 (Classification of torus knot)**.** *Suppose that $T(p,q)$ and $T(s,r)$ are two torus knots, and that $|p|$, $|q|$, $|s|$, $|r| \geq 2$. Then*

$$T(p,q) \approx T(s,r) \qquad \Longleftrightarrow \qquad \{p,q\} = \{s,r\} \text{ or } \{p,q\} = \{-s,-r\}.$$

Proof. The proof can be found in [Mur08, Theorem 7.4.1.] □

This classification shows that torus knots are completely determined by the unordered pair $\{|p|,|q|\}$.

The standard Diagram

Torus knots admit particularly simple diagrammatic representations arising from their natural braid structure.

Definition 1.68 (standard diagram of $T(p,q)$). The standard diagram of the torus knot $T(p,q)$ is obtained by projecting the standard torus $\mathbb{T}^2$ onto the plane in such a way that the curve appears as p strands arranged in a symmetric pattern, with each pair of adjacent strands crossing a total of q times. All crossings in this diagram have the same sign, determined by the orientation of the winding. See Figure 1.28.

Remark 1.69. The standard diagram of $T(2,n)$ for odd n is a reduced alternating diagram with exactly n crossings. Therefore, by the Kauffman-Murasugi-Thistlethwaite theorem (Theorem 1.35), this diagram realizes the crossing number:

$$c(T(2,n)) = n.$$

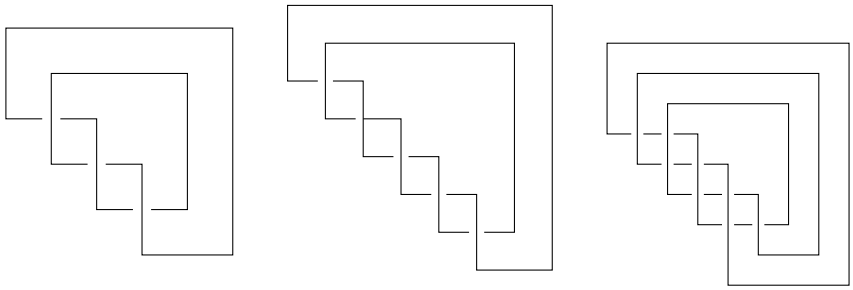

$T(2,3)$ $T(2,5)$ $T(2,4)$

Figure 1.28: *Canonical diagrams of torus knots $T(2,3)$, trefoil with 3 crossings, $T(2,5)$ cinquefoil with 5 crossings, and $T(3,4)$ 8 crossings.*

More generally, the crossing number of all torus knots is known:

Theorem 1.70 ([Mur08])**.** *The crossing number of a torus knot $T(p,q)$ is*

$$c(T(p,q)) = \min\{|p|(|q|-1), |q|(|p|-1)\}.$$

Example 1.71. For the trefoil $T(2,3)$, we have $c(T(2,3)) = \min\{2\cdot 2, 3\cdot 1\} = \min\{4,3\} = 3$. For $T(3,4)$, we get $c(T(3,4)) = \min\{3\cdot 3, 4\cdot 2\} = \min\{9,8\} = 8$.

The Genus of Torus Knots

We now compute the genus of torus knots using the Seifert algorithm.

Theorem 1.72. *The genus of the torus knot $T(p,q)$ for coprime $p,q \geq 1$ is given by*

$$g(T(p,q)) = \frac{(p-1)(q-1)}{2}.$$

Proof. See [Lic97, Theorem 8.6] or the original paper [Sei34]. □

Remark 1.73. This general formula will be crucial in Chapter 4 for the proof of the Milnor conjecture, where the genus of torus knots provides the key lower bound that the Rasmussen s-invariant must match.

Example 1.74. We compute the genus for several torus knots by using Theorem 1.72:

- $g(T(2,3)) = \frac{(2-1)(3-1)}{2} = \frac{2}{2} = 1$ (trefoil),
- $g(T(2,5)) = \frac{(2-1)(5-1)}{2} = \frac{4}{2} = 2$ (cinquefoil),
- $g(T(3,4)) = \frac{(3-1)(4-1)}{2} = \frac{6}{2} = 3$,

- $g(T(3,5)) = \frac{(3-1)(5-1)}{2} = \frac{8}{2} = 4$.

Corollary 1.75. *For coprime integers $p, q \geq 2$, the torus knot $T(p,q)$ is non-trivial.*

Proof. Since $p, q \geq 2$, we have

$$g(T(p,q)) = \frac{(p-1)(q-1)}{2} \geq \frac{1 \cdot 1}{2} = \frac{1}{2}.$$

Since the genus is an integer and $g(T(p,q)) \geq \frac{1}{2}$, we have $g(T(p,q)) \geq 1$. By Remark 1.54, any knot with positive genus is non-trivial. □

This corollary provides a simple proof that torus knots $T(p,q)$ with $p, q \geq 2$ are genuinely knotted, complementing the classification result of Theorem 1.67.

Chapter 2

Jones Polynomial

In the previous chapter, we have seen several numerical invariants, including numerical, combinatorial, and geometric ones. In the following, we will introduce a new Laurent polynomial invariant: the Jones polynomial. Discovered by Vaughan Jones in 1984 in his study of von Neumann algebras [Jon85], the *Jones polynomial* was soon recognized as a powerful new invariant of oriented links in three-dimensional space. The original construction was striking because it did not come from classical knot theory, but rather from operator algebras.

By analyzing inclusions of von Neumann algebras and the associated braid group representations, Jones discovered a trace function whose closure yielded a new link invariant. This unexpected connection between functional analysis and low-dimensional topology reshaped both fields and opened the door to entirely new methods in knot theory. For this groundbreaking work, Vaughan Jones was awarded the Fields Medal in 1990, with the Jones polynomial cited as a central achievement. Nowadays, it has gained importance since it serves as a gateway to a rich network of ideas linking knot theory, statistical mechanics, quantum groups, and topological quantum field theory. Many later invariants, including the HOMFLY-PT polynomial and Khovanov homology, can be viewed as extensions or categorifications of the Jones polynomial. In this chapter, we present the definition of the Jones polynomial via the Kauffman bracket, which offers a combinatorial and diagrammatic approach that is independent of its original operator- algebraic origins. This formulation, introduced by Louis Kauffman [Kau87] shortly after Jones's discovery, makes the invariant accessible through planar link diagrams and local relations.

We observe that, given a diagram D, there are two ways of "smoothing" a singularity at a crossing point, i.e., we can remove a double point in D by erasing

a small neighborhood of it and by connecting the four resulting ends by a pair of simple, nonintersecting arcs:

Figure 2.1: *The two was of smoothing or resolving a crossing.*

In the following sections, we firstly present an approach to Jones polynomial using Kauffman brackets. We then discuss several fundamental properties of the Jones polynomial and conclude by illustrating its computation through explicit examples using both types of brackets. In all the chapter we will follow [Cro04] approach.

2.1 Definition via Kauffman Bracket

The first polynomial invariant we will see is the canonical Jones polynomial; the one defined by Kauffman in [Kau87].

The Kauffman bracket $\langle D \rangle \in \mathbb{Z}[A^{\pm}]$ is defined for an unoriented link diagram D by a recursive procedure based on three rules:

i. $\langle \bigcirc \rangle = 1$

ii. $\langle D \cup \bigcirc \rangle = d\langle D \rangle$

iii. $\langle \times \rangle = A\langle \asymp \rangle + B\langle) (\rangle$

The third property means that the three diagrams that appear differ only in a portion of the diagram around the considered crossing and is often called the *Kauffman skein relation*. An *A-smoothing* (or A-resolution) of the crossing $\times$ is defined as the resolution of the crossing into $\asymp$, while a *B-smoothing* (or B-resolution) is the resolution of the same crossing into $) ($.

Remark 2.1. From the last rule, rotating the $\langle \times \rangle$ by $\pi/2$ we get:

$$\langle \times \rangle = A\langle) (\rangle + B\langle \asymp \rangle.$$

The definition of the bracket is given recursively; hence, we would like to find a general formula for a link diagram. To do this, we first notice that, applying i. and ii. $k-1$ times, we get $\langle \bigcirc_k \rangle = d^{k-1}$, where $\bigcirc_k$ represents the disjoint union of

$k \in \mathbb{N}$ unknot. Furthermore, each time the Kauffman bracket resolves a crossing in our diagram, the number of terms on the right side of our equation doubles. Hence, for a diagram D with n crossings, we need to apply the Kauffman bracket n times to end up, on the right side, with the sum of 2^n monomials in the unknowns A and B, multiplied by the brackets of a certain number of unknots (see Figure 2.2). More precisely, if we call *state* s of a given diagram D a choice at each crossing of an A or a B smoothing. Resuming all these observations, we get the following:

$$\langle D \rangle = \sum_{s \in S(D)} d^{k(s)-1} A^{a(s)} B^{b(s)}$$

where $S(D)$ is the set of all 2^n states of D and $k(s)$ the number of connected components obtained by performing all the resolutions of the state. $a(s)$ and $b(s)$ denote the numbers of A-resolutions and B-resolutions in the state s, respectively.

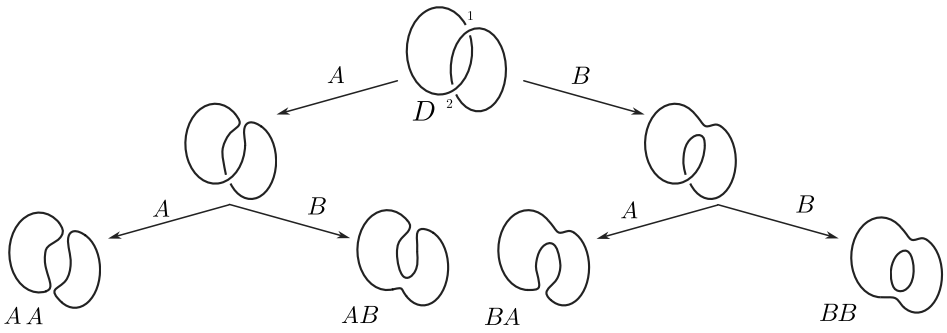

Figure 2.2: *A resolution tree for the diagram D representing the Hopf link. We firstly apply the Kauffman skein relation on crossing 1 and then on 2. At the end we get four states: one state of AA and one of BB with two components and two AB states with one component. Hence, the Kauffman bracket of this diagram D is $\langle D \rangle = dA^2 + 2AB + dB^2$.*

We would like this bracket to be an invariant for links, but, as we will see later, we can only adjust A, B and d so that it is an invariant under $R2$ and $R3$ but, sadly, it cannot be an invariant under $R1$. To solve this last problem, we can multiply the bracket by a quantity able to balance the change of $\langle \cdot \rangle$ under $R1$.

Lemma 2.2 (Invariance under R2). *Let $B = A^{-1}$ and $d = -A^2 - A^{-2}$, then the Kauffman bracket is an invariant under R2, i.e.* $\langle$  $\rangle = \langle$  $\rangle$ *for all diagrams.*

Proof. We will prove that

$\langle$  $\rangle = AB\langle$  $\rangle + (ABd + A^2 + B^2)\langle$  $\rangle$.

Resolving the singularity from the top to the bottom, we get:

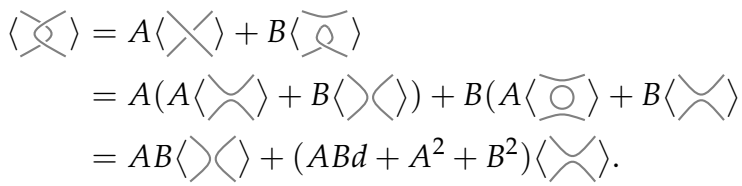

Imposing $AB = 1$ and $dAB + A^2 + B^2 = 0$, from the first equation we get $B = A^{-1}$ and from the second one we get $dAA^{-1} + A^2 + A^{-2} = 0$ and hence $d = (-A^2 - A^{-2})$. With this choice of B and d we can conclude $\langle$  $\rangle = \langle\rangle\langle\rangle$. This proves the statement. □

Lemma 2.3 (Invariance under R3). *The invariance under R2 implies type R3 invariance.*

Proof.

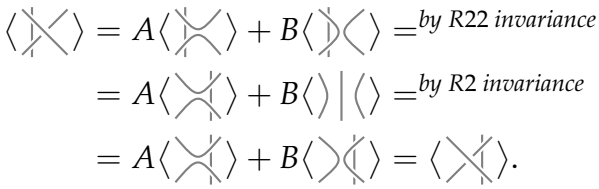

□

From now on, we work with the assumption of B and d as chosen in Lemma 2.2. The polynomial we get resolving a diagram is an element of $\mathbb{Z}[A, A^{-1}]$, is known as the *bracket polynomial* and is an invariant for unoriented framed links (i.e.,invariance under $R2$ and $R3$).

Definition 2.4 (Kauffman bracket). Let D be a diagram of a link. We define the *Kauffman bracket* of D, as the Laurent polynomial $\langle D\rangle \in \mathbb{Z}[A^{\pm}]$ obtained by this recursive procedure:

i. $\langle$  $\rangle = 1$

ii. $\langle D \cup$  $\rangle = (-A^2 - A^{-2)}\langle D\rangle$

iii. $\langle$  $\rangle = A\langle$ $\rangle + A^{-1}\langle\rangle\langle\rangle$.

Let us see what happens when we try to determine the bracket under $R1$:

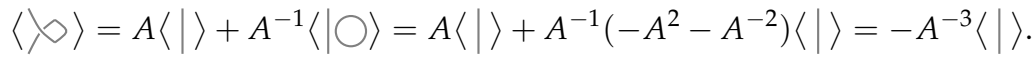

Similarly, $\langle \rangle = -A^3 \langle \; \rangle$.

We just have proved that the bracket polynomial is an invariant under $R2$ and $R3$ but not under $R1$. To transform the bracket from an invariant of framed unoriented links to one of oriented links, we can try to adjust it with an other invariant of framed links which takes in count its orientation. The simplest invariant for oriented framed links is the *writhe* (or twist number) $w(D)$:

Definition 2.5 (Writhe). Let D be an oriented link diagram. The *writhe* $w(D)$ is the sum of sings of all crossings. If we note n_+ and n_- the number of positive and negative crossings of D respectively, the writhe of D is:

$$w(D) = n_+ - n_-.$$

We observe that the writhe is an invariant for $R2$ and $R3$ in fact, when we do a $R2$ and change the diagram from $\times$ to $)($ two crossings with opposite sing disappear so the writhe $w(\times) = w()() + 1 - 1 = w()()$. For $R3$ move, the number and sign of the crossings do not change, the crossings are only in a different position, so the writhe remains the same (see Figure 2.3).

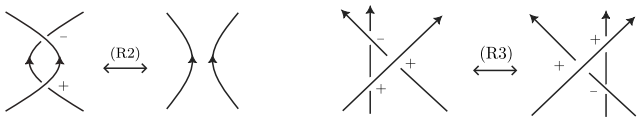

Figure 2.3: *How crossing sings change when we do a R2 or an R3 with some chosen orientations.*

Remark 2.6. We can observe that, regardless of the orientation we choose:

$$w(\;) = w(\;) - 1 \quad \text{and} \quad w(\;) = w(\;) + 1.$$

If we multiply the bracket by $(-A)^{-3w(D)}$, we get a polynomial invariant for links. This is due to the fact that, when a $R1$ move is performed, a $-A^{\pm 1}$ appears in the bracket depending on the crossings and this quantity is well balanced by the writhe.

Definition 2.7 (Jones Polynomial). Let D be a diagram of a link L. The *Jones polynomial* of the link L, $f_L(A) \in \mathbb{Z}[A, A^{-1}]$ is:

$$f_L(A) = (-A)^{-3w(D)} \langle D \rangle.$$

Remark 2.8. In the literature, the Jones polynomial is usually defined as $V_L(t) = f_L(A)_{|_{A=t^{-\frac{1}{4}}}} \in \mathbb{Z}[t^{\frac{1}{2}}, t^{-\frac{1}{2}}]$. The reason behind this change of variable is due to the skein relation of Jones polynomials, which will be studied in Section (2.2).

In this Section, we will use the first definition of Jones polynomial, i.e. the one with the A variable.

Proposition 2.9. *The Jones polynomial $f_L(A)$ is an invariant for oriented links.*

Proof. By Reideimeiser Theorem 1.27, to show that the Jones polynomial of a link diagram is a link invariant, it suffices to verify its invariance under the three Reidemeister moves. The invariance under $R2$ and $R3$ follows from the fact that the bracket and the writhe are both invariants for framed links.

For the $R1$ invariance, let us write on formula what we have said before. We will indicate as $f_{\curvearrowright}(A)$ the Jones polynomial of the knot diagram with a left twist and with $f_{\uparrow}(A)$ the Jones polynomial of the same diagram but without the twist.

$$f_{\curvearrowright}(A) = (-A)^{-3w(\curvearrowright)}\langle \curvearrowright \rangle = (-A)^{-3(w(\uparrow)-1)}(-A)^{-3}\langle \uparrow \rangle =$$

$$= (-A)^{-3w(\uparrow)}\langle \uparrow \rangle = f_{\uparrow}(A).$$

For the right twist it's the same but with inverted sign in the writhe and in the factor that appears in the bracket. □

2.2 Properties

In this Section, we will explore some useful properties of Jones polynomial and a skein relation used to compute the invariant.

Proposition 2.10. *Let L, L_1 and L_2 be links. It holds:*

i. $f_{L^*}(A) = f_L(A^{-1})$, *where L^* is the mirror image of L,*

ii. $f_{-L}(A) = f_L(A)$, *where $-L$ is the link obtained by reversing the orientation of each component of L,*

iii. $f_{L_1 \# L_2}(A) = f_{L_1}(A) f_{L_2}(A)$,

iv. $f_{L_1 \sqcup L_2}(A) = (-A^2 - A^{-2}) f_{L_1}(A) f_{L_2}(A)$.

Proof. We first notice that $w(D) = w(-D) = -w(D^*)$ since, if we change all orientations, the signs of crossings do not change, and, on the other hand, the mirror image of a knot has the same crossings but with opposite sign, i.e $n_+(D) = n_-(D^*)$ and $n_-(D) = n_+(D^*)$ so $w(D) = n_+(D) - n_(D) = n_-(D^*) - n_+(D^*) = -w(D^*)$ (see Figure 2.4).

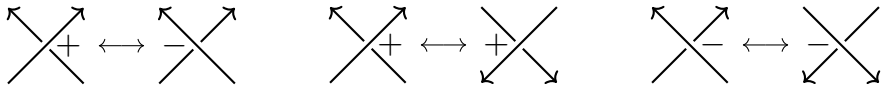

Figure 2.4: *On the left how the sign differ under taking mirror image. In the center and on the right, changing the orientation of both strands involved in a crossing does not change its sign.*

i. From Kauffman bracket's definition we deduce that $\langle D^* \rangle(A) = \langle D \rangle(A^{-1})$:

Hence, using the observation above, we have:

$$f_{D^*}(A) = (-A)^{-3w(D^*)}\langle D^*(A)\rangle = (-A)^{-3w(D)}\langle D\rangle(A^{-1}) = f_L(A^{-1}).$$

ii. The bracket $\langle D \rangle$ does not depend on the orientation of D, therefore:

$$f_{-L}(A) = (-A)^{-3w(-D)}\langle -D\rangle = (-A)^{-3w(D)}\langle D\rangle = f_L(A).$$

iii. Let D_1 and D_2 be two diagrams of L_1 and L_2 such that $D_1\#D_2$ is a diagram of $L_1\#L_2$ with $cr(D_1) + cr(D_2) = cr(D_1\#D_2)$. We observe that $w(D_1\#D_2) = w(D_1)w(D_2)$ considering that the connected sum preserves the orientation of the original diagrams. Now, we start to resolve the crossings of the first diagram, without touching the crossing of the second one. When we complete all the smoothing of D_1 we get: $\langle D_1\#D_2\rangle = \langle D_1\rangle\langle \bigcirc \#D_2\rangle = \langle D_1\rangle\langle D_2\rangle$. Combining the two results we get:

$$\begin{aligned} f_{L_1\#L_2}(A) &= (-A)^{-3w(D_1\#D_2)}\langle D_1\#D_2\rangle = (-A)^{-3(w(D_1)+w(D_2))}\langle D_1\rangle\langle D_2\rangle = \\ &= (-A)^{-3w(D_1)}\langle D_1\rangle(-A)^{-3w(D_2)}\langle D_2\rangle = \\ &= f_{L_1}(A)f_{L_2}(A). \end{aligned}$$

iv. We use the same procedure as in iii. On the one hand, we have $w(D_1 \sqcup D_2) = w(D_1) + w(D_2)$, on the other hand, after all the resolutions of D_1, an

additional disjoint circle appears near D_2, i.e. $\langle D_1 \sqcup D_2 \rangle = \langle D_1 \rangle \langle \bigcirc \sqcup D_2 \rangle = (-A^2 - A^{-2}) \langle D_1 \rangle \langle D_2 \rangle$. So:

$$\begin{aligned} f_{L_1 \sqcup L_2}(A) &= (-A)^{-3w(D_1 \sqcup D_2)} \langle D_1 \sqcup D_2 \rangle = \\ &= (-A)^{-3w(D_1)+w(D_2)} \langle D_1 \rangle (-A^2 - A^{-2}) \langle D_2 \rangle = \\ &= (-A^2 - A^{-2})(-A)^{-3w(D_1)} \langle D_1 \rangle (-A)^{-3w(D_2)} \langle D_2 \rangle = \\ &= (-A^2 - A^{-2}) f_{L_1}(A) f_{L_2}(A). \end{aligned}$$

□

Let now D be a diagram of an oriented knot and c, one of its crossings. We search for a skein relation for Jones polynomials similar to Kauffman's: $\langle \times \rangle_D = A \langle \times \rangle + A^{-1} \langle) (\rangle$. We consider three diagrams obtained by D by switching the crossing c or by eliminating it according to the orientation of the knot. We call D_+, D_- and D_0, respectively, the diagrams with positive, negative crossing c or without c (see Figure 2.5).

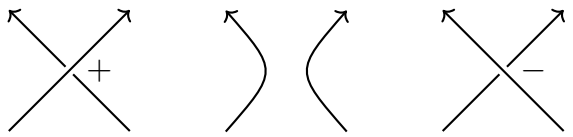

Figure 2.5: *The difference at c of the three diagrams.*

If we evaluate the bracket of D_+ and D_-, D_0 appears:

$$\langle \times \rangle_{D_-} = A \langle \times \rangle + A^{-1} \langle) (\rangle_{D_0}$$

$$\langle \times \rangle_{D_+} = A^{-1} \langle \times \rangle + A \langle) (\rangle_{D_0}$$

Multiplying the first and the second equation by A^{-1} and A, respectively, subtracting the second from the first equation we get:

$$A^{-1} \langle \times \rangle_{D_-} - A \langle \times \rangle_{D_+} = (A^{-2} - A^2) \langle) (\rangle_{D_0}.$$

We already know that $w(D_+) - 1 = w(D_0) = w(D_-) + 1$; so multiplying by $A^{w(D_0)}$ we get:

$$A^{-4} f_{L-}(A) - A^4 f_{L+}(A) = (A^{-2} - A^2) f_{L_0}.$$

Where L_+, L_- and L_0 are the links associated to the diagrams D_+, D_- and D_0, respectively. By multiplying the equation by -1 we get the Jones polynomial's skein relation:

Theorem 2.11. *If L_+, L_- and L_0 are three links having diagrams D_+, D_- and D_0 that differs as in Figure 2.5 in a specific crossing, we have:*

$$A^4 f_{L+}(A) - A^{-4} f_{L-}(A) = (A^2 - A^{-2}) f_{L_0}(A). \tag{2.1}$$

Remark 2.12. Changing the variable $A = t^{\frac{1}{4}}$ we get

$$t f_{L_+} - t^{-1} f_{L_-} = (t^{\frac{1}{2}} - t^{-\frac{1}{2}}) f_{L_0}.$$

2.3 Jones polynomial of type q

In this section, we will introduce another type of bracket, it is defined in a similar way to the Kauffman's one and, as for the other, this bracket gives rise to a version of Jones polynomial. We will use this version of Jones polynomial in Chapter 3, when defining Khovanov homology. We start by giving a recursive definition of the bracket.

Definition 2.13 (Kauffman q-bracket). Let D be a link diagram. The *q-bracket polynomial* $\langle\langle D \rangle\rangle$ is a Laurent polynomial $\langle\langle D \rangle\rangle \in \mathbb{Z}[q, q^{-1}]$ and it is defined by the following recursive properties:

i. $\langle\langle \bigcirc \rangle\rangle = q + q^{-1}$

ii. $\langle\langle D \cup \bigcirc \rangle\rangle = (q + q^{-1})\langle\langle D \rangle\rangle$

iii. $\langle\langle \times \rangle\rangle = \langle\langle \asymp \rangle\rangle - q\langle\langle)(\rangle\rangle$

Remark 2.14. We observe that in this definition the q-bracket of the unknot is not equal to 1, the reason why we did not initialized it as one will be clear in Chapter 3.

Notation 2.15. From now on, we will call the $A-$smoothing $\asymp$ of a crossing $\times$ a $0-$*smoothing* and the $B-$smoothing $)($ a $1-$*smoothing*.

As in Section 2.1, also the q-bracket of a link diagram D is computed via a recursive decomposition process represented by a resolution tree. At each crossing, one of two possible smoothings is chosen: a 0-smoothing or a 1-smoothing. This process yields a set of states $S(D)$, where each state $s \in S(D)$ corresponds to a unique collection of disjoint circles, denoted as the smoothed diagram D_s. To each state, we assign a weight based on the number of 1-smoothings performed,

denoted by $r(s)$; specifically relation *iii.* in Definition 2.13 implies that, each 1-smoothing contributes a factor of $-q$, resulting in a total weight of $(-1)^{r(s)}q^{r(s)}$. Since each disjoint circle in the resulting diagram D_s evaluates to the value $(q + q^{-1})$, a state with $k(s)$ circles contributes $(q + q^{-1})^{k(s)}$. By summing the weighted contributions of all possible states in the resolution tree, we get the state sum formula for the Kauffman q-bracket:

Proposition 2.16. *Let D be a diagram of a link. Then its q-bracket can be expressed as:*

$$\langle\langle D\rangle\rangle = \sum_{s\in S(D)} (-1)^{r(s)}q^{r(s)}\langle\langle D_s\rangle\rangle = \sum_{s\in S(D)} (-1)^{r(s)}q^{r(s)}(q+q^{-1})^{k(s)}.$$

Where $r(s)$ and $k(s)$ are the weight of the state and the number of circles in the smoothed diagram D_s, respectively.

Proposition 2.17. *The q-bracket $\langle\langle\ \cdot\ \rangle\rangle$ is invariant under $R3$ and it holds:*

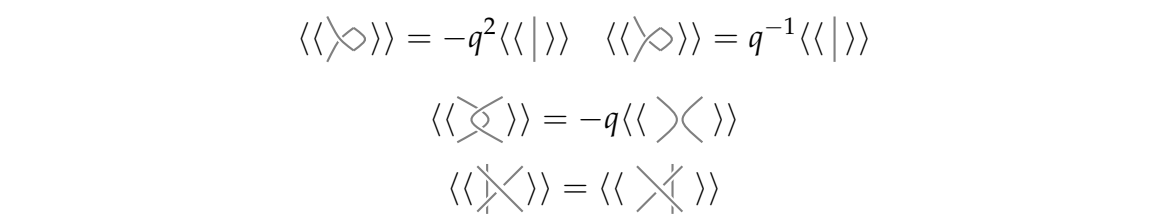

Proof. It is only a matter of computation:

Similarly,

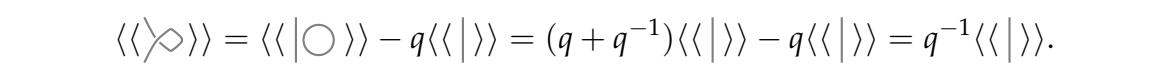

For $R2$ we use (2.1) with $A = 1$ $B = -q$ and $d = q + q^{-1}$

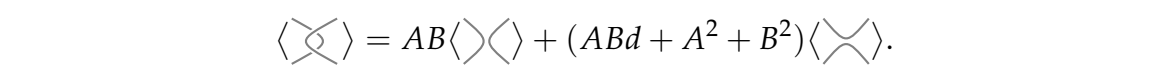

$AB = -q$ and $dAB + A^2 + B^2 = -q(q + q^{-1}) + 1 + q^2 = -q^2 - 1 + 1 + q^2 = 0$ and so:

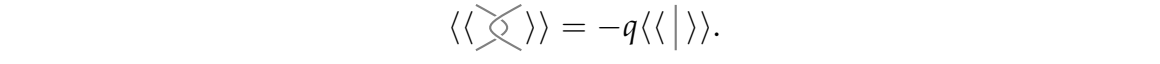

Finally, for $R3$, looking at the way the q-bracket behaves under $R2$, we get:

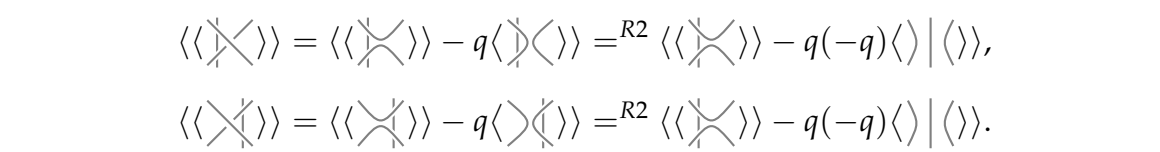

□

However, we can define an oriented link polynomial invariant by multiplying the bracket by a quantity depending on the number of positive and negative crossings in our diagram:

Definition 2.18 (Unnormalised Jones q-polynomial). Let D be an oriented link diagram. n_+ and n_- be the number of positive and negative crossings in D, respectively, and $n = n_+ + n_-$. The *unnormalised Jones q-polynomial* of D, $\hat{J}(D)$, is:

$$\hat{J}(D) = (-1)^{n_-} q^{n_+ - 2n_-} \langle\langle D \rangle\rangle.$$

Remark 2.19. It is called unormalised because the Jones q-polynomial of the unknot it is equal to $q + q^{-1}$ and not equal to one.

Proposition 2.20. *The unnormalised Jones q-polynomial $\hat{J}(D)$ is an invariant of oriented links.*

The proof is a consequence of Theorem 2.23, where we prove that $\hat{J}(D)$ is essentially the usual Jones polynomial but with a different variable.

Notation 2.21. Since we stated that $\hat{J}(D)$ does not depend on the diagram of the link, we can note it as $\hat{J}_L(q)$.

Definition 2.22 (Jones q-polynomial). Let L be a link and D one of its diagrams. The *Jones q-polynomial* of the link L is :

$$J_L(q) = (q + q^{-1})^{-1} \hat{J}_L(q).$$

We have seen how the two Kauffman brackets differ, in particular the q-bracket is not even invariant under $R2$. Nevertheless there is a relation between the unnormalised Jones q-polynomial of a link L with diagram D, $\hat{J}_L(q) = (-1)^{n_-} q^{n_+ - 2n_-} \langle\langle D \rangle\rangle$, and the classical Jones polynomial $f_L(A) = (-A)^{-3w(D)} \langle D \rangle$:

Theorem 2.23. *The Jones polynomial from Definition 2.7 and the Jones q-polynomial from Definition 2.22 are equivalent. More precisely, given a link L it holds:*

$$\hat{J}_L(q)\Big|_{q=-A^{-2}} = (-A^2 - A^{-2}) f_L(A).$$

In other words:

$$J_L(q)\Big|_{q=-A^{-2}} = f_L(A).$$

Proof. Given a diagram D representing L, with n_+ and n_- its number of positive and negative crossings, we have:

$$\begin{aligned}
\hat{J}_L(q)\big|_{q=-A^{-2}} &= (-1^{n_-})(-A^{-2})^{n_+-2n_-}\sum_{s\in S(D)}(-A^{-2}-A^2)^{k(s)}(-1)^{r(s)}(-A^{-2})^{r(s)} = \\
&= (-1^{n_-})(-1)^{n_+-2n_-}A^{4n_--2n_+}(-A^{-2}-A^2) \\
&\qquad \sum_{s\in S(D)}(-A^{-2}-A^2)^{k(s)-1}(-1)^{2r(s)}A^{-2r(s)} = \\
\overset{r(s)=b(s)}{} &= (-A^{-2}-A^2)(-1)^{n_+-n_-}A^{3n_--3n_+}A^{n_++n_-}\sum_{s\in S(D)}(-A^{-2}-A^2)^{k(s)-1}A^{-2b(s)} = \\
&= (-A^{-2}-A^2)(-A)^{3n_--3n_+}\sum_{s\in S(D)}(-A^{-2}-A^2)^{k(s)-1}A^{n-2b(s)} = \\
\overset{n=a(s)+b(s)}{} &= (-A^{-2}-A^2)(-A)^{3n_--3n_+}\sum_{s\in S(D)}(-A^{-2}-A^2)^{k(s)-1}A^{a(s)-b(s)} = \\
&= (-A^2-A^{-2})f_L(A).
\end{aligned}$$

□

This relation allows us to use both definitions based on needs.

2.4 Examples

To illustrate the computation of the Jones polynomial, we now present two explicit calculations for the trefoil knot. Although both methods yield the same invariant, they approach the computation from different perspectives and emphasize different structural features of the theory. The first uses the tree resolution method with the A variable, while the second employs the cube of resolutions with the q variable. In particular, the cube of resolutions anticipates the structure underlying Khovanov homology, which will be discussed in subsequent chapters.

Jones polynomial of the right-handed trefoil knot via tree resolution

Example 2.24. To compute the Jones polynomial of the right-handed trefoil knot we consider the following diagram D with three positive crossings.

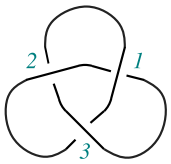

We firstly need to evaluate its Kauffman braket $\langle D \rangle$. Enumerating each crossings from 1 to 3, we resolve each crossings as a A-smoothing with coefficient A and a B-smoothing with coefficient A^{-1}. Resolving all three crossings produces a binary resolution tree as the one in Figure 2.6 with $2^3 = 8$ terminal states. Each terminal

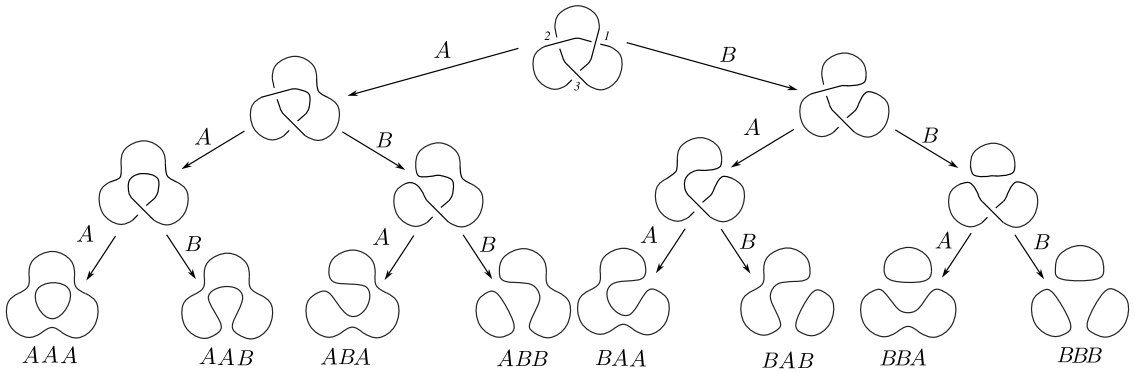

Figure 2.6: *The tree resolution of a diagram of the right-handed trefoil knot.*

state s is a collection of disjoint circles and its contribution is the product of the smoothing coefficients times $(-A^2 - A^{-2})^{k(s)-1}$, where $k(s)$ is the number of circles in s To evaluate the Kauffman bracket we need to sum up all contributions of the 8 states:

$$\begin{aligned}\langle \text{⊗} \rangle &= A^3(-A^2 - A^{-2}) + 3A + 3A^{-1}(-A^2 - A^{-2}) + A^{-3}(-A^2 - A^{-2})^2 = \\ &= -A^5 - A + 3A - 3A - 3A^{-3} + (-A^{-1} - A^{-5})(-A^2 - A^{-2}) = \\ &= -A^5 - A - 3A^{-3} + A + 2A^{-3} + A^{-7} = -A^5 - A^{-3} + A^{-7}.\end{aligned}$$

To obtain the Jones polynomial of the right-handed trefoil knot, we normalize by the writhe $w(D) = n_+ - n_- = 3$, using $f_L(A) = (-A)^{-3w(D)}\langle D \rangle$.

$$f_L(A) = -A^{-9}\langle \text{⊗} \rangle = A^{-4} + A^{-12} - A^{-16}.$$

Jones q-polynomial of the right-handed trefoil knot via cube resolution

Example 2.25. We will evaluate the Jones q-polynomial of the right-handed trefoil knot using a cube resolution. We consider the same diagram D as in Example 2.24.

We recall that for the Jones q polynomial and the q-bracket we named a  A-smoothing a $0-$*smoothing* and a  B-smoothing a $1-$*smoothing* of  . Let χ be the set of crossings of D, and let $n = |\chi| = 3$ denote the number its crossings. We label the crossings of D arbitrarily by the integers $1, 2, 3$, and we write $n = n_+ + n_-$, where $n_+ = 3$ and $n_- = 0$ are the number of positive and negative crossings of D, respectively.

With this notation, we can associate to each state s, corresponding to vertex of an n-dimensional cube $\{0,1\}^\chi$, a complete resolution D_s. For clarity and visual symmetry, we arrange the vertices of the cube such that states of the same height, $r = |s|$, occupy the same column and we complete the cube by connecting states which differ by exactly one smoothing.

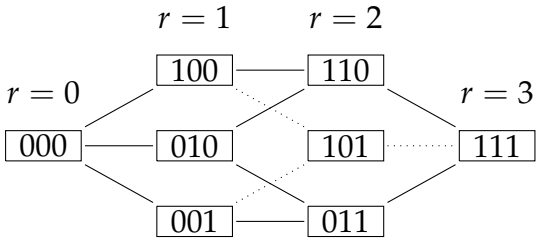

We then associate to each state a coefficient of the form

$$(-1)^{r(s)} q^{r(s)} (q + q^{-1})^{k(s)},$$

where $r = |s|$ is its height and $k(s)$ is the number of connected components of D_s. See Figure 2.7.

Summing up all the coefficients we get the Kauffman q-bracket of D:

$$\langle\langle D \rangle\rangle = (q+q^{-1}) + 3(-q(q+q^{-1})) + 3q^2(q+q^{-1})^2 - q^3(q+q^{-1}) = q^{-2} + 1 + q^2 - q^6.$$

Using $\hat{J}(L) = (-1)^{n_-(D)} q^{n_+(D) - 2n_-(D)} \langle\langle D \rangle\rangle$ with $n_+(D) = 3$ and $n_-(D) = 0$, we get

$$\hat{J}_L(q) = (q^{-2} + 1 + q^2 - q^6)(-1)^0 q^3 = q + q^3 + q^5 - q^9.$$

We normalize it and get the Jones q-polynomial of the right-handed trefoil knot:

$$\begin{aligned} J_L(q) &= (q + q^3 + q^5 - q^9)(q + q^{-1})^{-1} = \\ &= [q^2(q^{-1} + q) + q^7(q^{-1} + q)(q^{-1} - q)](q + q^{-1})^{-1} = \\ &= q^2 + q^6 - q^8. \end{aligned}$$

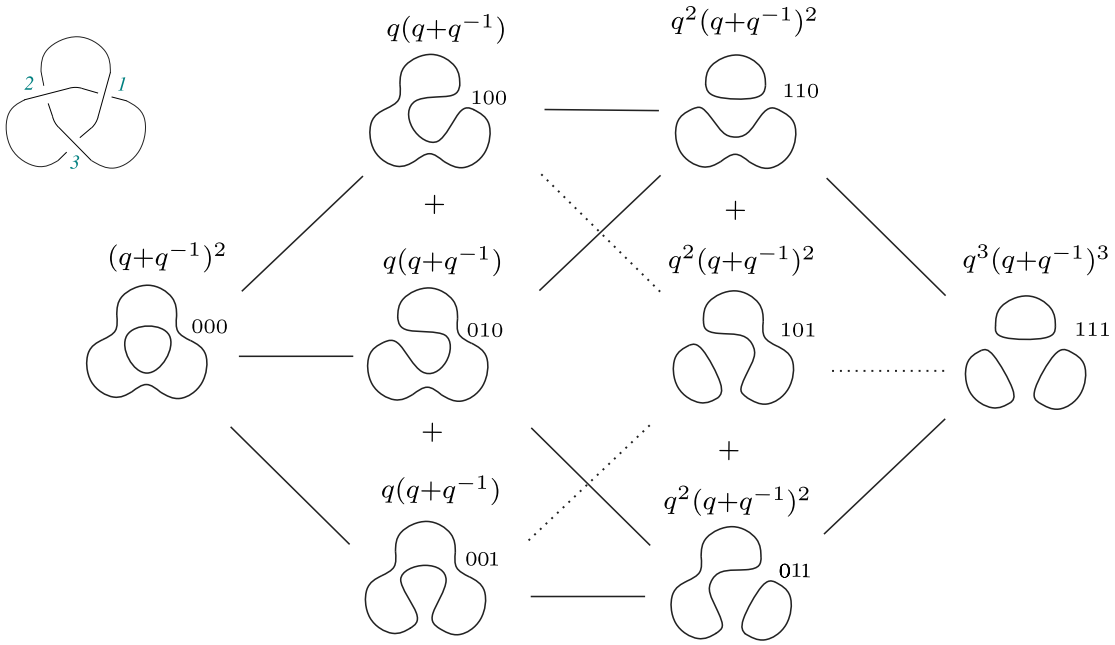

Figure 2.7: *The cube of resolutions and the computation of Jones polynomial of the right-handed trefoil knot.*

Comparison between the two types of Jones polynomial.

Now that we have computed the two versions of the Jones polynomial for the trefoil knot, we can have a tangible example of the fact that Theorem 2.23 holds:

$$J_L(q)_{|q=-A^{-2}} = (q^2 + q^6 - q^8)_{|q=-A^{-2}} = A^{-4} + A^{-12} - A^{-16} = f_L(A).$$

Chapter 3

Khovanov Homology

In this chapter, we introduce Khovanov homology, a homological invariant that categorifies the Jones polynomial. This theory was first introduced by M. Khovanov [Kho00] and later reformulated and developed by several authors, notably Viro [Vir04] and Bar-Natan [Bar02]. Throughout this chapter, we follow the notation and approach introduced by D. Bar-Natan, which provides a diagrammatic and conceptually transparent framework for the theory.

In the first section, we will define the *Khovanov Complex* $\mathcal{C}(D)$ and its *homology* $\mathcal{H}(D)$. The second Section is devoted to prove invariance under Reideimeister moves of this homological invariant. The third section is devoted to illustrate some examples of Khovanov homology coputations. In the fourth section, we explain the relation between the Khovanov complex and a $(1+1)$-dimensional Topological Quantum Field Theory TQFT, which clarifies the algebraic structure underlying the construction. The fifth section focuses on framed homology and presents an application of this theory.

Throughout this chapter, we will work with the unormilised Jones polynomial $\hat{J}_L(q)$.

3.1 Khovanov homology construction

The idea of Khovanov was, given a diagram D of a link, to associate a bigraded chain complex $\mathcal{C}^{*,*}(D)$ of graded vector spaces to it so that the resulting homology is a link invariant and has graded Euler characteristic equal to the unormalised Jones polynomial. We base this section in the paper [Bar02] by Bar-Natan.

3.1.1 Chain groups

Before starting with the actual process of creating a chain complex of graded vector spaces, we need to give some preliminary definitions. We will work with $\mathbb{Z}$ coefficients, so when we talk about vector spaces we will mean vector spaces over $\mathbb{Z}$ unless specified.

Definition 3.1 (Graded vector space and quantum dimension). A *graded vector space* W is a vector space that can be decomposed into a direct sum of vector spaces indexed by integers. Let $W = \oplus_m W_m$ be a graded vector space with homogeneous components W_m, i.e. $W_i = \langle w_i \rangle$ with $grade(w_i) = i$. The *graded dimension* of W is the power series

$$qdimW = \sum_m q^m dim(W_m).$$

The graded dimension satisfies the following:

1. $qdim(W \oplus W') = qdim(W) + qdim(W')$,
2. $qdim(W \otimes W') = qdim(W) qdim(W')$.

Definition 3.2 (Graded shift). Given a graded vector space $W = \oplus_m W_m$ and $l \in \mathbb{Z}$, we define the *shift degree* operation $\cdot\{l\}$ on W as the new graded vector space $W\{l\}$ such that $W\{l\}_m := W_{m-l}$, and

$$qdimW\{l\} = q^l qdimW.$$

To construct the Khovanov homology of a link L, we first define a two-dimensional graded vector space V spanned by the basis $\{v^+, v^-\}$. The degrees are assigned as $\deg(v^\pm) = \pm 1$, so that the resulting graded dimension of V is $q \dim V = q + q^{-1}$.

Following the conventions for 0-smoothings ( ) and 1-smoothings ( ) of a crossing , we arrange the resolutions of a diagram D into an n-dimensional cube of resolutions as we did in Example 2.25, where $n = |\chi|$ is the number of crossings.

To each vertex of the cube, corresponding to a state $s \in \{0,1\}^\chi$, we assign the graded vector space:

$$V_s(D) := V^{\otimes k}\{r\},$$

where $k(s)$ denotes the number of disjoint circles in the smoothed diagram D_s, and $r = |s| = \sum s_i$ represents the height of the state, i.e., the number of 1-smoothings in s.

With this construction, the graded dimension $qdim V_s(D)$ coincides with the polynomial assigned to the state s in the computation of the Kauffman bracket, as illustrated in Figure 2.7.

We set the r^{th} chain complex $[\![D]\!]^r$, for $r = 0, .., n$ as the direct sum of all graded vector space $V_s(D)$ with height r:

$$[\![D]\!]^r := \oplus_{s:|s|=r} V_s(D) \qquad r = 0, ..., n$$

and $[\![D]\!]^r = 0$ for all other values of r.

At this stage, since no differential has yet been defined, the collection $[\![D]\!] = ([\![D]\!]^r)_{r\in\mathbb{Z}}$ does not form a chain complex. For the moment, however, we focus on the construction of the graded chain groups and postpone the definition of the differential to the next section.

To proceed in our discussion, we need to recall some notions of homology theory.

Theorem 3.3 (Graded Euler Characteristic[Bar02]). *The graded Euler characteristic $\chi_q(\mathcal{C})$ of a chain complex $\cdots \mathcal{C}^r \xrightarrow{d^r} \mathcal{C}^{r+1} \cdots$ is defined to be the alternating sum of the graded dimension of its homology groups.*

$$\chi_q(\mathcal{C}) = \sum_i (-1)^i rk(\mathcal{H}^i).$$

Moreover, if the differential is of degree 0 and all chain groups are finite dimensional, it is also equal to the alternating sum of the graded dimension of the chain groups.

$$\chi_q(\mathcal{C}) = \sum_i (-1)^i qdim(\mathcal{C}^i).$$

Definition 3.4 (Height shift). Let s be an integer, we define the *height shift* operation $\cdot[s]$ on a chain complex as: if $\bar{\mathcal{C}}$ is a chain complex $\cdots \bar{\mathcal{C}}^r \xrightarrow{d^r} \bar{\mathcal{C}}^{r+1} \cdots$ of (graded) vector space, calling r the height of $\bar{\mathcal{C}}^r$ and of the r^{th} differential, the height shift define a new chain complex with all height shifted by s: if $\mathcal{C} = \bar{\mathcal{C}}[s]$ then $\mathcal{C}^r := \bar{\mathcal{C}}^{r-s}$.

Remark 3.5. If we endow $[\![D]\!]$ with a zero degree differential, we have $\chi_q([\![D]\!]) = \langle\langle D \rangle\rangle$:

$$\chi_q([\![D]\!]) = \sum_{r=0}^{n} (-1)^r qdim(\mathcal{C}^r(D))$$

Hence, substituting the expression for $qdim([\![D]\!]^r)$ into the sum, we have :

$$\chi_q([\![D]\!]) = \sum_{r=0}^{n} (-1)^r \left(\sum_{|s|=r} q^r (q + q^{-1})^{k(s)} \right).$$

We can consolidate the two sums into a single sum over all possible states $s \in \{0,1\}^n$:

$$\chi_q([\![D]\!]) = \sum_{s\in\{0,1\}^n} (-1)^{|s|} q^{|s|} (q+q^{-1})^{k(s)} = \langle\langle D \rangle\rangle$$

Recall that our objective is to associate to a diagram D a chain complex whose Euler characteristic is the unnormalised Jones polynomial. In order to achieve this, it is necessary to apply appropriate shifts in both the homological and internal gradings. Accordingly, we define the Khovanov chain complex associated to D by

$$\mathcal{C}(D) := [\![D]\!][-n_-]\{n_+ - 2n_-\}.$$

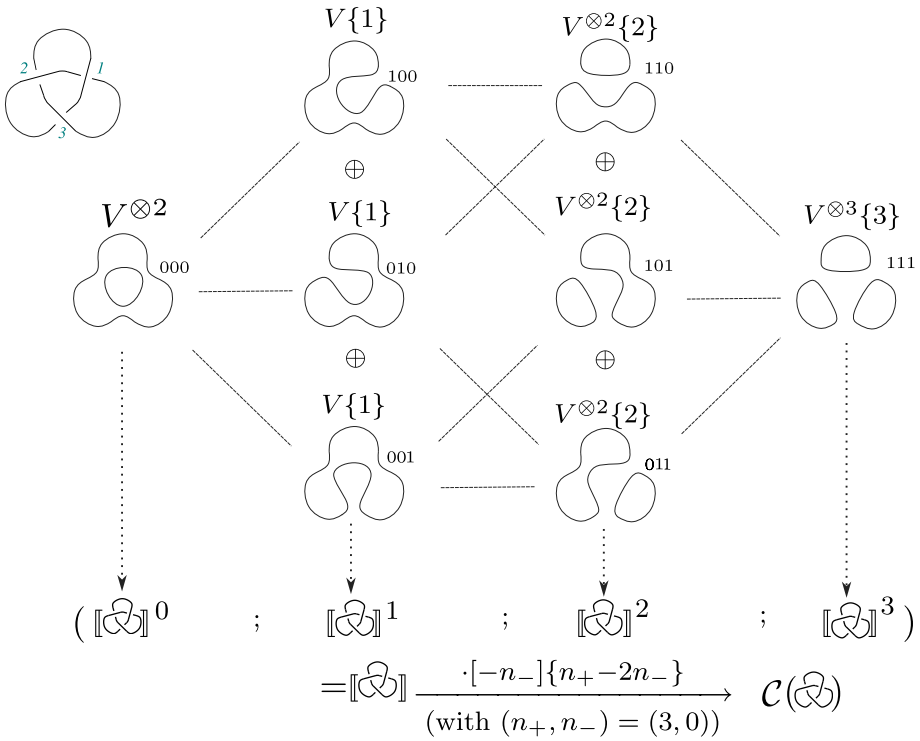

Figure 3.1: *Construction of the trefoil knot complex.*

Remark 3.6. The shift in the quantum grading by $n_+ - 2n_-$ corresponds to the factor $q^{n_+-2n_-}$ in the Definition 2.18 of the unnormalized Jones q-polynomial. The homological shift by n_- accounts for the factor $(-1)^{n_-}$ that appears in $\hat{J}(D)$.

Theorem 3.7. *([Bar02, Theorem 1]) The graded Euler characteristic of $\mathcal{C}(D)$ is the unnormalised Jones q-polynomial of the knot L:*

$$\chi_q(\mathcal{C}(D)) = \hat{J}_L(q).$$

Proof. Suppose we endowed the chain complex $\mathcal{C}(D)$ with a 0 degree differential, for Theorem 3.7 we need to show that the alternating sum of the graded dimension of the chain groups of $\mathcal{C}(D)$ is equal to the unormalised Jones q- polynomial of L. It directly follows from Remark 3.5 and Remark 3.6.

□

Definition 3.8 (Homological degree). We call *homological degree* i of a group chain $\mathcal{C}$ its height. Hence, if we consider $\mathcal{C}(D) = [\![D]\!][-n_-]\{n_+ - 2n_-\}$, the homological degree of $[\![D]\!]^r$ is

$$i = r - n_-.$$

Definition 3.9 (Quantum degree). The *quantum degree* of an element $v \in V_s(D)$ is defined as:

$$j = qdeg(v) = deg(v) + r + n_+ - 2n_-.$$

Remark 3.10. We observe that if L is a link with m components, then

$$j - m = 0 \quad mod\ 2,$$

in other words, j has the same parity as the number of components. Hence we conclude that for a knot j is always odd and for a 2 component link is even.

3.1.2 Differentials

We now aim to endow the sequence of graded vector spaces $\mathcal{C}(D)$ with a chain complex structure by defining a differential d of degree zero. Geometrically, the differential is built from maps assigned to the edges of the cube of resolutions. A vector space at homological degree i is connected to one at degree $i+1$ if and only if their corresponding states, s and s', differ by exactly one smoothing-specifically, a transition from a 0-smoothing to a 1-smoothing in one of the crossings. See Figure 3.2.

To formalize this, we label each edge ξ of the cube with a tuple in $\{0, 1, \star\}^\chi$. This tuple matches the starting state s at every position except for a single entry $\star$, which marks the crossing where the resolution changes from 0 to 1.

Each edge ξ induces a linear map between the corresponding vector spaces:

$$d_\xi : V_s \longrightarrow V_{s'}.$$

The height of an edge, denoted $|\xi|$, is defined as the height of its tail (the number of 1s in the tuple), representing the homological degree from which the map

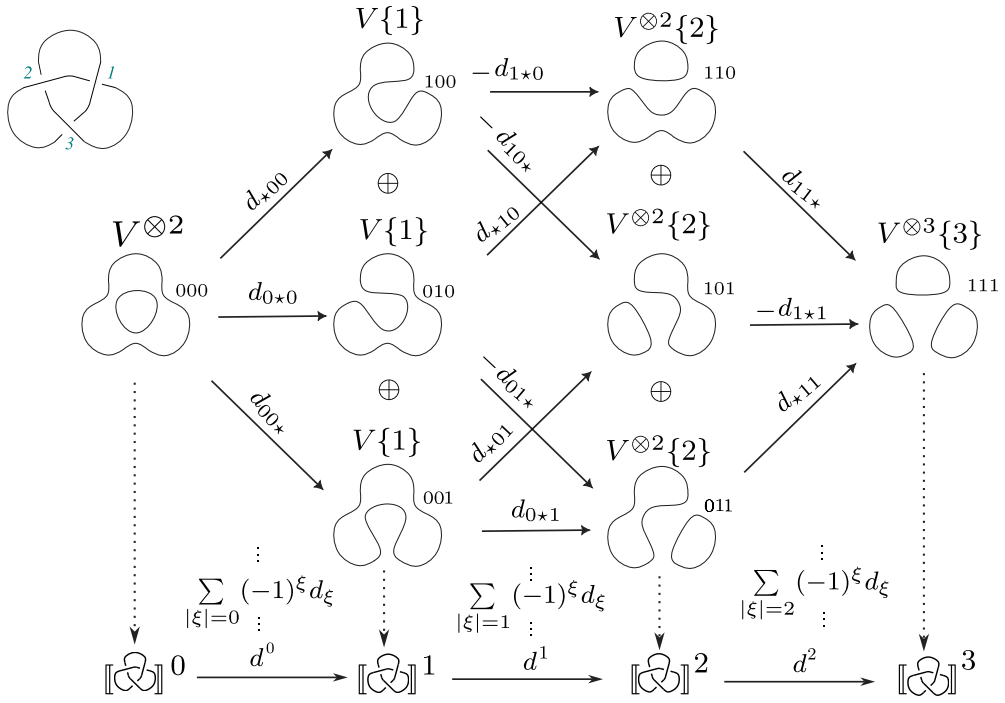

Figure 3.2: *The complex $\mathcal{C}(\mathcal{D})$ of the right-handed trefoil knot with the relative differentials d^i.*

originates.

Since each chain group $\mathcal{C}^r(D)$ is defined as the direct sum of the vector spaces associated with states of height r, we define the total *differential* $d^r : \mathcal{C}^r(D) \to \mathcal{C}^{r+1}(D)$ as the signed sum of all edge maps d_ξ:

$$d^r := \sum_{|\xi|=r} (-1)^\xi d_\xi,$$

where the sign is determined by $(-1)^\xi := (-1)^{\sum_{i<j_\star} \xi_i}$ and $j_\star$ denotes the position of $\star$in the tuple associated with ξ.

The specific assignment of the signs $(-1)^\xi$ is designed to satisfy the chain complex condition $d \circ d = 0$. In the context of the n-dimensional cube, this is equivalent to ensuring that every 2-dimensional square face anticommutes. Under the assumption that the component edge maps d_ξ commute, the introduction of the sign $(-1)^\xi$ ensures the necessary anticommutativity.

To demonstrate this, consider a generic square face of the cube involving the smoothing of two crossings at indices i and j, with $i < j$, as the one in Figure 3.3. Let the initial vertex be $s_{0,0}$, where the i-th and j-th entries are both 0. We define define $m = \sum_{k=1,\dots,i-1} s_k$ as the number of 1-smoothings preceding index i in $s_{0,0}$

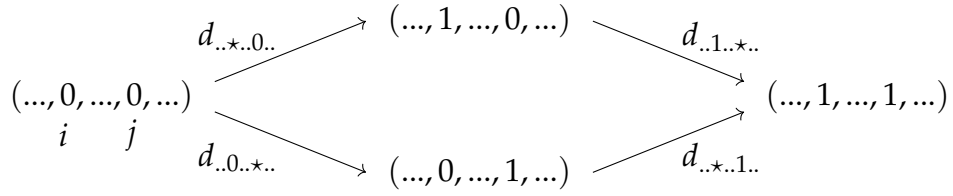

Figure 3.3: *A face of the n- cube.*

and $l = \sum_{k=i+1,..,j-1} s_k$ as the number of 1-smoothings between indices i and j in it. The edges of the square correspond to the following maps:

$$d_{\xi_1} = d_{..\star..0..} : s_{0,0} \longrightarrow s_{1,0},$$

$$d_{\xi_3} = d_{..0..\star..} : s_{0,0} \longrightarrow s_{0,1},$$

$$d_{\xi_4} = d_{..\star..1..} : s_{0,1} \longrightarrow s_{1,1},$$

$$d_{\xi_2} = d_{..1..\star..} : s_{1,0} \longrightarrow s_{1,1}.$$

Assuming that the maps d_ξ commute

$$d_{\xi_2} \circ d_{\xi_1} = d_{\xi_4} \circ d_{\xi_3},$$

we show that the sign convention induces anticommutativity. The product of the signs along the two paths is: $(-1)^{\xi_1}(-1)^{\xi_2} = (-1)^m(-1)^{m+1+l} = (-1)(-1)^{m+l}(-1)^m = -(-1)^{\xi_3}(-1)^{\xi_4}$. This confirms that the square anticommutes, ensuring that $d^{r+1} \circ d^r = 0$.

It remains to define the maps d_ξ so that they have degree 0 and make the cube commute. When changing the smoothing, two possibilities can occur: either two cycles merge into one, or a single cycle splits into two.

For each ξ we define d_ξ to act as the identity on the tensor factor corresponding to the cycles that are unchanged by the smoothing; and we complete the definition by defining two linear maps corresponding to the local change of the smoothing; $m : V \otimes V \longrightarrow V$ and $\Delta : V \longrightarrow V \otimes V$ defined as follows:

$(V \otimes V \xrightarrow{m} V)$ $\quad m : \begin{cases} v_+ \otimes v_- \mapsto v_- & v_+ \otimes v_+ \mapsto v_+ \\ v_- \otimes v_+ \mapsto v_- & v_- \otimes v_- \mapsto 0 \end{cases}$

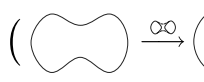

$(V \xrightarrow{\Delta} V \otimes V)$ $\quad \Delta : \begin{cases} v_+ \mapsto v_+ \otimes v_- + v_- \otimes v_+ \\ v_- \mapsto v_- \otimes v_- \end{cases}$

This definition of $d_{\tilde{\zeta}}$ is determined by the requirement of having degree 0 together with the grading shifts induced in the definition of V_s. Since the homological degree increases by one along each edge of the cube, the maps m and Δ must be of degree -1 to ensure that overall differential preserving grading. Furthermore, there is no canonical ordering of the circles in a resolution S_s, and hence no natural ordering of the tensor factor in V_s. As a result, m and Δ must be *commutative* and *co-commutative*. For instance, this justifies the choice $m(v_+ \otimes v_-) = m(v_- \otimes v_+)$.

Remark 3.11. The $d_{\tilde{\zeta}}$ maps have quantum degree 0, in the sense that the maps send vectors with quantum degree j in vectors with quantum degree j.

Definition 3.12. We define the chain complex with homological degree i and quantum degree j as the subgroup of $\mathcal{C}(D)^i$ which elements have quantum degree j.

$$\mathcal{C}(D)^{i,j} = \{v \in \mathcal{C}(D)^i : qdeg(v) = j\}.$$

We are finally able to announce the following theorem.

Theorem 3.13. *The sequence of chain complexes $\mathcal{C}(D)^r$ endowed with the differential d^r is a chain complex such that its Euler characteristic is equal to the unnormalised Jones polynomial.*

Proof. The proof is in the construction of the chain complex $\mathcal{C}(D)$ and of Theorem 3.3 and Theorem 3.7. □

Definition 3.14 (Khovanov complex). Let D be the diagram of an oriented link. The chain complex defined before $\mathcal{C}(D)$ is the *Khovanov complex* of D.

Remark 3.15. The Khovanov complex is not an invariant of knots, in fact, it strictly depends on the chosen diagram.

Example 3.16. Let us construct the Khovanov complex of the unknot with diagrams ◯ and ◇◇ :

The diagram ◯ has no crossings, hence a single state consisting of one circle. This yields the chain complex:

$$\mathcal{C}(\bigcirc) : \ 0 \longrightarrow (\llbracket \bigcirc \rrbracket^0 = V) \longrightarrow 0.$$

The diagram ◇◇, independently from the chosen orientation has one negative crossing ($n_=1$ and $n_+ = 0$). The cube of resolutions is one-dimensional, with two states:

- 0-**smoothing** (height $r = 0$): Resolving the crossing with a 0-smoothing produces a single circle, so $k(s_0) = 1$. The associated graded vector space is

$$[\![\bigcirc\bigcirc]\!]^0 = V,$$

with homological grading $i = 0$ and quantum grading

$$j = n_+ - n_- + 2r - k = 0 - 1 + 2(0) - 1 = -1.$$

- 1-**smoothing** (height $r = 1$): Resolving the crossing with a 1-smoothing produces a diagram with two disjoint circles, so $k(s_1) = 2$. The associated graded vector space is:

$$[\![\bigcirc\bigcirc]\!]^1 = V^{\otimes 2},$$

with homological grading $i = 1$ and quantum grading

$$j = n_+ - n_- + 2r - k = 0 - 1 + 2(1) - 2 = -1.$$

Applying the quantum shift $\cdot\{n_+ - 2n_-\} = \cdot\{-2\}$ and the homological shift $\cdot[-n_-] = \cdot[-1]$ and introducing the differential d we get the following chain complex:

$$\mathcal{C}(\bigcirc\bigcirc) : \ 0 \longrightarrow ([\![\bigcirc\bigcirc]\!]^{-1} = V\{-2\}) \xrightarrow{\Delta} ([\![\bigcirc\bigcirc]\!]^0 = V^{\otimes 2}\{-1\}) \longrightarrow 0$$

3.1.3 Homology

Definition 3.17 (Khovanov homology). Let L be a link and D one of its diagrams. We define the *Khovanov homology* of D, $\mathcal{H}(D)$, as the (co)homology of the Khovanov complex $\mathcal{C}(D)$.

Let now $\mathcal{H}^r(D) = \frac{Ker(d^r)}{Im(d^{r-1})}$ be the r^{th} (co)homology of $\mathcal{C}(D)$. It is a graded vector space depending on D. Similarly, let $\mathcal{H}^{i,j}(D)$ be the subspace of $\mathcal{H}^i(D)$ whose elements have all quantum degree j.

The Khovanov homology of a link L is conventionally represented as a two-dimensional grid, called the *Khovanov homology table*, reflecting the bigraded nature of the theory. In this representation, the horizontal axis corresponds to the homological grading i, while the vertical axis corresponds to the quantum grading j.

In the resulting table, each cell (i, j) displays the group $\mathcal{H}^{i,j}(L)$. The power of this visualization lies in its relation to the Jones polynomial: the graded Euler

characteristic of the table, calculated as the alternating sum of the ranks across the columns weighted by the quantum grading q^j, recovers the original polynomial invariant.

Example 3.18. We compute the Khovanov homology of the unknot:

$$0 \longrightarrow ([\![\bigcirc]\!]^0 = V) \longrightarrow 0$$

Since all differentials are zero maps, we get $\mathcal{H}^0(\bigcirc) = \frac{Ker(d^0)}{Im(d^{-1})} = Ker(d^0) = V \simeq \mathbb{Z} \otimes \mathbb{Z}$, with generators v^+ and v^- which have degree 1 and -1, hence the Khovanov homology of the unknot is:

$$\mathcal{H}^{i,j}(\bigcirc) = \mathbb{Z} \quad if\ (i,j) = (0, \pm 1) \qquad\qquad 0 \text{ otherwise.}$$

Hence the Khovanov homoloy table of the unknot is:

j \ i	0
1	$\mathbb{Z}$
-1	$\mathbb{Z}$

To provide the necessary framework for Section 3.4, we now introduce several fundamental definitions following Viro's approach [Vir04].

Definition 3.19 (Enhanced Kauffman state). A state s associate with a choice of a plus or a minus in each connected components is called an *enhanced Kauffman state* and is denoted by S. We denote the set of all enhanced states associated with s as $S(D_s)$.

Example 3.20. Let D be a diagram of a knot, and $s \in s(D)$ one of its states with k components. To each circle of s we can choose a $+$ or a $-$, therefore, as we can see in the figure below, we have 2^k enhanced states coming form s.

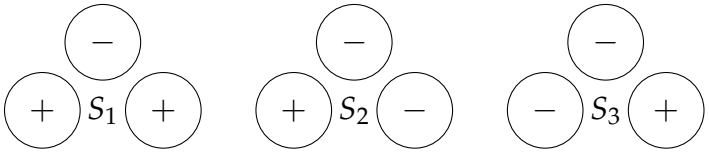

Remark 3.21. There exists a natural bijection between the enhanced states associated with a state s and the canonical basis of the graded vector space $V_s(D) := V^{\otimes k(s)}\{r\}$. Given that V is spanned by the basis $\{v^+, v^-\}$, the canonical basis for the tensor power $V^{\otimes k(s)}$ consists of all possible $k(s)$-tuples of these vectors.

We formally define the bijection ρ as follows:

$$\begin{aligned}\rho : V_s(D) &\longrightarrow \mathcal{S}(D_s)\\ v^{\epsilon_1} \otimes \cdots \otimes v^{\epsilon_{k(s)}} &\longmapsto (\epsilon_1, \epsilon_2, \ldots, \epsilon_{k(s)}),\end{aligned}$$

where $\epsilon_i \in \{+, -\}$ for each $i \in \{1, \ldots, k(s)\}$.

Under this map, each basis element is identified with an enhanced Kauffman state, where a choice of label ($+$ or $-$) is assigned to each of the $k(s)$ disjoint circles in the resolution D_s. To ensure this bijection is well-defined, the ordering of the tensor factors must be fixed consistently with the ordering of the circles in D_s. Specifically, the i-th vector in the tensor product corresponds to the label assigned to the i-th circle of the smoothed diagram.

Example 3.22. Applying the bijection τ to the enhanced states introduced in Example 3.20, we identify each state with an element of the canonical basis of $V^{\otimes 3}$. By ordering the circles as indicated in the figure below, where labels $1, 2$, and 3 correspond to the first, second, and third tensor factors respectively, we obtain the following mappings: $S_1 \mapsto (v^+ \otimes v^- \otimes v^+)$, $S_2 \mapsto (v^+ \otimes v^- \otimes v^-)$ and $S_3 \mapsto (v^- \otimes v^- \otimes v^+)$.

This correspondence is visualized below for the state S_1, illustrating how the assignment of signs to the disjoint circles determines the specific basis vector in the graded vector space:

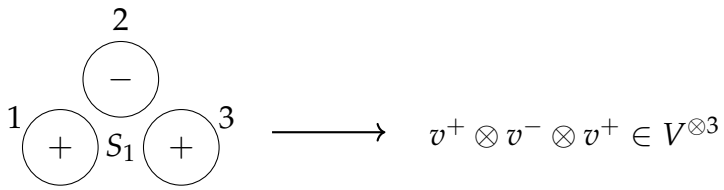

Definition 3.23 (Graded Poincaré polynomial). Given a diagram D of a knot, we can define the *graded Poincaré polynomial* $Kh(D)$ of the Khovanov complex $\mathcal{C}(D)$ in the variable t as:

$$Kh(D) := \sum_r t^r q\dim \mathcal{H}^r(D).$$

Finally, we are able to state the main theorem of this chapter.

Theorem 3.24 (Khovanov Theorem)**.** *The graded dimensions of the homology groups $\mathcal{H}^r(D)$ are link invariants and, therefore $Kh(D)$, a polynomial in the variable t and q, is a link invariant that specializes the unnormalized Jones polynomial in $t = -1$.*

Proof. For the first part of the theorem, we proved in Theorem 3.7 that the graded Euler characteristic is equal to the unormalized Jones q-polynomial. Hence, being the unormalized Jones q-polynomial a link invariant, it follows that the dimensions of the homology groups $\mathcal{H}^r(D)$ are link invariants.

The second part will be proved in the following section. □

Before proceeding, we observe that Khovanov homology is a finer invariant for knots than Jones polynomial. Let us see some known examples:

Example 3.25. A known example of a pair of knots with same Jones polynomial but different Khovanov homology are the knots 5_1 and 10_{132} of Rolfsen knot table [Rol76].

Figure 3.4: *The Rolfsen diagrams of* 5_1 *on the left and of* 10_{132} *on the right [Rol76].*

Their Jones polynomials are

$$J_{5_1}(q) = J_{10_{132}}(q) = -q^{-7} + q^{-6} - q^{-5} + q^{-4} + q^{-2}.$$

The Khovanov homology table of the two knots, taken from [BM+05], are shown in Figure 3.5:

As illustrated by the two Khovanov homology tables, the knots under consideration have different homology groups. Consequently, they are not equivalent, even though they share the same Jones polynomial. Another notable example is the knot 9_{42}; Khovanov homology detects that it is distinct from its mirror image, demonstrating the enhanced discriminatory power of this homological invariant compared to the Jones polynomial alone.

However, it is not a complete invariant; in fact, L. Watson proved in Theorem 6.2 of [Wat07] that there exists an infinite family of distinct knots with identical Khovanov homology.

Moreover, P.B. Krohemer and T.S. Krowka in [KM11], were able to prove the following result:

j \ i	-5	-4	-3	-2	-1	0
-3						$\mathbb{Z}$
-5						$\mathbb{Z}$
-7				$\mathbb{Z}$		
-9						
-11		$\mathbb{Z}$	$\mathbb{Z}$			
-13						
-15	$\mathbb{Z}$					

j \ i	-7	-6	-5	-4	-3	-2	-1	0
-1							$\mathbb{Z}$	$\mathbb{Z}$
-3								$\mathbb{Z}$
-5					$\mathbb{Z}$	$\mathbb{Z}^2$		
-7				$\mathbb{Z}$				
-9				$\mathbb{Z}$	$\mathbb{Z}$			
-11		$\mathbb{Z}$	$\mathbb{Z}$					
-13								
-15	$\mathbb{Z}$							

Figure 3.5: *The Khovanov homology table of 5_1 (on the left) and 10_{132} (on the right). In blue the groups that get canceled when computing the Euler characteristic to give rise to the Jones polynomial.*

Theorem 3.26. *[KM11] The Khovanov homology is an unknot detector, i.e., if a diagram D of a knot has the same Khovanov homology as the unknot, the the diagram is a diagram of the unknot.*

3.2 Invariance

To prove Theorem 3.24 we need to understand the behavior of $[\![D]\!]$ under the three Reidemeister moves. In this section, we demonstrate the invariance under $R1$ and $R2$ for Khovanov homology, following the proofs established by Bar-Natan in [Bar02]. Invariance of type $R3$ can be found in [Bar02] or in [Kho00]. Furthermore, for those interested in a more geometric perspective, an articulate proof of invariance can be found in [Bar05], where Bar-Natan use cobordisms and a special category to construct an invariant for tangles which can be related to Khovanov homology via functor (see Section 3.5 to get an idea of it).

Before starting, let us see some useful properties of complexes and homology (see Appendix 5.2) that will be practical to use in our proof.

Lemma 3.27. *Let $\mathcal{C}$ be a chain complex and $\mathcal{C}' \subseteq \mathcal{C}$ be one of its subchain complexes; then:*

- *If $\mathcal{C}'$ is acyclic, i.e., it has no homology, then the homology $\mathcal{H}(\mathcal{C})$ of $\mathcal{C}$ is equal to the homology $\mathcal{H}(\mathcal{C}/\mathcal{C}')$ of $\mathcal{C}/\mathcal{C}'$.*

- *If $\mathcal{C}/\mathcal{C}'$ is acyclic, then $\mathcal{H}(\mathcal{C}) = \mathcal{H}(\mathcal{C}')$.*

Proof. Consider the following sequence:

$$0 \longrightarrow \mathcal{C}' \xrightarrow{i} \mathcal{C} \xrightarrow{q} \mathcal{C}/\mathcal{C}' \longrightarrow 0$$

where i is the inclusion map and q is the quotient map. From how it is built, this sequence is exact and hence it gives rise to the long exact sequence in homology:

$$\cdots \longrightarrow \mathcal{H}^r(\mathcal{C}') \xrightarrow{i_*} \mathcal{H}^r(\mathcal{C}) \xrightarrow{q_*} \mathcal{H}^r(\mathcal{C}/\mathcal{C}') \longrightarrow \mathcal{H}^{r+1}(\mathcal{C}') \longrightarrow \cdots.$$

- If $\mathcal{C}'$ is acyclic, then $\mathcal{H}^r(\mathcal{C}')$ is trivial $\forall\, r \in \mathbb{Z}$, therefore, q_* is an isomorphism between $\mathcal{H}^r(\mathcal{C})$ and $\mathcal{H}^r(\mathcal{C}/\mathcal{C}')$.
- If $\mathcal{C}/\mathcal{C}'$ is acyclic, then $\mathcal{H}^r(\mathcal{C}/\mathcal{C}')$ is trivial $\forall\, r \in \mathbb{Z}$, therefore, i_* is an isomorphism between $\mathcal{H}^r(\mathcal{C}')$ and $\mathcal{H}^r(\mathcal{C})$.

□

3.2.1 R1 invariance

Let us denote  the diagram of our knot with the crossing appearing in numbered as the last crossing and  the diagram of the knot without that crossing. We need to check that $\mathcal{H}($ $) = \mathcal{H}($ $)$. When computing $\mathcal{H}($ $)$ we look at the complex:

$$\mathcal{C} = [\![\text{}]\!] = ([\![\text{}]\!] \xrightarrow{m} [\![\text{}]\!]\{1\}). \tag{3.1}$$

With this notation, we mean that the complex $[\![$ $]\!]$ is the direct sum of the two complexes $[\![$ $]\!]$ (the complex with a 0 resolution on the last crossing) and $[\![$ $]\!]\{1\}$ (the complex with a 1 resolution on the last crossing) with the addition of the maps $m = d_{\dots\star}$ from the first complex to the second one. We define $[\![$ $]\!]_{v^+}$ as the subcomlpex of $[\![$ $]\!]$ associating v^+ to the "special circle". (If we consider $[\![$ $]\!] \cong [\![$ $]\!] \otimes V$ then $[\![$ $]\!]_{v^+}$ can be seen as $[\![$ $]\!] \otimes < v^+ >$.) The complex $\mathcal{C}$ in (3.1) has as a subcomplex

$$\mathcal{C}' = ([\![\text{}]\!]_{v^+} \xrightarrow{m} [\![\text{}]\!]\{1\}). \tag{3.2}$$

Since v^+ acts as a unit($m(v^\pm \otimes v^+) = m(v^+ \otimes v^\pm) = v^\pm$), $\mathcal{C}'$ is acyclic. Thus, for Lemma 3.27 we need to study the quotient

$$\mathcal{C}/\mathcal{C}' = ([\![\text{}]\!]_{/v^+=0} \xrightarrow{m} 0),$$

where "$v^+ = 0$" means mod out by $v^+ = 0$ in the last circle. But $V_{/v^+=0} =< v^- >$ hence - if we do not consider the shift degree - $[\![\bigcirc]\!]_{/v^+=0}$ is isomorphic to $[\![\; | \;]\!]$. We notice that $[\![\; | \;]\!]\{1\}$ has a positive crossing less than $[\![\bigcirc]\!]_{/v^+=0}$ and therefore the degree shift $\cdot\{1\}$ is well balanced by the shift $\cdot[-n_-]\{n_+ - 2n_-\}$ in the definition of $\mathcal{C}(D)$.

3.2.2 R2 invariance

When studying $\mathcal{H}($  $)$ we need to study the complex $\mathcal{C}$ as a direct sum of the complexes $[\![$  $]\!]$, $[\![$  $]\!]\{1\}$, $[\![$  $]\!]\{1\}$ and $[\![$  $]\!]\{2\}$ with the corresponding connecting differentials as in Figure 3.6. This complex has a subcomplex $\mathcal{C}'$ as in Figure 3.6 (we use the same notation used in the proof of the invariance under $R1$). As before, since v^+ acts as a unit for m, m is an isomorphism between $[\![$  $]\!]\{1\}_{/v^+}$ and $[\![$  $]\!]\{2\}$, hence $\mathcal{C}'$ is acyclic.

Figure 3.6: *The complex $\mathcal{C}$ and its acyclic subcomplex $\mathcal{C}'$.*

For Lemma 3.27 $\mathcal{H}(\mathcal{C}) = \mathcal{H}(\mathcal{C}/\mathcal{C}')$, so we can study the quotient $\mathcal{C}/\mathcal{C}'$, which, as well, has a subcomplex we get $\mathcal{C}''$ as shown in Figure 3.7.

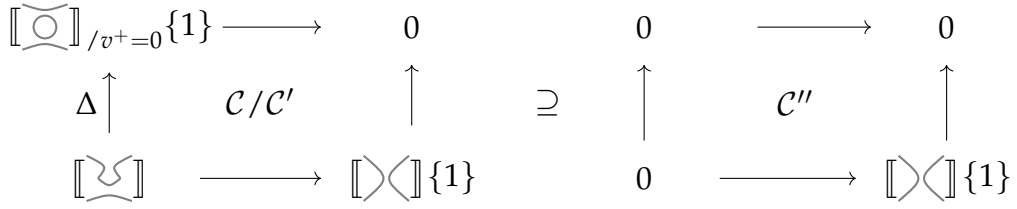

Figure 3.7: *The quotient $\mathcal{C}/\mathcal{C}'$ and its subcomplex $\mathcal{C}''$.*

We observe that the quotient $(\mathcal{C}/\mathcal{C}')/\mathcal{C}''$, shown in Figure 3.8, is acyclic because the map $\Delta : [\![$  $]\!] \longrightarrow [\![$  $]\!]_{/v^+=0}\{1\}$ is an isomorphism.

Applying both statements of Lemma 3.27, we establish that:

$$\mathcal{H}(\mathcal{C}) \cong \mathcal{H}(\mathcal{C}/\mathcal{C}') \cong \mathcal{H}(\mathcal{C}'').$$

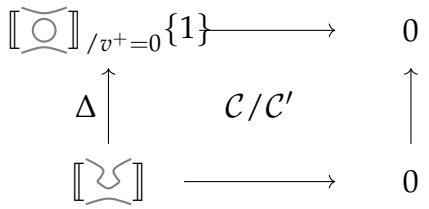

Figure 3.8: *The quotient* $(\mathcal{C}/\mathcal{C}')/\mathcal{C}''$

However, up to homological and quantum shift, $\mathcal{C}''$ is isomorph to the complex $[\![\rangle\langle]\!]$.

To show that the invariance under $R2$, we must verify that the total shifts cancel out. Recall that the normalized Khovanov complex $\mathcal{C}(L)$ for a link L is defined by:

$$\mathcal{C}(L) = [\![D]\!][-n_-]\{n_+ - 2n_-\}$$

where n_+ and n_- denote the number of positive and negative crossings in the diagram D. Let n_+ and n_- be the numbers of positive and negative crossings, respectively, for the diagram $\rangle\langle$. The diagram $\rangle\!\langle$ introduces exactly one additional positive crossing and one additional negative crossing. Thus, the shifted complex for $\rangle\!\langle$ is:

$$\mathcal{C}(\rangle\!\langle) = [\![\rangle\!\langle]\!][-(n_-+1)]\{(n_++1)-2(n_-+1)\} = [\![\rangle\!\langle]\!][-n_--1]\{n_+-2n_--1\}.$$

Our algebraic reduction identifies $[\![\rangle\!\langle]\!]$ with $[\![\rangle\langle]\!][1]\{1\}$ (accounting for the internal shifts in $\mathcal{C}''$). Substituting this into the equation above, we find:

$$\mathcal{C}(\rangle\!\langle) \cong ([\![\rangle\langle]\!][1]\{1\})[-n_- - 1]\{n_+ - 2n_- - 1\}$$

$$\mathcal{C}(\rangle\!\langle) \cong [\![\rangle\langle]\!][-n_-]\{n_+ - 2n_-\} = \mathcal{C}(\rangle\langle).$$

This confirms that the total shifts are perfectly balanced, resulting in the desired isomorphism in homology.

3.3 Examples

In this section, we transition from the abstract algebraic definition of Khovanov homology to explicit computations for two fundamental examples: the Hopf link and the right-handed trefoil knot (3_1). Utilizing the diagrammatic framework established by Bar Natan [Bar02] and detailed in Chapter 3, we provide a concrete demonstration of the construction of the Khovanov chain complex $\mathcal{C}(L)$

from a planar link diagram D. A central aim of these examples is to elucidate the role of Khovanov homology as the categorification of the Jones polynomial $J_L(q)$.

By calculating the homology groups $\mathcal{H}^{i,j}(L)$, we will explicitly show how the Jones polynomial is recovered as the graded Euler characteristic of the complex:

$$J_L(q) = \sum_i (-1)^i q dim(\mathcal{H}^i(L)).$$

Furthermore, these case studies will illustrate the mechanical application of the smoothing rules, where the merging and splitting of circles in the resolution diagram correspond directly to the multiplication and comultiplication operations.

Khovanov homology of the right handed trefoil knot

Example 3.28. We compute the Khovanov homology of the right-handed trefoil knot 3_1 explicitly, working over $\mathbb{Z}$. This extended example illustrates all steps of the construction: building the cube of resolutions, constructing the chain complex, computing the differentials, and extracting the homology groups.

The Cube of Resolutions

Consider the standard diagram D of the right-handed trefoil knot with three positive crossings, labeled $1, 2, 3$ as shown in Figure 3.9:

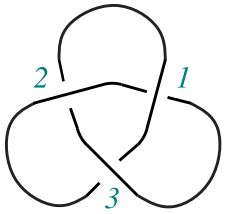

Figure 3.9: *The right-handed trefoil knot standard diagram with labeled crossings.*

Since D has $n = 3$ crossings, the cube of resolutions has $2^3 = 8$ vertices, corresponding to all possible ways of resolving the three crossings. Each state $s \in \{0,1\}^3$ is assigned a vector space

$$V_s = V^{\otimes k(s)}\{r(s)\}[r(s)],$$

where $k(s)$ is the number of circles in the resolved diagram D_s and $r(s) = |s|$ is the height (number of 1-smoothings). The cube of chain complexes is illustrated in Figure 3.10.

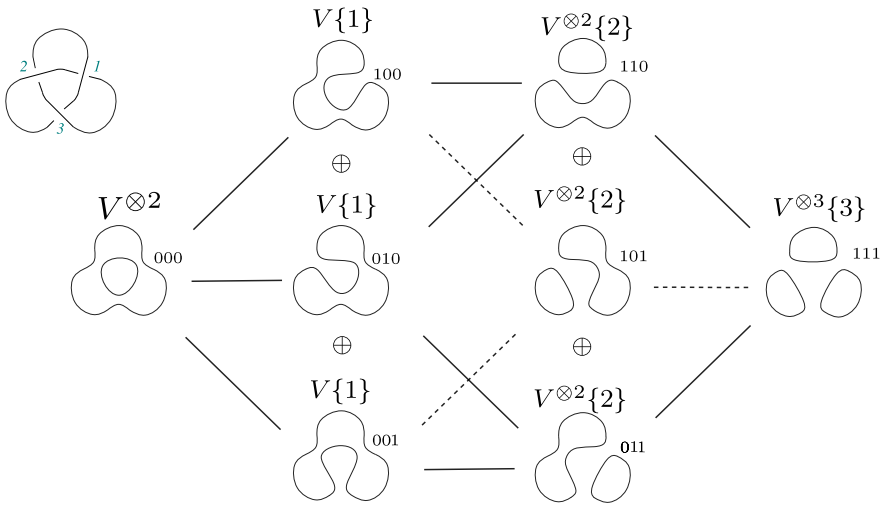

Figure 3.10: *The cube of resolutions for the right-handed trefoil knot.*

To specify the differentials explicitly, we adopt the labeling convention of Bar-Natan [Bar02]. Starting from crossing 1, we label each edge from 1 to n, with the numbering increasing as we traverse crossings in a counterclockwise direction. Each circle in a resolution is then labeled by the minimum edge number it contains. See Figure 3.11.

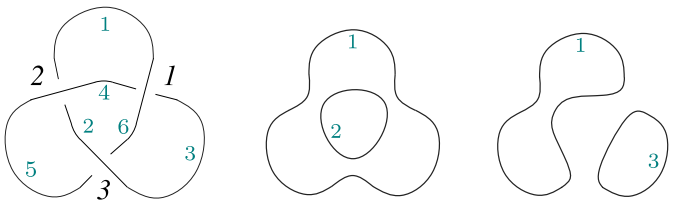

Figure 3.11: *Edge and circle labeling for the trefoil knot.*

The Chain Complex

Since $(n_+, n_-) = (3, 0)$, and $[\![D]\!] = (V^{\otimes 2}; (V \oplus V \oplus V)\{1\}; (V^{\otimes 2} \oplus V^{\otimes 2} \oplus V^{\otimes 2})\{2\}; V^{\otimes 3}\{3\})$, the Khovanov complex is

$$\mathcal{C}(D) = [\![D]\!][0]\{3\} = (V^{\otimes 2}\{3\}; (V \oplus V \oplus V)\{4\}; (V^{\otimes 2} \oplus V^{\otimes 2} \oplus V^{\otimes 2})\{5\}; V^{\otimes 3}\{6\}).$$

We now describe explicit bases for each chain group and compute the differentials. For a visual representation of the cube of resolutions and the structure of the differentials, see Figure 3.12.

For $[\![D]\!]^0 = (V_1 \otimes V_2)\{0\}$, there are 4 generators, all of them with homological degree $i = 0$:

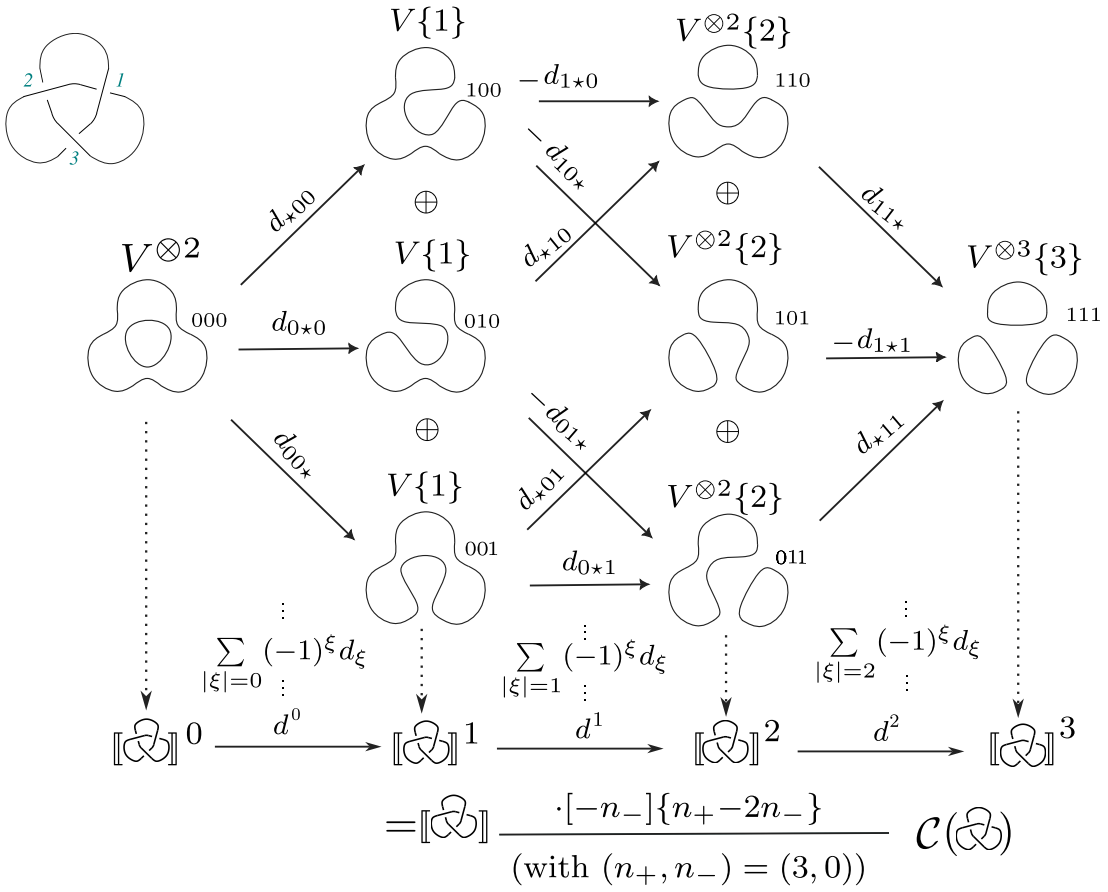

Figure 3.12: *Right-handed trefoil Chain complex*

$$
\begin{aligned}
e_1^0 &= v^+ \otimes v^+ \quad \textit{of degree } 2.\\
e_2^0 &= v^+ \otimes v^- \quad \textit{of degree } 0.\\
e_3^0 &= v^- \otimes v^+ \quad \textit{of degree } 0.\\
e_4^0 &= v^- \otimes v^- \quad \textit{of degree } -2.
\end{aligned}
$$

For $[\![D]\!]^1 = (V_1 \oplus V_1 \oplus V_1)\{1\}$, there are 6 generators, all of them with homological degree $i = 1$:

$$
\begin{aligned}
e_1^1 &= (v^+,0,0) \quad \textit{of degree } 1+i=2.\\
e_2^1 &= (v^-,0,0) \quad \textit{of degree } -1+i=0.\\
e_3^1 &= (0,v^+,0) \quad \textit{of degree } 1+i=2.\\
e_4^1 &= (0,v^-,0) \quad \textit{of degree } -1+i=0.\\
e_5^1 &= (0,0,v^+) \quad \textit{of degree } 1+i=2.\\
e_6^1 &= (0,0,v^-) \quad \textit{of degree } -1+i=0.
\end{aligned}
$$

For $[\![\infty]\!]^2 = ((V_1 \otimes V_2) \oplus (V_2 \otimes V_1) \oplus (V_1 \otimes V_3))\{2\}$, there are 12 generators all with homological degree $i = 2$:

$$
\begin{aligned}
e_1^2 &= (v^+ \otimes v^+, 0, 0) \quad \textit{of degree } 2 + i = 4.\\
e_2^2 &= (v^+ \otimes v^-, 0, 0) \quad \textit{of degree } 0 + i = 2.\\
e_3^2 &= (v^- \otimes v^+, 0, 0) \quad \textit{of degree } 0 + i = 2.\\
e_4^2 &= (v^- \otimes v^-, 0, 0) \quad \textit{of degree } -2 + i = 0.\\
e_5^2 &= (0, v^+ \otimes v^+, 0) \quad \textit{of degree } 2 + i = 4.\\
e_6^2 &= (0, v^+ \otimes v^-, 0) \quad \textit{of degree } 0 + i = 2.\\
e_7^2 &= (0, v^- \otimes v^+, 0) \quad \textit{of degree } 0 + i = 2.\\
e_8^2 &= (0, v^- \otimes v^-, 0) \quad \textit{of degree } -2 + i = 0.\\
e_9^2 &= (0, 0, v^+ \otimes v^+) \quad \textit{of degree } 2 + i = 4.\\
e_{10}^2 &= (0, 0, v^+ \otimes v^-) \quad \textit{of degree } 0 + i = 2.\\
e_{11}^2 &= (0, 0, v^- \otimes v^+) \quad \textit{of degree } 0 + i = 2.\\
e_{12}^2 &= (0, 0, v^- \otimes v^-) \quad \textit{of degree } -2 + i = 0.
\end{aligned}
$$

For $[\![\infty]\!]^3 = (V_1 \otimes V_2 \otimes V_3)\{3\}$, there are 8 generators all with homological degree $i = 3$:

$$
\begin{aligned}
e_1^3 &= v^+ \otimes v^+ \otimes v^+ \quad \textit{of degree } 3 + i = 6.\\
e_2^3 &= v^+ \otimes v^+ \otimes v^- \quad \textit{of degree } 1 + i = 4.\\
e_3^3 &= v^+ \otimes v^- \otimes v^+ \quad \textit{of degree } 1 + i = 4.\\
e_4^3 &= v^- \otimes v^+ \otimes v^+ \quad \textit{of degree } 1 + i = 4.\\
e_5^3 &= v^- \otimes v^- \otimes v^+ \quad \textit{of degree } -1 + i = 2.\\
e_6^3 &= v^- \otimes v^+ \otimes v^- \quad \textit{of degree } -1 + i = 2.\\
e_7^3 &= v^+ \otimes v^- \otimes v^- \quad \textit{of degree } -1 + i = 2.\\
e_8^3 &= v^- \otimes v^- \otimes v^- \quad \textit{of degree } -3 + i = 0.
\end{aligned}
$$

The groups $[\![\infty]\!]^r = 0$ for $r \neq 0, 1, 2, 3$.

The differentials

Now, let us understand how the differentials act on these vector spaces, taking into account the definition of these maps $d^r = \sum_{|\tilde{\xi}|=r}(-1)^{\tilde{\xi}} d_{\tilde{\xi}}$.

$$\begin{aligned} d^0 :&(V_1 \otimes V_2)\{0\} \longrightarrow (V_1 \oplus V_1 \oplus V_1)\{1\} \\ &(v_1 \otimes v_2) \quad \longmapsto (m(v_1 \otimes v_2),\, m(v_1 \otimes v_2),\, m(v_1 \otimes v_2)) \end{aligned}$$

The matrix associated with this map $M(d^0)$ is:

$$M(d^0) = \begin{array}{c} \begin{matrix} e_1^0 & e_2^0 & e_3^0 & e_4^0 \end{matrix} \\ \begin{pmatrix} 1 & 0 & 0 & 0 \\ 0 & 1 & 1 & 0 \\ 1 & 0 & 0 & 0 \\ 0 & 1 & 1 & 0 \\ 1 & 0 & 0 & 0 \\ 0 & 1 & 1 & 0 \end{pmatrix} \end{array}$$

The rank of the matrix is two; hence,

$$\begin{aligned} Ker(d^0) &= Span\{e_3^0 - e_2^0,\, e_4^0\} = Span\{v^- \otimes v^+ - v^+ \otimes v^-,\, v^- \otimes v^-\} \\ Im(d^0) &= Span\{e_1^1 + e_3^1 + e_5^1,\, e_2^1 + e_4^1 + e_6^1\} = Span\{(v^+, v^+, v^+),\, (v^-, v^-, v^-)\}. \end{aligned}$$

$$\begin{aligned} d^1 :&(V_1 \oplus V_1 \oplus V_1)\{1\} \longrightarrow ((V_1 \otimes V_2) \oplus (V_1 \otimes V_2) \oplus (V_1 \otimes V_3))\{2\} \\ &(v_1,\, v_2,\, v_3) \quad \longmapsto (-\Delta(v_1) + \Delta(v_2),\, -\Delta(v_1) + \Delta(v_3),\, -\Delta(v_2) + \Delta(v_3)) \end{aligned}$$

The associated matrix $M(d^1)$ is:

$$M(d^1) = \begin{array}{c} \begin{matrix} e_1^1 & e_2^1 & e_3^1 & e_4^1 & e_5^1 & e_6^1 \end{matrix} \\ \begin{pmatrix} 0 & 0 & 0 & 0 & 0 & 0 \\ -1 & 0 & 1 & 0 & 0 & 0 \\ -1 & 0 & 1 & 0 & 0 & 0 \\ 0 & -1 & 0 & 1 & 0 & 0 \\ 0 & 0 & 0 & 0 & 0 & 0 \\ -1 & 0 & 0 & 0 & 1 & 0 \\ -1 & 0 & 0 & 0 & 1 & 0 \\ 0 & -1 & 0 & 0 & 0 & 1 \\ 0 & 0 & 0 & 0 & 0 & 0 \\ 0 & 0 & -1 & 0 & 1 & 0 \\ 0 & 0 & -1 & 0 & 1 & 0 \\ 0 & 0 & 0 & -1 & 0 & 1 \end{pmatrix} \end{array} \rightarrow \begin{array}{c} \begin{matrix} -e_1^1 & -e_2^1 & -e_3^1 - e_1^1 & a & b & c \end{matrix} \\ \begin{pmatrix} 0 & 0 & 0 & 0 & 0 & 0 \\ 1 & 0 & 0 & 0 & 0 & 0 \\ 1 & 0 & 0 & 0 & 0 & 0 \\ 0 & 1 & 0 & 0 & 0 & 0 \\ 0 & 0 & 0 & 0 & 0 & 0 \\ 1 & 0 & 1 & 0 & 0 & 0 \\ 1 & 0 & 1 & 0 & 0 & 0 \\ 0 & 1 & 0 & 1 & 0 & 0 \\ 0 & 0 & 0 & 0 & 0 & 0 \\ 0 & 0 & 1 & 0 & 0 & 0 \\ 0 & 0 & 1 & 0 & 0 & 0 \\ 0 & 0 & 0 & 1 & 0 & 0 \end{pmatrix} \end{array}$$

with $a = -e_4^1 - e_2^1$, $b = e_5^1 + e_1^1 + e_3^1$ and $c = e_6^1 + e_2^1 + e_4^1$.
Hence, we have $rank(A_1(D)) = 4$ and

$$Ker(d^1) = Span\{e_5^1 + e_1^1 + e_3^1,\ e_6^1 + e_2^1 + e_4^1\} = Span\{(v^+, v^+, v^+),\ (v^-, v^-, v^-)\}$$
$$Im(d^1) = Span\{(v^+ \otimes v^- + v^- \otimes v^+,\ v^+ \otimes v^- + v^- \otimes v^+,\ 0), (v^- \otimes v^-,\ v^- \otimes v^-,\ 0),$$
$$(0,\ v^+ \otimes v^- + v^- \otimes v^+,\ v^+ \otimes v^- + v^- \otimes v^+), (0,\ v^- \otimes v^-,\ v^- \otimes v^-)\}.$$

$$d^2 : ((V_1 \otimes V_2) \oplus (V_1 \otimes V_2) \oplus (V_1 \otimes V_3))\{2\} \longrightarrow (V_1 \otimes V_2 \otimes V_3)\{3\}$$
$$(v_{1,1} \otimes v_{1,2},\ v_{2,1} \otimes v_{2,2},\ v_{3,1} \otimes v_{3,3}) \quad \longmapsto \Delta(v_{1,2}) - \Delta(v_{2,1}) + \Delta(v_{3,1})$$

$$M(d^2) = \begin{array}{c} \begin{matrix} e_1^2 & e_2^2 & e_3^2 & e_4^2 & e_5^2 & e_6^2 & e_7^2 & e_8^2 & e_9^2 & e_{10}^2 & e_{11}^2 & e_{12}^2 \end{matrix} \\ \begin{pmatrix} 0 & 0 & 0 & 0 & 0 & 0 & 0 & 0 & 0 & 0 & 0 & 0 \\ 1 & 0 & 0 & 0 & -1 & 0 & 0 & 0 & 0 & 0 & 0 & 0 \\ 1 & 0 & 0 & 0 & 0 & 0 & 0 & 0 & 1 & 0 & 0 & 0 \\ 0 & 0 & 0 & 0 & -1 & 0 & 0 & 0 & 1 & 0 & 0 & 0 \\ 0 & 0 & 1 & 0 & 0 & -1 & 0 & 0 & 0 & 0 & 1 & 0 \\ 0 & 0 & 1 & 0 & 0 & 0 & -1 & 0 & 0 & 1 & 0 & 0 \\ 0 & 1 & 0 & 0 & 0 & -1 & 0 & 0 & 0 & 1 & 0 & 0 \\ 0 & 0 & 0 & 1 & 0 & 0 & 0 & -1 & 0 & 0 & 0 & 1 \end{pmatrix} \end{array}$$

That can be reduced to the matrix:

$$M(d^2) = \begin{array}{c} \begin{matrix} e_1^2 & e_5^2+e_1^2 & e_9^2-e_5^2-e_1^2 & e_{11}^2 & -e_7^2 & e_2^2 & e_4^2 & a & b & c & d & f \end{matrix} \\ \begin{pmatrix} 0 & 0 & 0 & 0 & 0 & 0 & 0 & 0 & 0 & 0 & 0 & 0 \\ 1 & 0 & 0 & 0 & 0 & 0 & 0 & 0 & 0 & 0 & 0 & 0 \\ 1 & 1 & 0 & 0 & 0 & 0 & 0 & 0 & 0 & 0 & 0 & 0 \\ 0 & -1 & 2 & 0 & 0 & 0 & 0 & 0 & 0 & 0 & 0 & 0 \\ 0 & 0 & 0 & 1 & 0 & 0 & 0 & 0 & 0 & 0 & 0 & 0 \\ 0 & 0 & 0 & 0 & 1 & 0 & 0 & 0 & 0 & 0 & 0 & 0 \\ 0 & 0 & 0 & 0 & 0 & 1 & 0 & 0 & 0 & 0 & 0 & 0 \\ 0 & 0 & 0 & 0 & 0 & 0 & 1 & 0 & 0 & 0 & 0 & 0 \end{pmatrix} \end{array}$$

where $a = e_3^2 + e_7^2 - e_{11}^2$, $b = e_6^2 + e_{11}^2 + e_2^2$, $c = e_8^2 + e_4^2$, $d = e_{10}^2 + e_7^2 - e_2^2$ and $f = e_8^2 + e_{12}^2$. Hence,

$$\begin{aligned} Ker(d^2) &= Span\{e_3^2 + e_7^2 - e_{11}^2,\ e_6^2 + e_{11}^2 + e_2^2,\ e_8^2 + e_4^2,\ e_{10}^2 + e_7^2 - e_2^2,\ e_8^2 + e_{12}^2\} \\ &= Span\{(v^- \otimes v^+,\ v^- \otimes v^+,\ -v^- \otimes v^+),\ (v^+ \otimes v^-,\ v^+ \otimes v^-,\ v^- \otimes v^+), \\ &\quad (v^- \otimes v^-,\ v^- \otimes v^-,\ 0), (-v^+ \otimes v^-,\ v^- \otimes v^+,\ v^+ \otimes v^-), (0,\ v^- \otimes v^-,\ -v^- \otimes v^-)\} \\ Im(d^2) &= Span\{v^+ \otimes v^+ \otimes v^- + v^+ \otimes v^- \otimes v^+,\ v^+ \otimes v^- \otimes v^+ - v^- \otimes v^+ \otimes v^+, \\ &\quad 2v^- \otimes v^+ \otimes v^+,\ v^- \otimes v^- \otimes v^+,\ v^- \otimes v^+ \otimes v^-,\ v^+ \otimes v^- \otimes v^-,\ v^- \otimes v^- \otimes v^-\}. \end{aligned}$$

Now, we just need to compute the homology of the Khovanov complex $\mathcal{C}(K)$ of the trefoil knot by shifting the complex $[\![D]\!]$:

$$\mathcal{C}(K) = [\![D]\!][-n_-]\{n_+ - 2n_-\} = [\![D]\!]\{3\}.$$

Recall that the quantum grading of a vector v in homological degree i with internal grading $deg(v)$ is defined as

$$j(v) = deg(v) + r + n_+ - 2n_-,$$

hence for the right-handed trefoil knot we have $j(v) = deg(v) + i + 3$.

$$\mathcal{H}^0(K) = \frac{Ker(d^0)}{Im(d^{-1})} = Ker(d^0) = \langle e_3^0 - e_2^0,\ e_4^0 \rangle \cong \mathbb{Z} \oplus \mathbb{Z}$$

Its generators are $e_3^0 - e_2^0 = v^- \otimes v^+ - v^+ \otimes v^-$ and $e_4^0 = v^- \otimes v^-$ with quantum degree $j(e_3^0 - e_2^0) = 0 + 0 + 3 = 3$ and $j(e_4^0) = -2 + 0 + 3 = 1$.

$$\mathcal{H}^1(K) = \frac{Ker(d^1)}{Im(d^0)} = \frac{< e_5^1 + e_1^1 + e_3^1,\ e_6^1 + e_2^1 + e_4^1 >}{< e_5^1 + e_1^1 + e_3^1,\ e_6^1 + e_2^1 + e_4^1 >} = 0,$$

$$\mathcal{H}^2(\circledS) = \frac{Ker(d^2)}{Im(d^1)} = \frac{< e_3^2 + e_7^2 - e_{11}^2,\ e_6^2 + e_{11}^2 + e_2^2,\ e_8^2 + e_4^2,\ e_{10}^2 + e_7^2 - e_2^2,\ e_8^2 + e_{12}^2 >}{< e_6^2 + e_7^2 + e_{10}^2 + e_{11}^2,\ e_8^2 + e_{12}^2,\ e_2^2 + e_3^2 + e_6^2 + e_7^2,\ e_4^2 + e_8^2 >}$$

$$=< e_3^2 + e_7^2 - e_{11}^2 > \cong \mathbb{Z},$$

Its generator is $e_3^2 + e_7^2 - e_{11}^2 = (v^- \otimes v^+,\ v^- \otimes v^+,\ -v^- \otimes v^+)$ which has quantum degree $j(e_3^2 + e_7^2 - e_{11}^2) = 0 + 2 + 3 = 5$.

$$\mathcal{H}^3(\circledS) = \frac{Ker(d^3)}{Im(d^2)} = \frac{V_1 \otimes V_2 \otimes V_3\{6\}}{< e_2^3 + e_3^3,\ e_3^3 - e_4^3,\ 2e_4^3,\ e_5^3,\ e_6^3,\ e_7^3,\ e_8^3 >} = \frac{< e_1^3,\ e_4^3 >}{< 2e_4^3 >} \cong \mathbb{Z} \oplus \mathbb{Z}_2,$$

The generator $e_1^3 = v^+ \otimes v^+ \otimes v^+$ of $\mathbb{Z}$ has quantum degree $j(e_1^3) = 3+3+3 = 9$ and the one of $\mathbb{Z}_2$ which is $e_4^3 = v^- \otimes v^+ \otimes v^+$ has quantum degree $j(e_4^3) = 1+3+3 = 7$.

The Khovanov table and Jones polynomial

We now present the computed homology in a compact form by arranging the homology groups in a table, which allows the results to be easily visualized. This table is called the Khovanov table of the knot.

j \ i	0	1	2	3
9				$\mathbb{Z}$
7				$\mathbb{Z}_2$
5			$\mathbb{Z}$	
3	$\mathbb{Z}$			
1	$\mathbb{Z}$			

The (unnormalized) Jones polynomial is recovered as the graded Euler characteristic:

$$\hat{J}_{3_1}(q) = \sum_{i,j}(-1)^i q^j \dim \mathcal{H}^{i,j}(3_1) = (-1)^0 q^1 + (-1)^0 q^3 + (-1)^2 q^5 + (-1)^3 q^9$$

$$= q + q^3 + q^5 - q^9,$$

which agrees with the computation in Example 2.25.

Khovanov homology of the Hopf link

Example 3.29. Consider the diagram of the Hopf link with two positive crossings ($n_+ = 2$ and $n_- = 0$) shown in Figure 3.13. We label the crossings as indicated in the figure.

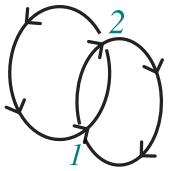

Figure 3.13: *A diagram of the Hopf link with labeled positive crossings.*

We consider the Khovanov complex as in the figure below.

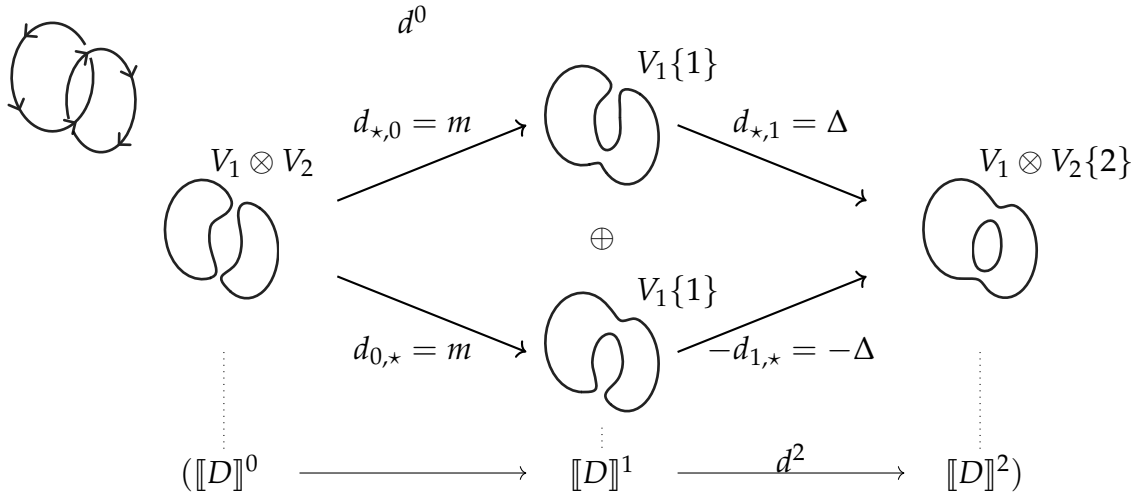

The Khovanov complex is given by

$$\mathcal{C}(D) = [\![D]\!]\{2\}.$$

where the quantum shift $\{n_+ - 2n_-\} = \{2\}$ arises from the crossing data $(n_+, n_-) = (2, 0)$. Having illustrated the general construction in the previous example, we now focus directly on computing the differential maps and their action on basis vectors of the chain groups.

$$\begin{aligned} d^0 : V_1 \otimes V_2 &\longrightarrow V_1 \oplus V_1\{1\} \\ v_1 \otimes v_2 &\longmapsto (m(v_1 \otimes v_2),\, m(v_1 \otimes v_2)) \end{aligned}$$

Hence, if the ordered base of $V_1 \otimes V_2$ and $V_1 \oplus V_2$ are $\{v^+ \otimes v^+, v^+ \otimes v^-, v^- \otimes v^+, v^- \otimes v^-\}$ and $\{(v^+, 0), (0, v+), (v^-, 0), (0, v^-)\}$ respectively; the resulting associated matrix is:

$$M(d^0) = \begin{pmatrix} 1 & 0 & 0 & 0 \\ 1 & 0 & 0 & 0 \\ 0 & 1 & 1 & 0 \\ 0 & 1 & 1 & 0 \end{pmatrix}$$

We deduce that:

$$ker(d^0) = Span\{v^- \otimes v^-, v^+ \otimes v^- - v^- \otimes v^+\},$$

$$Im(d^0) = Span\{(v^+, v^+), (v^-, v^-)\}.$$

Now for d^1 we consider the same ordered base for $V_1 \oplus V_1\{1\}$ and for $V_1 \otimes V_2\{2\}$ the ordered base $\{v^+ \otimes v^+, v^+ \otimes v^-, v^- \otimes v^+, v^- \otimes v^-\}$.

$$\begin{aligned} d^1 : & V_1 \oplus V_1\{1\} \longrightarrow V_1 \otimes V_2\{2\} \\ & (v_1, v_2) \longmapsto \Delta(v_1) - \Delta(v_2) \end{aligned}$$

and its associated matrix is:

$$M(d^1) = \begin{pmatrix} 0 & 0 & 0 & 0 \\ 1 & -1 & 0 & 0 \\ 1 & -1 & 0 & 0 \\ 0 & 0 & 1 & -1 \end{pmatrix}$$

Hence,

$$Ker(d^1) = Span\{(v^+, v^+), (v^-, v^-)\}$$

$$Im(d^1) = Span\{v^- \otimes v^-, v^+ \otimes v^- + v^- \otimes v^+\}$$

We compute the Khovanov homology:

$$\mathcal{H}(D)^0 = Ker(d^0) = Span\{v^- \otimes v^-, v^+ \otimes v^- - v^- \otimes v^+\} \cong \mathbb{Z} \oplus \mathbb{Z}.$$

It is generated by two vectors of quantum degree 0 and 2.

$$\mathcal{H}^1(D) = \frac{Ker(d^1)}{Im(d^0)} = \frac{Span\{(v^+, v^+), (v^-, v^-)\}}{Span\{(v^+, v^+), (v^-, v^-)\}} = 0$$

$$\begin{aligned} \mathcal{H}^2(D) = \frac{V_1 \otimes V_2\{4\}}{Im(d^1)} = \frac{V_1 \otimes V_2\{4\}}{Span\{v^- \otimes v^-, v^+ \otimes v^- + v^- \otimes v^+\}} = \\ = Span\{v^+ \otimes v^+, v^+ \otimes v^-\} \cong \mathbb{Z} \oplus \mathbb{Z} \end{aligned}$$

It's generators have quantum degree 6 and 4. Therefore, its Khovanov homology table is

j \ i	0	1	2
6			$\mathbb{Z}$
4			$\mathbb{Z}$
2	$\mathbb{Z}$		
0	$\mathbb{Z}$		

From it we can easily recover the Jones polynomial of the Hopf link oriented as in the example:

$$(-1)^2 q^0 + (-1)^2 q^2 + (-1)^4 q^4 + (-1)^4 q^6 = 1 + q^2 + q^4 + q^6$$

If we normalize it, we get:

$$J_L(q) = (q + q^{-1})^{-1}(1 + q^2 + q^4 + q^6) = q + q^5.$$

3.4 Framed Khovanov homology and applications

Khovanov homology is a homological refinement of the Jones polynomial, providing a categorification whose graded Euler characteristic recovers the Jones invariant. Constructed from a link diagram via a cube of resolutions, Khovanov homology is invariant under the Reidemeister moves $R1$, $R2$ and $R3$, and therefore defines a powerful invariant of oriented links up to isotopy. Beyond recovering the Jones polynomial, Khovanov homology contains strictly more information, distinguishing links that share the same polynomial invariant.

Framed Khovanov homology, denoted by $\mathcal{H}_{a,b}(D)$, arises by modifying this construction to ignore the orientation of the link and removing the grading shift responsible for invariance under the first Reidemeister move. In this setting, the graded Euler characteristic no longer yields the Jones polynomial but instead recovers the Kauffman bracket. Consequently, framed Khovanov homology may be viewed as a categorification of the Kauffman bracket and defines an invariant of framed, unoriented links. As expected from the framed setting, this theory is invariant under the Reidemeister moves $R2$ and $R3$, but not under $R1$. Moreover, ordinary Khovanov homology can be recovered from its framed counterpart by choosing an orientation of the diagram D, which determines a writhe w, and applying the following relation:

$$\mathcal{H}^{i,j}(D) = \mathcal{H}_{w-2i,3w-2j}(D).$$

An additional advantage of the homological framework is that classical skein relations admit natural categorical analogues. In particular, the skein relation defining the Kauffman bracket is lifted to a long exact sequence in framed Khovanov homology, relating the homology groups associated to a diagram and the diagrams associated to the two local resolutions of a crossing. This exact sequence, defined in detail in Section 3.4.2, plays a central role in computations and highlights the deeper structural insight gained through categorification. In particular, we will use it to compute the homology of the torus knots $T(2,n)$, $n \geq 0$.

3.4.1 Framed Khovanov homology

Framed Khovanov homology was first introduced by Viro in [Vir04], for this reason , in this section we adopt Viro's notation [Vir04] for the homological and quantum grading in Khovanov homology. We make a minor modification to Viro's definition of the quantum grading in order to ensure compatibility with Bar-Natan's definition of the differential.

Notation 3.30. Let s be a state of D and S one of its enhanced Kauffman state defined in 3.19. Let us note:

- $\sigma(s)$ the difference between the number of 0-smoothing and the number of 1-smoothing.
- $\tau(S)$ the difference between the pluses and minuses assigned to D_s.

With this notation, the bijection introduced in Remark 3.21 implies that $\tau(S) = deg(v)$, where v is the counter-image of S through the isomorphism ρ defined in 3.21. Moreover, since $\sigma(s) = (n - r(s)) - r = n - 2r(s)$, with n the number of crossing in D and r the height of s, we obtain $r = \frac{n-\sigma(s)}{2}$. Using these relations, the homological and quantum degrees i and j can be rewritten as follows:

$$\begin{aligned} i(S) =& r - n_- = \frac{n_+ + n_- - \sigma(s) - 2n_-}{2} = \frac{w(D) - \sigma(s)}{2}. \\ j(S) =& deg(v) + r + n_+ - 2n_- = \frac{2\tau(S) + n_+ + n_- - \sigma(s) + 2n_+ - 4n_-}{2} = \\ & - \frac{\sigma(s) - 2\tau(S) - 3w(D)}{2}. \end{aligned}$$

The aim is to define a chain complex and a Khovanov homology for framed unoriented links. For an enhanced Kauffman state S associated to a state s of an unoriented diagram D we define the following gradings:

$$I(S) = \sigma(s) \quad \text{and} \quad J(S) = \sigma(s) - 2\tau(S).$$

When the diagram D is oriented and its writhe $w(D)$ is defined, Equation (3.30) shows that these gradings are related to the usual Khovanov gradings by:

$$I(S) = w(D) - 2i(S) \quad \text{and} \quad J(S) = 3w(D) - 2j(S).$$

We denote as $\mathcal{C}_{a,b}(D)$ the free abelian group generated by the enhanced Kauffman states S of D satisfying $I(S) = a$ and $J(S) = b$. If we choose an orientation for D and denote by $\overrightarrow{D}$ the resulting oriented diagram with writhe w, then the framed and oriented Khovanov chain groups are related by:

$$\mathcal{C}^{i,j}(\overrightarrow{D}) = \mathcal{C}_{w-2i,3w-2j}(D) \qquad \mathcal{C}_{a,b}(D) = \mathcal{C}^{\frac{w-a}{2},\frac{3w-b}{2}}(\overrightarrow{D}). \tag{3.3}$$

Under this identification, $d^i : \mathcal{C}^{i,j}(D) \longrightarrow \mathcal{C}^{i+1,j}$ corresponds to:

$$\partial_{a,b} : \mathcal{C}_{a,b}(D) \longrightarrow \mathcal{C}_{a-2,b}.$$

Since the orientation of the diagram only affects the grading shifts, the complex remains well defined regardless of the orientation. We denote its homological group $\mathcal{H}_{a,b}(D)$ and refer to them as the *framed Khovanon homology group* of D.

Theorem 3.31. *With the previous notation $\partial_{a-2,b} \circ \partial_{a,b} = 0$ and the framed Khovanov homology groups of D:*

$$\mathcal{H}_{a,b} = \frac{Ker\partial_{a,b}}{Im\partial_{a-2,b}}$$

are invariant under R2 and R3, so they are invariants for unoriented framed links.

3.4.2 Khovanov skein sequence

Let D be a diagram of a link L with n crossings, an χ be its set of crossings. Choose one crossing $c \in \chi$, and enumerate all crossings so that c is the last one $\chi = \{c_1, ..., c_{n-1}, c\}$. Let D_0 and D_1 denote the two diagrams obtained by resolving c with a 0 or a 1-smoothing, respectively, as shown in Figure 3.14. As we have seen, these three diagrams satisfy the *Kauffman skein relation*:

$$\langle D \rangle = A\langle D_o \rangle + A^{-1}\langle D_1 \rangle.$$

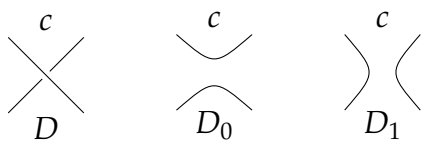

Figure 3.14: *The diagrams D, D_0 and D_1, respectively.*

We want to categorify this skein relation.

To do this, it is convenient to view a state s as a map $s : \chi \longrightarrow \{0,1\}$ assigning to each crossing of D a choice of 0 or 1.

Consider the map $\alpha : \mathcal{C}_{a+1,b+1}(D_1) \longrightarrow \mathcal{C}_{a,b}(D)$ which sends an enhanced Kauffman state S of D_1 to the corresponding enhanced Kauffman state of D in which all smoothings and signs of the circles (i.e., elements in each copy of V in Bar-Natan approach) are preserved.

$$\begin{array}{rccc} \alpha : & \mathcal{C}_{a+1,b+1}(D_1) & \longrightarrow & \mathcal{C}_{a,b}(D) \\ & (s(c_1),...,s(c_{n-1})) & \longmapsto & (s(c_1),...,s(c_{n-1}),1) \end{array}$$

Similarly, we construct the map $\beta : \mathcal{C}_{a,b}(D) \longrightarrow \mathcal{C}_{a-1,b-1}(D_0)$ which maps an enhanced Kauffman state of D with $s(c) = 0$ to the enhanced Kauffman state of D_0, preserving all smoothings of the first $n-1$ crossings and the sings of the circles, and all other states (i.e., those with $s(c) = 1$) to 0.

$$\begin{array}{rccc} \beta : & \mathcal{C}_{a,b}(D) & \longrightarrow & \mathcal{C}_{a-1,b-1}(D_0) \\ & (s(c_1),...,s(c_{n-1}),0) & \longmapsto & (s(c_1),...,s(c_{n-1})) \\ & (s(c_1),...,s(c_{n-1}),1) & \longmapsto & 0 \end{array}$$

The maps α and β are homomorphisms constructed so that

$$Ker(\beta) = \{(s(c_1),...,s(c_{n-1}),1), \ \ with \ \ s(c_i) \in \{0,1\}\} = Im(\alpha),$$

which ensures that they fit into a short exact sequence of complexes:

$$0 \longrightarrow \mathcal{C}_{*+1,*+1}(D_1) \xrightarrow{\alpha} \mathcal{C}_{*,*}(D) \xrightarrow{\beta} \mathcal{C}_{*-1,*-1}(D_0) \longrightarrow 0$$

From this short exact sequence, Viro [Vir04, Section 3.3] obtained a long exact sequence in homology of the form:

$$\cdots \xrightarrow{\partial *} \mathcal{H}_{a+1,b+1}(D_1) \xrightarrow{\alpha_*} \mathcal{H}_{a,b}(D) \xrightarrow{\beta_*} \mathcal{H}_{a-1,b-1}(D_0) \tag{3.4}$$

$$\xrightarrow{\partial_*} \mathcal{H}_{a-1,b+1}(D_1) \xrightarrow{\alpha_*} \mathcal{H}_{a-2,b}(D) \xrightarrow{\beta_*} \mathcal{H}_{a-3,b-1}(D_0) \xrightarrow{\partial_*} \cdots$$

This sequence provides a practical way to compute Khovanov homology of a link: if we can identify a crossing whose smoothings produces two links with known Khovanov homology, the sequence allows us to deduce some facts of the homology of the original link. We will illustrate this with a concrete example in the following subsection.

When passing from framed Khovanov homology to the canonical one, three writhes appear, depending on the chosen orientation of the three diagrams involved in the skein relation. Let us now examine the two possible cases, firstly presented in [Muk+18, Lemma 2.2]:

a) Let D be oriented in such a way that c is positive. Let us call w its writhe. We take the orientation of D_0 that is coherent with the one of D and choose one for D_1 that is equal to the one of D in the components that are not involved in c. We call w_0 and w_1 the relative writhes (see figure 3.15). We observe that $w_0 = w - 1$.

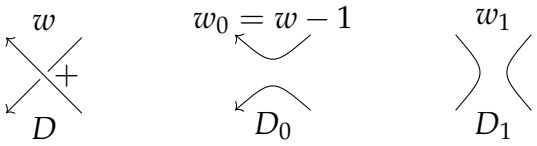

Figure 3.15

With this choice of orientation and the expression (3.4.1), the previous exact sequence:

$$\cdots \xrightarrow{\partial *} \mathcal{H}_{a+1,b+1}(D_1) \xrightarrow{\alpha_*} \mathcal{H}_{a,b}(D) \xrightarrow{\beta_*} \mathcal{H}_{a-1,b-1}(D_0) \xrightarrow{\partial_*} \cdots$$

becomes:

$$\cdots \xrightarrow{\partial *} \mathcal{H}^{\frac{w_1-a-1}{2},\frac{3w_1-b-1}{2}}(D_1) \xrightarrow{\alpha_*} \mathcal{H}^{\frac{w-a}{2},\frac{3w-b}{2}}(D) \xrightarrow{\beta_*} \mathcal{H}^{\frac{w_0-a+1}{2},\frac{3w_0-b+1}{2}}(D_0) \xrightarrow{\partial_*} \cdots$$

We substitute $w_0 = w - 1$ and we set $i = \frac{w-a}{2}$ and $j = \frac{3w-b}{2}$ ($a = w - 2i$ and $b = 3w - 2j$). With this substitution, the first homology group indexes become $\frac{w_1-a-1}{2} = \frac{w_1-w-1}{2} + i$ and $\frac{3w_1-b-1}{2} = \frac{3(w_1-w)-1}{2} + j$. For D_0 we have $\frac{w_0-a+1}{2} = \frac{w-a}{2} = i$ and $\frac{3w_0-b+1}{2} = \frac{3w-b-2}{2} = j - 1$. Finally, we get:

$$\cdots \xrightarrow{\partial *} \mathcal{H}^{\frac{w_1-w-1}{2}+i,\frac{3(w_1-w)-1}{2}+j}(D_1) \xrightarrow{\alpha_*} \mathcal{H}^{i,j}(D) \xrightarrow{\beta_*} \mathcal{H}^{i,j-1}(D_0) \xrightarrow{\partial_*} \cdots$$

b) Let D be oriented so that c is negative. When choosing an orientation for D with writhe w there is only one possible choice of orientation for D_1 coherent

with D, we call its writhe $w_1 = w + 1$. As in the case a) we choose an orientation of D_0 so that is equal to the one of D and D_1 for all components not involved in c and we call its writhe w_0 (see Figure 3.16). With this choice

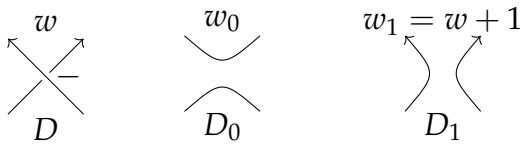

Figure 3.16

we get that:

$$\cdots \xrightarrow{\partial *} \mathcal{H}^{\frac{w_1-a-1}{2},\frac{3w_1-b-1}{2}}(D_1) \xrightarrow{\alpha_*} \mathcal{H}^{\frac{w-a}{2},\frac{3w-b}{2}}(D) \xrightarrow{\beta_*} \mathcal{H}^{\frac{w_0-a+1}{2},\frac{3w_0-b+1}{2}}(D_0) \xrightarrow{\partial_*} \cdots$$

Performing the same substitution as before, we get: $\frac{w_1-a-1}{2} = \frac{w+1-w-1}{2} + i = i$, $\frac{3w_1-b-1}{2} = \frac{3w+3-3w-1}{2} + j = j + 1$. For D_0, they become $\frac{w_0-a+1}{2} = \frac{w_0-w+1}{2} + i$ and $\frac{3w_0-b+1}{2} = \frac{3(w_0-w)+1}{2} + j$. Finally:

$$\cdots \xrightarrow{\partial *} \mathcal{H}^{i,j+1}(D_1) \xrightarrow{\alpha_*} \mathcal{H}^{i,j}(D) \xrightarrow{\beta_*} \mathcal{H}^{\frac{w_0-w+1}{2}+i,\frac{3(w_0-w)+1}{2}+j}(D_0) \xrightarrow{\partial_*} \cdots$$

3.4.3 Application: Torus Knots $T(2, n)$

A nice application of this sequence can be found in [Mon23], where the authors explicitly compute the Khovanov homology of all positive torus knots with two strands, $T(2, n)$ with $n \geq 0$, in a straightforward way. The key idea is that performing a 0-smoothing on a chosen crossing produces the torus knot with one less crossing, $T(2, n-1)$, while performing a 1-smoothing gives a diagram of the unknot with $n-1$ twist, as shown in Figure 3.17.

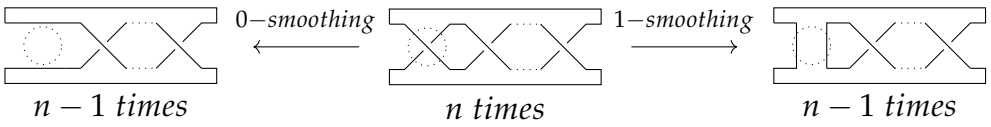

Figure 3.17: *Torus knot $T(2, n)$ for $n \geq 0$(center), torus knot $T(2, n-1)$ (left) and trivial knot with $n-1$ positive twist (right).*

Remark 3.32. Torus knot $T(2, n)$ is a knot if n is odd and a two component link otherwise.

Let $D(2, n)$ denote the standard diagram of $T(2, n)$ as the one in Figure 3.17.

We will prove, step by step, the following theorem:

Theorem 3.33. *Let $T(2,n)$ be the two strands torus knot, with $n > 0$, and $D(2,n)$ its standard diagram. Its framed Khovanov homology $\mathcal{H}_{a,b}(D(2,n)$ is given by:*

$$\mathcal{H}_{a,b}(D(2,n)) = \begin{cases} \mathbb{Z} & \text{for } (a,b) = (n,n), \\ \mathbb{Z} & \text{for } (a,b) = (-n,-3n) \text{ if } n \text{ is even}, \\ \mathbb{Z} & \text{for } a = n-2s,\ b = n-4s+4 \text{ where } s \text{ is even and } 0 \leq s \leq n, \\ \mathbb{Z} & \text{for } a = n-2s,\ b = n-4s \text{ where } s \text{ is odd and } 3 \leq s \leq n, \\ \mathbb{Z}_2 & \text{for } a = n-2s,\ b = n-4s+4 \text{ where } s \text{ is odd and } 3 \leq s \leq n, \\ 0 & \text{otherwise.} \end{cases}$$

Proof. Let $\bigcirc^k$ be the diagram of the trivial knot with k negative twists.

We argue by induction on n.

1. Basic step

Case $n = 1$:

For $T(2,1)$, its standard diagram is the unknot with a positive crossing  (considering a rotation of 90 degrees).Using Example 3.18, the Khovanov homology of the unknot is

$$\mathcal{H}^{i,j}(\bigcirc) = \mathbb{Z} \qquad \text{if } (i,j) = (0, \pm 1),$$

and vanishes otherwise.

Since the writhe of $D(2,1)$ is $w($$) = 1$, equation (3.4.1) implies:

$$\mathcal{H}_{w,3w\pm 2}(D(2,1)) = \mathcal{H}_{1,3\pm 2}(D(2,n)) = \mathbb{Z}$$

with all other homology groups trivial.

Case $n = 2$:

In Section 3.3, Example 3.29, we computed the Khovanov homology of the Hopf link. Using the expression (3.4.1), we recover the Khovanov framed homology of the diagram $D(2,2)$, showed in the table below:

j \ i	-2	0	2
6			$\mathbb{Z}$
2			$\mathbb{Z}$
-2	$\mathbb{Z}$		
-6	$\mathbb{Z}$		

This coincides with the values predicted by the theorem for $n = 2$, in fact, the theorem states that the Khovanov framed homology of $D(2,2)$ should be $\mathbb{Z}$ when:

* $(a,b) = (2,2)$, $(a,b) = (-2,-6)$ (second line of the statement),
* $(a,b) = (2, 2+4) = (2,6)$ (case $s = 0$),
* $(a,b) = (2-4, 2-8+4) = (-2,-2)$ (case $s = 2$).

2. **Inductive step**:

Assume that the theorem holds for $D(2,k)$, where $k \leq n-1$, and consider $D(2,n)$, with $n \geq 3$.

Performing a 1-smoothing on $D(2,n)$ produces an unknot with framing $1-n$. Hence, its Khovanov homology is:

$$\mathcal{H}_{a,b}(\bigcirc^{1-n}) = \begin{cases} \mathbb{Z} & \text{if } (a,b) = (1-n, 3-3n \pm 2), \\ 0 & \text{otherwise.} \end{cases} \tag{3.5}$$

The long exact sequence defined in (3.4) becomes:

$$\to \mathcal{H}_{a+1,b+1}(\bigcirc^{1-n}) \xrightarrow{\alpha_*} \mathcal{H}_{a,b}(D(2,n)) \xrightarrow{\beta_*} \mathcal{H}_{a-1,b-1}(D(2,n-1)) \xrightarrow{\partial_*} \mathcal{H}_{a-1,b+1}(\bigcirc^{1-n}) \to .$$

We observe that β_* an isomorphism whenever $\mathcal{H}_{a+1,b+1}(\bigcirc^{n-1})$ and $\mathcal{H}_{a-1,b+1}(\bigcirc^{n-1})$ are trivial. Therefore, for

$$(a,b) \neq \{(-n,-3n), (2-n,-3n), (-n,4-3n), (2-n,4-3n)\},$$

we have

$$\mathcal{H}_{a,b}(D(2,n)) = \mathcal{H}_{a-1,b-1}(D(2,n-1)).$$

Applying the inductive hypothesis we get:

$$\mathcal{H}_{a,b}(D(2,n)) = \begin{cases} \mathbb{Z} & \text{for } (a,b) = (n,n) \\ \mathbb{Z} & \text{for } a = n-2s,\ b = n-4s+4 \text{ where } s \text{ is even and } 0 \leq s \leq n-1, \\ \mathbb{Z} & \text{for } a = n-2s,\ b = n-4s \text{ where } s \text{ is odd and } 3 \leq s \leq n-1, \\ \mathbb{Z}_2 & \text{for } a = n-2s,\ b = n-4s+4 \text{ where } s \text{ is odd and } 3 \leq s \leq n-1, \\ 0 & \text{for } (a,b) \neq \{(-n,-3n), (2-n,-3n), (-n,4-3n), (2-n,4-3n)\}, \\ 0 & \text{otherwise;} \end{cases}$$

We now treat the remaining bidegrees individually. Specifically, we need to verify that

$$\mathcal{H}_{-n,-3n}(D(2,n)) = \mathbb{Z},$$

(second line of the statement when n is even, fourth line of the statement case $s = n$ when n is odd),

$$\mathcal{H}_{2-n,-3n}(D(2,n)) = \mathcal{H}_{2-n,4-3n}(D(2,n)) = 0$$

and that:

* when n is even (third line of the statement case $s = n$):

$$\mathcal{H}_{-n,4-3n}(D(2,n)) = \mathbb{Z}.$$

* When n is odd (fifth line of the statement case $s = n$):

$$\mathcal{H}_{-n,4-3n}(D(2,n)) = \mathbb{Z}_2.$$

Case i.) Let us consider the case $(a,b) = (-n,-3n)$:

The long exact sequence in a neighborhood of $\mathcal{H}_{-n,-3n}(D(2,n))$ is:

$$\begin{aligned}\to\ \mathcal{H}_{1-n,-1-3n}(D(2,n-1)) &\xrightarrow{\partial_*} \mathcal{H}_{1-n,1-3n}(\bigcirc^{n-1}) \xrightarrow{\alpha_*}\\ \mathcal{H}_{-n,-3n}(D(2,n)) &\xrightarrow{\beta_*} \mathcal{H}_{-n-1,-3n-1}(D(2,n-1)) \to\end{aligned}$$

By the inductive hypothesis, $\mathcal{H}_{-n,-3n}(D(2,n))$ and $\mathcal{H}_{-n-1,-3n-1}(D(2,n))$ are trivial. Hence, the previous exact sequence reduces to:

$$0 \xrightarrow{\partial_*} \mathcal{H}_{1-n,1-3n}(\bigcirc^{n-1}) \xrightarrow{\alpha_*} \mathcal{H}_{-n,-3n}(D(2,n)) \xrightarrow{\beta_*} 0$$

which shows that α_* is an isomorphism between $\mathcal{H}_{1-n,1-3n}(\bigcirc^{n-1}) = \mathbb{Z}$ and $\mathcal{H}_{-n,-3n}(D(2,n))$.

We can conclude:

$$\mathcal{H}_{-n,-3n}(D(2,n)) = \mathbb{Z}.$$

Case ii) Consider $(a,b) = (2-n,-3n)$:

In a neighborhood of $\mathcal{H}_{2-n,-3n}(D(2,n))$, the long exact sequence reads:

$$\to\ \mathcal{H}_{2-n,1-3n}(\bigcirc^{n-1})\ \xrightarrow{\alpha_*}\ \mathcal{H}_{2-n,-3n}(D(2,n))\ \xrightarrow{\beta_*}\ \mathcal{H}_{1-n,-3n-1}(D(2,n-1))\ \to$$

By the inductive hypothesis, $\mathcal{H}_{1-n,-3n-1}(D(2,n))$ is trivial. Thus, the exact sequence reduces to:

$$0\ \xrightarrow{\alpha_*}\mathcal{H}_{-n,-3n}(D(2,n))\ \xrightarrow{\beta_*}\ 0.$$

Therefore:

$$\mathcal{H}_{-n,-3n}(D(2,n)) = 0.$$

Case iii) We consider $(a,b) = (-n,4-3n)$ so that $(a+2,b) = (2-n,4-3n)$:

Consider the neighborhood of $\mathcal{H}_{-n,4-3n}(D(2,n))$, in this region, the long exact sequence has the form:

$$0\to\ \mathcal{H}_{2-n,4-3n}(D(2,n))\ \xrightarrow{\beta_*}\ \mathcal{H}_{1-n,3-3n}(D(2,n-1))\ \xrightarrow{\partial_*}\ \mathcal{H}_{1-n,5-3n}(\bigcirc^{n-1})\ \xrightarrow{\alpha_*}$$
$$\xrightarrow{\alpha_*}\mathcal{H}_{-n,4-3n}(D(2,n))\ \xrightarrow{\beta_*}\ \mathcal{H}_{-n-1,3-3n}(D(2,n-1))\ \to$$

By inductive hypothesis,

$$\mathcal{H}_{-n-1,3-3n}(D(2,n-1)) = 0$$

and

$$\mathcal{H}_{1-n,3-3n}(D(2,n-1)) = \mathcal{H}_{-(n-1),-3(n-1)}(D(2,n-1)) = \mathbb{Z}.$$

Thus, the exact sequence simplifies to:

$$0\to\ \mathcal{H}_{2-n,4-3n}(D(2,n))\ \xrightarrow{\beta_*}\ \mathbb{Z}\ \xrightarrow{\partial_*}\ \mathbb{Z}\ \xrightarrow{\alpha_*}\ \mathcal{H}_{-n,4-3n}(D(2,n))\ \xrightarrow{\beta_*}\ 0\ \to$$

To establish $\mathcal{H}_{2-n,4-3n}(D(2,n))$ and $\mathcal{H}_{-n,4-3n}(D(2,n))$ we analyze the group homomorphism:

$$(\partial_*)_{1-n,3-3n} : \mathbb{Z} \longrightarrow \mathbb{Z}.$$

The map $(\partial_*)_{1-n,3-3n}$is an homomorphism, hence, it is the zero map or it is a multiplication by $k > 0$.

- If it is the null map, the exactness of the sequence gives:

$$\mathcal{H}_{2-n,4-3n}(D(2,n)) = \mathcal{H}_{1-n,3-3n}(D(2,n-1)) = \mathbb{Z}$$

and

$$\mathcal{H}_{-n,4-3n}(D(2,n)) = \mathcal{H}_{1-n,3-3n}(D(2,n-1)) = \mathbb{Z}.$$

- If it is the multiplication by $k > 0$, the exactness implies that $Ker\partial_* = Im\beta_* = 0$ and $Im\partial_* = k\mathbb{Z} = Ker\alpha_*$. Therefore, we have $\mathcal{H}_{2-n,4-3n}(D(2,n)) = 0$ and $\mathcal{H}_{-n,4-3n}(D(2,n))) = \mathbb{Z}_k$.

The study made by M.Pabiniak, J.H.Przytycky and R.Sazdanovic in [PPS09] established that the map $(\partial_*)_{1-n,3-3n}$ is the zero map when n is even and the multiplication by 2 when n is odd.

Therefore, we conclude that:

$$\mathcal{H}_{-n,4-3n}(D(2,n)) = \mathcal{H}_{2-n,4-3n}(D(2,n)) = \mathbb{Z} \quad \textit{when } n \textit{ is even,}$$

$$\mathcal{H}_{2-n,4-3n}(D(2,n)) = 0 \qquad \mathcal{H}_{-n,4-3n}(D(2,n))) = \mathbb{Z}_2 \qquad \textit{when } n \textit{ is odd.}$$

This concludes the proof.

□

3.5 Cobordism and Khovanov homology

In this section, we provide an overview of the relationship between Khovanov homology and $(1+1)$ *dimensional topological quantum field theory* (TQFT); see Appendix 5.3 for a brief introduction to this framework. Although this material is not required for the proofs of the main results of the dissertation, it offers valuable conceptual insight into the construction of Khovanov homology and highlights its intrinsic topological nature. A detailed and systematic treatment of this viewpoint can be found in the work of Bar-Natan [Bar05], which we very briefly summarize here.

From the perspective of topological quantum field theory, Khovanov homology can be understood as arising from a functorial assignment of algebraic data to 1-manifolds and 2-dimensional cobordisms. In general, a $(1+1)$-dimensional TQFT is a symmetric monoidal functor from the category Cob_{1+1} of compact 1-manifolds and 2-dimensional cobordisms to the category of vector spaces, satisfying compatibility with disjoint unions and gluing of cobordisms. Such a functor

encodes the principle that topological operations on manifolds, such as cutting, gluing, merging, and splitting, are reflected algebraically by linear maps. In this framework, the algebraic structure underlying Khovanov homology is not ad hoc, but is dictated by the topology of surfaces and their compositions.

We begin by obseving that the algebraic data introduced earlier, namely the graded vector space V together with the multiplication m and a comultiplication Δ, can be extended to a Frobenius algebra by adjoining a unit ι and a counit ϵ defined by:

$$\iota(1) = v^+ \qquad \epsilon(v^+) = 0 \quad \textit{and} \quad \epsilon(v^-) = 1.$$

With these operations, V becomes a Frobenius algebra isomorphic to

$$A = \mathbb{Q}[x]/x^2.$$

Remark 3.34. In much of the literature, the generators of V are denoted by $v^+ = \mathbf{1}$ and $v^- = \mathbf{x}$. This notation emphasizes the algebraic structure of V. In particular, the relation $\mathbf{x}^2 = 0$ corresponds to the fact that the multiplication map satisfies $m(v^- \otimes v^-) = 0$.

Building on this algebraic structure, Khovanov [Kho00] and Bar-Natan [Bar05] constructed a functor

$$\mathcal{F} : Cob_{1+1} \longrightarrow Vect$$

which assigns to a 1-dimensional manifold consisting of n disjoint circles the vector space $V^{\otimes n}$, and to a cobordism between such manifolds a linear map determined by the Frobenius algebra structure on V. The basic cobordisms and their algebraic counterparts are illustrated in Figure 3.18, and are given explicitly by:

$$\mathcal{F}(\bigcirc) = id : V \longrightarrow V,$$

$$\mathcal{F}(\bigcirc) = \iota : \mathbb{Z} \longrightarrow V,$$

$$\mathcal{F}(\bigcirc) = \epsilon : V \longrightarrow \mathbb{Z},$$

$$\mathcal{F}(\bigcirc) = \Delta : V \longrightarrow V \otimes V,$$

$$\mathcal{F}(\bigcirc\bigcirc) = m : V \otimes V \longrightarrow V.$$

This functorial perspective provides a conceptual explanation for the definition of the Khovanov differential. Indeed, adjacent vertices in the cube of resolutions of a link diagram differ by a single smoothing change, which corresponds topologically to an elementary cobordism describing either the merging of two

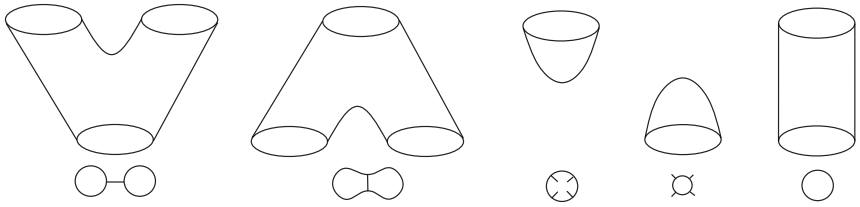

Figure 3.18: *Set of cobordisms and the way we encode them.*

circles, also called *pair of pants*, or the splitting of one circle into two, called *co-pair of pants* or *saddle cobordism*. Under the functor $\mathcal{F}$, these cobordisms are sent respectively to the multiplication map $m : V \otimes V \to V$ and the comultiplication map $\Delta : V \to V \otimes V$. The Khovanov differential is then defined as a signed sum of these linear maps, taken over all edges of the cube of resolutions.

From this viewpoint, Khovanov homology emerges naturally as the homology of a chain complex obtained by applying a $(1+1)$-dimensional TQFT to the cube of resolutions of a link diagram. This interpretation not only clarifies the algebraic structure underlying the theory.

Chapter 4

Lee Homology and Rasmussen s-invariant

In 2005, Eun Soo Lee [Lee05] introduced a deformation of Khovanov homology, now known as Lee homology, obtained by modifying the Frobenius algebra underlying the original construction. Although this deformation dramatically simplifies the resulting homology (collapsing it to a vector space of dimension 2 for knots) it retains a filtered structure whose interaction with the original grading contains meaningful topological information. In particular, Lee's deformation induces a spectral sequence from Khovanov homology to Lee homology, providing a powerful computational and conceptual tool.

Building on Lee's work, Jacob Rasmussen [Ras10] extracted from this filtered structure a numerical knot invariant, now called the *Rasmussen s-invariant*. The invariant $s(K) \in \mathbb{Z}$ is defined purely in terms of Lee homology, yet it has profound geometric consequences. Most notably, Rasmussen in [Ras10] proved a significant property of the s-invariant: $s(K)$ gives a lower bound on the *smooth slice genus* of a knot:

$$|s(K)| \leq 2g_*(K).$$

In this chapter, we will define this new homological invariant for links, showing in detail its structure and its canonical generators. We will then underline the spectral sequence arising from the induced filtration in Lee homology. This spectral sequence is relevant not only for the grading which lids to the definition of the s invariant, but also because has Khovanov homology as first page and converges to Lee homology, being a link between the two homologies.

At the end of this chapter, we will finally talk about the Rasmussen s-invariant

and some of its properties as bounding the slice genus. All this chapter will come up with multiple examples which will give a deeper understanding on these subjects.

4.1 Lee homology construction

The idea behind Lee homology is to modify the Khovanov chain complex by introducing a new differential that no longer preserves the quantum grading. We now explain how Lee constructed this complex.

4.1.1 Lee complex

Let D be a diagram of a link. Throughout this section, we will work over $\mathbb{Q}$: we define Lee chain groups in the same way as we did for Khovanov's one in Section 3.1, with the only difference that the vector space V is now regarded as a graded vector space over $\mathbb{Q}$.

The key modification lies in the differential. Lee defines a new differential as the sum of two components. The first one is the usual Khovanov differential d of degree $(1,0)$. The second one, denoted by ϕ, has degree $(1,4)$ and therefore increases the quantum degree. The Lee differential is then defined as $d' = d + \phi$ and the corresponding chain complex is denoted by $\mathcal{C}_{Lee}(D)$. Let us see how ϕ is defined:

As in the Khovanov case, the map ϕ acts as the identity on the tensor factors corresponding to circles preserved when changing the smoothing. On the other tensor factors it is defined linearly by the following maps on the generators:

$$\begin{aligned} m_\phi : V \otimes V &\longrightarrow V \\ v^+ \otimes v^+ &\longmapsto 0 \\ v^+ \otimes v^- &\longmapsto 0 \\ v^- \otimes v^+ &\longmapsto 0 \\ v^- \otimes v^- &\longmapsto v^+ \end{aligned} \qquad \begin{aligned} \Delta_\phi : V &\longrightarrow V \otimes V \\ v^+ &\longmapsto 0 \\ v^- &\longmapsto v^+ \otimes v^+ \end{aligned}$$

We observe that m_ϕ is commutative and associative and moreover:

$$m_\phi(m_\phi(x \otimes y) \otimes z) = m_\phi(x \otimes (m_\phi(y \otimes z)) = 0, \quad \forall x, y, z \in V.$$

The comultiplication is also cocommutative and coassociative, moreover:

$$(\Delta_\phi \otimes id) \circ \Delta_\phi(z) = (id \otimes \Delta_\phi) \circ \Delta_\phi(z) = 0, \quad \forall z \in V.$$

The maps Δ and m also satisfy the Frobenius condition (see Appendix 5.3), moreover:

$$\Delta_\phi \circ m_\phi(x \otimes y) = (m_\phi \otimes id)(x \otimes \Delta_\phi(y)) = 0, \quad \forall x, y \in V.$$

Hence, we have $\phi \circ \phi = 0$ and to show that d' is a differential ($d' \circ d' = 0$) we just need to see that ϕ commutes with d.

In [Lee05, Section 4.2.1] Lee proved it by proving the three following equalities:

i. $m \circ (m_\phi \otimes id) + m_\phi \circ (m \otimes id) = m \circ (id \otimes m_\phi) + m_\phi \circ (id \otimes m_\phi)$,

ii. $(\Delta \otimes id) \circ \Delta_\phi + (\Delta_\phi \otimes id) \circ \Delta = (id \otimes \Delta) \circ \Delta_\phi + (id \otimes \Delta_\phi) \circ \Delta$,

iii. $\Delta \circ m_\phi + \Delta_\phi \circ m = (m \otimes id) \circ (id \otimes \Delta_\phi) + (m_\phi \otimes id) \circ (id \otimes \Delta)$.

Finally, we can redefine d' in terms of a new multiplication $m' = m + m_\phi$ and comultiplication $\Delta' = \Delta + \Delta_\phi$.

$$\begin{aligned} m' : & V \otimes V \longrightarrow V \\ & v^+ \otimes v^+ \longmapsto v^+ \\ & v^+ \otimes v^- \longmapsto v^- \\ & v^- \otimes v^+ \longmapsto v^- \\ & v^- \otimes v^- \longmapsto \color{red}{v^+} \end{aligned} \qquad \begin{aligned} \Delta' : & V \longrightarrow V \otimes V \\ & v^+ \longmapsto v^+ \otimes v^- + v^- \otimes v^+ \\ & v^- \longmapsto v^- \otimes v^- + \color{red}{v^+ \otimes v^+} \end{aligned}$$

We use red color to indicate the contribution of m_ϕ and Δ_ϕ.

Definition 4.1 (Lee complex). Let D be a diagram of a link. We call the complex constructed above the *Lee complex* and denote it by $\mathcal{C}_{Lee}(D)$.

$$\mathcal{C}^{*,*}_{Lee}(D) \xrightarrow{d'=d+\phi} \mathcal{C}^{*+1,*}_{Lee}(D) \oplus \mathcal{C}^{*+1,*+4}_{Lee}(D)$$

Remark 4.2. We have already observed that the differential d' does not preserve the quantum grading; moreover, $\Delta'(v^-)$ is not even homogeneous. Nevertheless, for every homogeneous element $v \in \mathcal{C}_{Lee}(D)$, the quantum grading of each monomial appearing in $d'(v)$ is greater or equal to the quantum grading of v. As a consequence, the quantum grading induces a filtration on the Lee complex $\mathcal{C}_{Lee}(D)$. This will be explained in more detail in Section 4.2.

Although this complex may at first appear more complicated than the Khovanov complex, its structure turns out to be surprisingly simple. To make this apparent, we introduce a new basis $\{\mathbf{a}, \mathbf{b}\}$ for V, defined by

$$\mathbf{a} = v^- + v^+ \qquad \text{and} \qquad \mathbf{b} = v^- - v^+.$$

Let us compute how the modified multiplication m' and comultiplication Δ' act on this new basis, Using bilinearity and the definitions of m' and Δ', we have

$$\mathbf{a} \otimes \mathbf{a} = (v^- + v^+) \otimes (v^- + v^+) = v^+ \otimes v^+ + v^- \otimes v^- + v^+ \otimes v^- + v^- \otimes v^+,$$

$$\mathbf{b} \otimes \mathbf{b} = (v^- - v^+) \otimes (v^- - v^+) = v^+ \otimes v^+ + v^- \otimes v^- - v^+ \otimes v^- - v^- \otimes v^+$$

and

$$\mathbf{a} \otimes \mathbf{b} = (v^- + v^+) \otimes (v^- - v^+) = -v^+ \otimes v^+ + v^- \otimes v^- + v^+ \otimes v^- - v^- \otimes v^+ = \mathbf{b} \otimes \mathbf{a}.$$

From these computations, we obtain:

$$\begin{aligned}
m'(\mathbf{a} \otimes \mathbf{a}) &= m'(v^+ \otimes v^+ + v^- \otimes v^- + v^+ \otimes v^- + v^- \otimes v^+) = \\
&= v^+ + v^+ + v^- + v^- = \\
&= 2\mathbf{a}; \\
m'(\mathbf{a} \otimes \mathbf{b}) &= m'(\mathbf{b} \otimes \mathbf{a}) = m'(-v^+ \otimes v^+ + v^- \otimes v^- + v^+ \otimes v^- - v^- \otimes v^+) = \\
&= -v^+ + v^+ + v^- - v^- = \\
&= 0, \\
m'(\mathbf{b} \otimes \mathbf{b}) &= m'(v^+ \otimes v^+ + v^- \otimes v^- - v^+ \otimes v^- - v^- \otimes v^+) = \\
&= v^+ + v^+ - v^- - v^- = \\
&= -2\mathbf{b};
\end{aligned}$$

$$\begin{aligned}
\Delta'(\mathbf{a}) &= \mathbf{a} \otimes \mathbf{a}; \\
\Delta'(\mathbf{b}) &= \mathbf{b} \otimes \mathbf{b};
\end{aligned}$$

4.1.2 Lee homology canonical generators

Definition 4.3 (Lee homology). Let D be a diagram of an oriented link. We call *Lee homology* $\mathcal{H}_{Lee}(D)$ the homology of the Lee complex $\mathcal{C}_{Lee}(D)$.

Example 4.4. The unknot ◯ has same Khovanov and Lee homology. In fact:

$$0 \xrightarrow{d'} [\![\bigcirc]\!]^0 \xrightarrow{d'} 0,$$

where d' is the null map and hence

$$\mathcal{H}^0_{Lee}(\bigcirc) = V \cong \mathbb{Q} \oplus \mathbb{Q}.$$

Theorem 4.5. *Lee homology is an invariant for links.*

Proof. The entire proof can be found in [Lee05] and [Ras10]. The idea of the proof is that, given D and $\tilde{D}$ two equivalent diagrams related by the Reidemeister move Ri, defining a map $\rho_i : \mathcal{C}_{Lee}(D) \longrightarrow \mathcal{C}_{Lee}(D')$ for $i = 1, 2, 3$ which induces an isomorphism among homologies of both complexes. □

Now that we know Lee homology is a link invariant, we turn to a more detailed study of how to compute $\mathcal{H}_{Lee}(L)$ for a given link L.

Let D be a diagram of an unoriented n-component link L. Consider an orientation of its components $o \in Or(L)$. We call D_o the corresponding oriented resolution defined as follows: at each crossing of D, we take a 0-smoothing if the crossing is positive and a 1-smoothing if the crossing is negative. Observe that this is the same procedure used to construct a Seifert surface from an oriented link diagram, as explained in Section 1.2.3. The result is a collection of disjoint circles in the plane, each inheriting an orientation from o. We now label each circle of D_o with **a**'s or **b**'s according to the following rules: we assign **a** if the circle has a clockwise (resp. counterclockwise) orientation and there is an even (resp. odd) number of circles separating it from infinity, and we assign a label **b** otherwise. This rule can be summarized by:

$$\mathbf{a} \mapsto \begin{cases} \textit{if } \circlearrowright \textit{ and even number of circle separating it from } \infty, \\ \textit{if } \circlearrowleft \textit{ and odd number of circle separating it from } \infty, \end{cases} \tag{4.1}$$

$$\mathbf{b} \mapsto \begin{cases} \textit{if } \circlearrowright \textit{ and odd number of circle separating it from } \infty, \\ \textit{if } \circlearrowleft \textit{ and even number of circle separating it from } \infty. \end{cases} \tag{4.2}$$

Remark 4.6. When we refer to infinity, we mean the point in S^3 with respect to the chosen planar projection of the link.Note that the parity of the number of circles separating a given circle from infinity is equal to the number of circles in which it is nested.

Example 4.7. To illustrate the labeling rule, we assign the basis elements **a** and **b** to the oriented resolution of the standard diagram of the figure-eight knot for each of its two possible orientations. The resulting labeled resolutions are shown in Figure 4.1

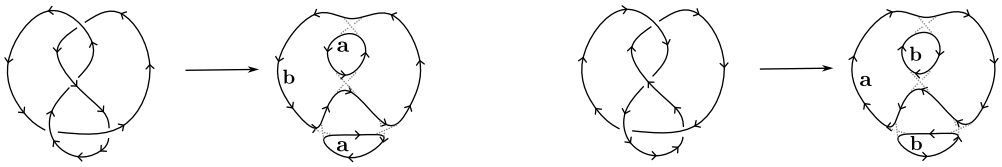

Figure 4.1: *A diagram representing the figure eight knot with its two oriented resolution, and the assciated labeling of circles.*

Remark 4.8. We observe that no circles labeled by **a** share a smoothed crossing; in other words, if we consider a graph whose vertices are in $1-1$ correspondence with the circle and whose edges are in $1-1$ correspondence with the smoothed crossings, the labeling by **a**, **b** defines a bipartition of this graph.

As a consequence, whenever two circles in D_o are connected by a smoothed crossing, they must carry different labels. Furthermore, it is easy to check that if a region of the diagram contains exactly two arc segments, then one of the following two situations occurs: either they have same orientations but different labels, or they share the same label but they have opposite orientations.

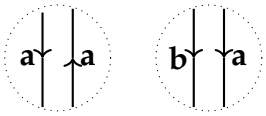

Figure 4.2: *Local behavior of the oriented state* $\mathfrak{s}_o$.

Example 4.9. Here is the bipartite graph associated to the rightmost diagram in Figure 4.2.

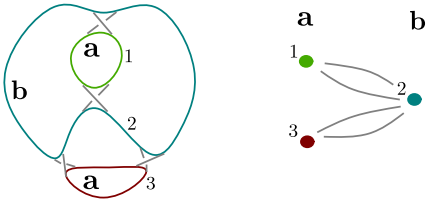

Definition 4.10 (Oriented state). Given a diagram D and an orientation of it $o \in Or(D)$, we define $\mathfrak{s}_o$ the *oriented state* obtained by the labeling described above.

Lemma 4.11. *Let D be a diagram of an n-component link L. We have $\mathfrak{s}_o \in \mathcal{H}_{Lee}(D)$ for all 2^n possible orientations of L. Moreover, if we consider the link oriented with orientation o, we have $\mathfrak{s}_o, \mathfrak{s}_{\bar{o}} \in \mathcal{H}^0_{Lee}(D)$, where $\bar{o} \in Or(D)$ is the reverse orientation of o.*

Proof. Let D be a diagram of L with m crossings and let $o \in Or(D)$ be one of its orientations. Denote by D_o be the corresponding oriented resolution. $\mathfrak{s}_o$ is a vector in V_α where $\alpha_o \in \{0,1\}^m$ is the vertex associated with the oriented resolution ($|\alpha_o| = m_-$) has height equal to the number of negative crossings. As observed in Remark 4.8, if two circles in D_o share a crossing, they must have different labels (**a** and **b**). Therefore, when we apply the Lee differential d' to $\mathfrak{s}_o$, each term corresponding to a merging of two circles labeled **a** and **b** vanishes, because

$$m'(\mathbf{a} \otimes \mathbf{b}) = 0,$$

as shown in (4.1.1)

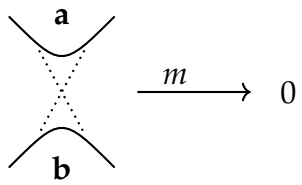

Hence $\mathfrak{s}_o \in Ker(d')$ is a cycle in $\mathcal{H}_{Lee}(D)$. We will not show here that $\mathfrak{s}_o$ is not a boundary. To prove this, one typically equips the chain complex with an inner product in which the basis elements **a** and **b** are orthonormal and then applies Hodge theory; for a detailed treatment, see [Lee05, Section 4.4.2] .

This completes the proof of the first part of the Lemma. To prove the last part, it is sufficient to give an orientation $o \in Or(D)$ to L and recall the definition of the Lee complex $\mathcal{C}_{Lee}(D) = [\![D]\!][-m_-]\{m_+ - 2m_-\}$ where m_- and m_+ denote the numbers of negative and positive crossings of D, respectively. We have already shown that $\mathfrak{s}_o$ has height m_-, hence

$$\mathfrak{s}_o \in [\![D]\!]^{m_-}[-m_-] = \mathcal{C}^0_{Lee}(D).$$

Similarly, the oriented resolution $D_{\bar{o}}$ corresponding to the opposite orientation $\bar{o}$ represents the same resolution of D_o and hence $\mathfrak{s}_{\bar{o}} \in \mathcal{C}^0_{Lee}(D)$. We conclude that both canonical cycles associated to the two orientations lie in the degree-zero part of the Lee complex:

$$\mathfrak{s}_o, \mathfrak{s}_{\bar{o}} \in \mathcal{C}^0_{Lee}(D).$$

□

The goal is to show that these are the generators of $\mathcal{H}_{Lee}(D)$, i.e., all cycles in $\mathcal{H}_{Lee}(D)$ are linear combinations of $\mathfrak{s}_o$ with $o \in Or(L)$.

Theorem 4.12. *[Lee05, Theorem 4.2] Let L be an oriented link with n components, then its Lee homology $\mathcal{H}_{Lee}(D)$ has dimension 2^n.*

Proof. From the previous lemma, since an n-components link has 2^n possible orientations and the corresponding canonical cycles $\mathfrak{s}_o$ are linearly independent (**a** and **b** form a base for V), we immediately obtain the lower bound:

$$dim(\mathcal{H}_{Lee}(L)) \geq 2^n.$$

To prove the reverse inequality, we will use a Khovanov-type skein sequence, as constructed in Section 3.4.2, but ignoring the quantum grading. For clarity, we will refer to the framed version of the Lee homology as $\bar{\mathcal{H}}^*_{Lee}$ where the homological grading is written as a superscript and the bar distinguishes it from the usual (oriented) version. The corresponding long exact sequence takes the form:

$$\cdots \longrightarrow \bar{\mathcal{H}}^{a+1}_{Lee}(D_0) \longrightarrow \bar{\mathcal{H}}^{a+1}_{Lee}(D_1) \longrightarrow \bar{\mathcal{H}}^{a}_{Lee}(D) \longrightarrow \bar{\mathcal{H}}^{a-1}_{Lee}(D_0) \longrightarrow \bar{\mathcal{H}}^{a-1}_{Lee}(D_1) \longrightarrow \cdots \tag{4.3}$$

Since this sequence is exact, we immediately get the inequality

$$dim(\bar{\mathcal{H}}^{a}_{Lee}(D)) \leq dim(\bar{\mathcal{H}}^{a-1}_{Lee}(D_0)) + dim(\bar{\mathcal{H}}^{a+1}_{Lee}(D_1)) \qquad \text{for all } \ a \in \mathbb{Z}.$$

Since $dim(\mathcal{H}_{Lee}(D)) = dim(\bar{\mathcal{H}}_{Lee}(D)) = \sum_{a\in\mathbb{Z}} dim(\bar{\mathcal{H}}^{a}_{Lee}(D))$, we have:

$$dim(\mathcal{H}_{Lee}(D)) \leq dim(\mathcal{H}_{Lee}(D_0)) + dim(\mathcal{H}_{Lee}(D_1)).$$

We first prove that $dim(\mathcal{H}_{Lee}(L)) \leq 2^n$ for knot and 2- components links, by working by induction on the number c of crossings and on the number of components of the link. The statement clearly holds for the unknot(Example 4.4) and for $\bigcirc^n$ since in these cases the Khovanov and Lee homologies coincide: $\mathcal{H}(\bigcirc^n) = V^{\otimes n}$ and $dim(V^{\otimes n}) = 2^n$.

Assume the statement holds for all diagrams with $c-1$ crossings. We will prove that it holds for all diagrams with c crossings.

Case 1: D is the diagram of a knot:

Let D be a diagram of a knot K with c crossings. Choose a crossing $\bar{c}$ to resolve. Performing a 0 or a 1 resolution at $\bar{c}$, we are left with two possibility:

1) D_0 is a knot and D_1 is a two component link.

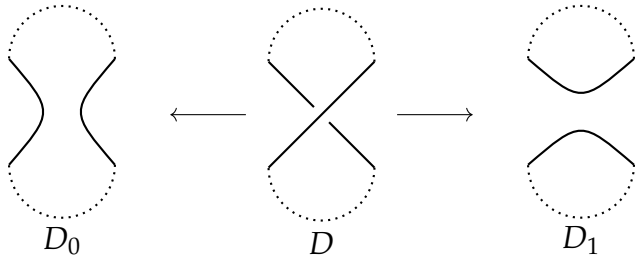

2) D_1 is a knot and D_0 is a two component link.

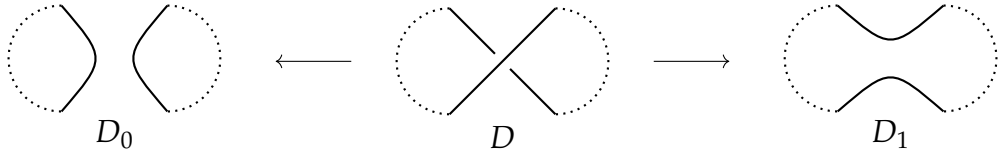

In both cases D_0 and D_1 have one fewer crossing than D. Therefore, we can apply the inductive hypothesis: D_0 and D_1 have either 2 or 4 generators of the Lee homology, depending on the number of their components. Next, let us analyze how orientations on D correspond to orientations on D_0 and D_1 considering the two previous cases:

1) D_0 is a knot and D_1 is a two component link:

   Given an orientation on D, the crossing $\bar{c}$ is necessarily negative. Note that once an orientation is chosen for a single strand, the orientation of the other is determined by the global connectivity of the knot; reversing this global orientation does not alter the sign of the crossing. Consequently, the two possible orientations of D are compatible with exactly two of the four possible orientations of D_1. Conversely, the two canonical orientations of D_0 are compatible with the remaining two orientations of D_1:

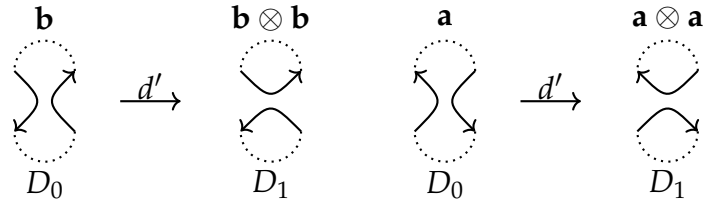

   As shown in the diagrams above, the induced map $d'^{*} : \bar{\mathcal{H}}_{Lee}(D_0) \longrightarrow \bar{\mathcal{H}}_{Lee}(D_1)$ sends the two generators of $\bar{\mathcal{H}}_{Lee}(D_0)$ to the two generators of $\bar{\mathcal{H}}_{Lee}(D_1)$ associated with orientations compatible with D_0.

2) D_0 is a two component link and D_1 is a knot:

   In this scenario, assigning an orientation to D results in $\bar{c}$ being a positive crossing. Under this choice, the two orientations of D are compatible with two of the orientations of D_0. Furthermore, the two orientations of D_0 are compatible with the two orientations of D_1 that do not arise directly from D:

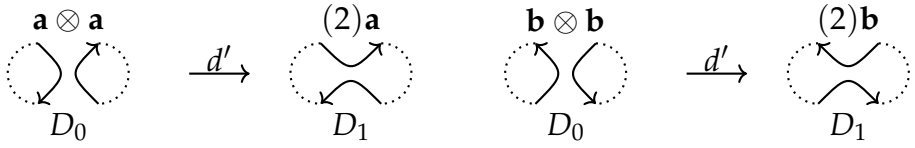

   In this case, the map $d'^{*} : \bar{\mathcal{H}}_{Lee}(D_0) \longrightarrow \bar{\mathcal{H}}_{Lee}(D_1)$ likewise maps the generators of $\bar{\mathcal{H}}_{Lee}(D_0)$ to the generators of $\bar{\mathcal{H}}_{Lee}(D_1)$ that inherit compatible relative orientations.

The exactness of the sequence (4.1.2) allows us to bound the dimension of the Lee homology. By accounting for the behavior of these generators, we obtain:

$$dim(\bar{\mathcal{H}}_{Lee}(D)) \leq dim(\bar{\mathcal{H}}_{Lee}(D_0)) + dim(\bar{\mathcal{H}}_{Lee}(D_0)) - 4.$$

Applying the inductive hypothesis for knots and 2-component links and using the fact that $dim(\bar{\mathcal{H}}_{Lee}(D)) = dim(\mathcal{H}_{Lee}(D))$ we conclude:

$$dim(\mathcal{H}_{Lee}(D)) \leq 2 + 4 - 4 = 2.$$

Together with the lower bound previously established, this proves the result for knots.

Case 2: D is the diagram of a 2 component link:

We now consider the case of a 2 component link L with diagram D having c crossings.

- If $D = D_1 \sqcup D_2$ is a disjoint union of two knot diagrams D_1 and D_2, with $c_{D_1}, c_{D_2} \leq c$, then the Lee homology satisfies $\bar{\mathcal{H}}_{Lee}(D) = \bar{\mathcal{H}}_{Lee}(D_1) \otimes \bar{\mathcal{H}}_{Lee}(D_2)$. By the knot case, we obtain

$$2^2 = 4 \leq dim(\bar{\mathcal{H}}_{Lee}(D)) \leq dim(\bar{\mathcal{H}}_{Lee}(D_1)) \cdot dim(\bar{\mathcal{H}}_{Lee}(D_2)) = 4.$$

- Otherwise, we can choose a crossing such that both D_0 and D_1 are diagrams of knots. In this case,

$$2^2 = 4 \leq dim(\bar{\mathcal{H}}_{Lee}(D)) \leq dim(\bar{\mathcal{H}}_{Lee}(D_1)) + dim(\bar{\mathcal{H}}_{Lee}(D_2)) = 4.$$

To prove that $\dim(\bar{\mathcal{H}}_{Lee}(D)) = 2^n$ for any n-component link, we assume the statement holds for all links with $k < n$ components. When we examine an n-component link diagram D, we encounter two possibilities:

- If D is a disjoint union of two sub-links, L_1 and L_2, with n_1 and n_2 components respectively ($n_1 + n_2 = n$), the homology decomposes via the tensor product:
$$\bar{\mathcal{H}}_{Lee}(D) \cong \bar{\mathcal{H}}_{Lee}(L_1) \otimes \bar{\mathcal{H}}_{Lee}(L_2)$$
By the inductive hypothesis, $\dim(\bar{\mathcal{H}}_{Lee}(L_1)) = 2^{n_1}$ and $\dim(\bar{\mathcal{H}}_{Lee}(L_2)) = 2^{n_2}$. Therefore:
$$\dim(\bar{\mathcal{H}}_{Lee}(D)) = 2^{n_1} \cdot 2^{n_2} = 2^{n_1+n_2} = 2^n.$$

- If the link is not a disjoint union, we can always identify a crossing between two different components. Changing or smoothing this crossing reduces the number of components. Specifically, we can choose a crossing such that the smoothings D_0 and D_1 result in diagrams with $n-1$ components. Applying the inductive hypothesis to these $(n-1)$-component links, we know:
$$\dim(\bar{\mathcal{H}}_{Lee}(D_0)) = 2^{n-1} \quad \text{and} \quad \dim(\bar{\mathcal{H}}_{Lee}(D_1)) = 2^{n-1}.$$
Using the dimension inequality derived from the long exact sequence (the same technique used in the 2-component case):
$$\dim(\bar{\mathcal{H}}_{Lee}(D)) \leq \dim(\bar{\mathcal{H}}_{Lee}(D_0)) + \dim(\bar{\mathcal{H}}_{Lee}(D_1))$$
$$\dim(\bar{\mathcal{H}}_{Lee}(D)) \leq 2^{n-1} + 2^{n-1} = 2^n.$$

Since we know from the construction of Lee homology that there are at least 2^n generators (two for each component's orientation), we have the lower bound $2^n \leq \dim(\bar{\mathcal{H}}_{Lee}(D))$. Combined with the inductive upper bound 2^n, we conclude that:
$$\dim(\bar{\mathcal{H}}_{Lee}(D)) = 2^n.$$

Finally, let D be an n-component link D. Either D is a disjoint union of link diagrams of fewer components, or there exists a crossing such that both D_0 and D_1 are diagrams of $(n-1)$-component links. Applying an induction hypothesis on the number of components and the same technique as for the 2 components case, we can deduce
$$dim(\mathcal{H}_{Lee}(D)) = dim(\bar{\mathcal{H}}_{Lee}(D)) = 2^n,$$
as required □

In view of the previous result, we have substantial information about Lee homology, we know its dimension and we have an explicit description of its generators. We can be even more precise and determine the homological degree supporting each generator.

Proposition 4.13. *[Lee05, Proposition 4.3] Let L be an oriented link with n-components $L_1, ..., L_n$. For each orientation $o \in Or(L)$, the corresponding generator $\mathfrak{s}_o$ lies in homological degree*

$$\mathfrak{s}_o \in \mathcal{H}^i_{Lee}(L) \qquad \text{where} \quad i = 2 \cdot \sum_{p \in E_o, q \notin E_o} lk(L_p, L_q).$$

Here, $E_o \subseteq \{1, 2, ..., n\}$ is the set of indices of the components of L whose orientations must be reversed in order to obtain the orientation o from the fixed reference orientation of L.

Proof. Let $\theta \in Or(L)$ be the given orientation of the link L, with diagram D and let $o \in Or(L)$ be another orientation. Define $E_o \subseteq \{1, ..., n\}$ to be the set of the indexes of components L_p of L whose orientations must be reversed in order to obtain o from θ. Denote by n_+ and n_- the number of positive and negative crossings of D with respect to the orientation θ, and by $n_+(o)$, $n_-(o)$ the corresponding numbers with respect to the orientation o.

Recall that, in the oriented resolution associated to $\mathfrak{s}_o$, a positive crossing is resolved by a 0-smoothing and a negative crossing by a 1-smoothing. The homological degree of a vector is defined as the number of 1-resolution minus the number of negative crossings of the diagram D with its given orientation θ. Hence, if denoted by $i_{(\mathfrak{s}_o)}$ the homological degree of $\mathfrak{s}_o$ we have

$$i_{(\mathfrak{s}_o)} = n_-^{\mathfrak{s}_o} - n_-,$$

where $n_-^{\mathfrak{s}_o}$ is the number of 0-smoothing appearing in the oriented resolution corresponding to o. Recall also that the linking number between two components L_p and L_q, with associated oriented diagrams D_p and D_q respectively, is given by:

$$2 \cdot lk(L_p, L_q) = 2 \cdot lk(D_p, D_q) = n_+(D_p, D_q) - n_-(D_p, D_q),$$

where $n_+(D_p, D_q)$ and $n_-(D_p, D_q)$ denote the number of positive and negative crossings involving an arc of the sub-diagrams D_p and another arc of the sub-diagrams D_q, respectively, with respect to the original orientation θ of D.

Observe that the sign of a crossings between two distinct components L_p and L_q changes if and only if exactly one of the two involved components has its orientation reversed. Thus,

$$\begin{aligned} n_+(D_p, D_q) - n_-(D_p, D_q) &= n_-(-D_p, D_q) - n_-(D_p, D_q) = \\ &= n_-(D_p, -D_q) - n_-(D_p, D_q), \end{aligned}$$

where $-D_p$ (resp.$-D_q$) denotes the correspoding diagram with reversed orientation. We can now decompose the difference $n_-^{\mathfrak{s}_o} - n_-$ according to the components of the link:

$$\begin{aligned} n_-^{\mathfrak{s}_o} - n_- = \sum_{p,q \in Eo} (n_-^{\mathfrak{s}_o}(D_p, D_q) - n_-(D_p, D_q)) + \sum_{p,q \notin Eo} (n_-^{\mathfrak{s}_o}(D_p, D_q) - n_-(D_p, D_q)) + \\ \sum_{p \in E_o, q \notin Eo} (n_-^{\mathfrak{s}_o}(D_p, D_q) - n_-(D_p, D_q)). \end{aligned} \tag{4.4}$$

For the previous remark, if both $p, q \in E_o$ or both $p, q \notin E_o$ the signs of crossings between them do not change. Hence, $n_-^{\mathfrak{s}_o}(D_p, D_q) = n_-(D_p, D_q)$ in these cases. Therefore, equation (4.4) becomes:

$$\begin{aligned} n_-^{\mathfrak{s}_o} - n_- &= \sum_{p \in E_o, q \notin E_o} (n_-^{\mathfrak{s}_o}(D_p, D_q) - n_-(D_p, D_q)) = \\ &= \sum_{p \in E_o, q \notin E_o} (n_-(-D_p, D_q) - n_-(D_p, D_q)) = \\ &= \sum_{p \in E_o, q \notin E_o} (n_+(D_p, D_q) - n_-(D_p, D_q)) = \\ &= \sum_{p \in E_o, q \notin E_o} 2 \cdot lk(D_p, D_q). \end{aligned}$$

Finally,

$$i_{(\mathfrak{s}_o)} = \sum_{p \in E_o, q \notin E_o} 2 \cdot lk(L_p, L_q),$$

which proves the Proposition. □

Definition 4.14 (Canonical generators). Let D be an oriented diagram of a link L. For each orientation $o \in Or(L)$, the elements $\mathfrak{s}_o$ constructed as described above are referred to as the *canonical generators* of the Lee homology $\mathcal{H}_{Lee}(L)$.

The name canonical generators is justified by the following proposition.

Proposition 4.15. *[Ras10] If L and $\tilde{L}$ are related by a Reidemeister moves, then an orientation $o \in Or(L)$ induces an orientation $\tilde{o}$ on $\tilde{L}$ and the induced isomorphism in homology $\rho_i * ([\mathfrak{s}_o])$ is a nonzero multiple of $[\mathfrak{s}_{\tilde{o}}]$*

Remark 4.16. The ρ_i are the maps defined by Lee in [Lee05].

Proof. The proof can be found in [Ras10, Section 6]. □

We can conclude that the Lee homology of a knot has the following structure.

$$\mathcal{H}^i_{Lee}(K) = \begin{cases} \mathbb{Q} \oplus \mathbb{Q} & \text{if } i = 0, \\ 0 & \text{otherwise.} \end{cases} \tag{4.5}$$

Moreover, for any m-component link, we have

$$dim(\mathcal{H}^i_{Lee}(L)) = |\{o \in Or(L) : \ i = 2 \cdot \sum_{p \in E_o, q \notin E_o} lk(L_p, L_q)\}|.$$

4.1.3 Example

Let us now compute the Lee homology of the Hopf link oriented as shown.

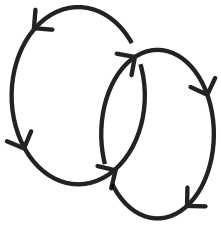

Figure 4.3

According to Theorem 4.12, the dimension of the Lee homology is expected to be 4, as the Hopf link is a 2 components link. Furthermore, Proposition 4.13 allows us to determine the specific homological degrees of its generators based on the link's internal data. In the diagram D in Figure 4.3, the link is composed of two components, L_1 and L_2, with linking number $lk(L_1, L_2) = 1$. Using these parameters, we obtain:

$$\mathcal{H}^i_{Lee}(L) = \begin{cases} \mathbb{Q} \oplus \mathbb{Q} & \text{if } i = 0, 2 \\ 0 & \text{otherwise.} \end{cases} \tag{4.6}$$

We will compute the Lee homology of the oriented Hopf link in two complementary ways. First, we will carry out the computation directly from the definition of the Lee complex. Then, we will reinterpret the result in terms of the canonical generators associated with the orientations of the link.

Computing Lee homology from the complex:

We begin by computing the Lee homology directly from the definition of the Lee complex $\mathcal{C}_{Lee}(D)$. We will refer to the complex constructed in Exercise 3.29, now equipped with the modified differential $d' = d + \phi$. Rather than reproducing the entire complex, we only present the matrix of the differential d'. In this matrix, the contributions coming from the Lee deformation ϕ are highlighted in red, in order to distinguish them from the original Khovanov differential.

$$M(d^0) = \begin{pmatrix} 1 & 0 & 0 & 1 \\ 1 & 0 & 0 & 1 \\ 0 & 1 & 1 & 0 \\ 0 & 1 & 1 & 0 \end{pmatrix}$$

We deduce:

$$ker(d^0) = Span\{v^+ \otimes v^+ - v^- \otimes v^-,\, v^+ \otimes v^- - v^- \otimes v^+\},$$

$$Im(d^0) = Span\{(v^+, v^+),\, (v^-, v^-)\}.$$

$$M(d^1) = \begin{pmatrix} 0 & 0 & 1 & -1 \\ 1 & -1 & 0 & 0 \\ 1 & -1 & 0 & 0 \\ 0 & 0 & 1 & -1 \end{pmatrix}$$

Hence,

$$Ker(d^1) = Span\{(v^+, v^+), (v^-, v^-)\}$$

$$Im(d^1) = Span\{v^+ \otimes v^+ + v^- \otimes v^-,\; v^+ \otimes v^- + v^- \otimes v^+\}$$

Hence the Lee homology is:

$$\mathcal{H}_{Lee}(D)^0 = Ker(d^0) = Span\{v^+ \otimes v^+ - v^- \otimes v^-,\; v^+ \otimes v^- - v^- \otimes v^+\} \cong \mathbb{Q} \oplus \mathbb{Q}.$$

$$\mathcal{H}^1(D) = \frac{Ker(d^1)}{Im(d^0)} = \frac{Span\{(v^+,\, v^+), (v^-,\, v^-)\}}{Span\{(v^+,\, v^+), (v^-,\, v^-)\}} = 0.$$

$$\mathcal{H}^2(D) = \frac{V_1 \otimes V_2\{4\}}{Im(d^1)} = \frac{V_1 \otimes V_2\{4\}}{Span\{v^+ \otimes v^+ + v^- \otimes v^-,\; v^+ \otimes v^- + v^- \otimes v^+\}} =$$

$$= Span\{v^+ \otimes v^+,\, v^+ \otimes v^-\} \cong \mathbb{Q} \oplus \mathbb{Q}.$$

Hence, $\mathcal{H}_{Lee}(D)^0$ is generated by two elements $(v^+ \otimes v^- - v^- \otimes v^+)$ and $(v^+ \otimes v^+ - v^- \otimes v^-)$ and $\mathcal{H}_{Lee}(D)^2$ is generated by $v^+ \otimes v^+$ and $v^+ \otimes v^-$.

Lee homology via canonical generators:

The Hopf link admits four distinct orientations. Denote by O the given orientation of the link L, by $\bar{O}$ its reversed orientation, by o the orientation in which only the first component is reversed with respect to O, and by $\bar{o}$ the orientation in which only the second component is reversed. Label the diagram D of the Hopf link such that the first component corresponds to the one on the left. The four oriented diagrams are illustrated in Figure 4.4.

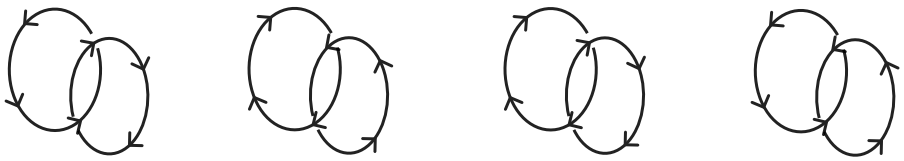

Figure 4.4: *The four possible oriented diagrams of D of the Hopf link. From left to right D_O, $D_{\bar{O}}$, D_o and $D_{\bar{o}}$, respectively.*

From these oriented diagrams, one can construct the canonical generators of the Lee homology following the procedure outlined previously. The process involves:

- resolve the diagram in the only orientation-preserving way,
- assign to each circle of the resolution a label **a** or **b** following the rules (4.1.2).

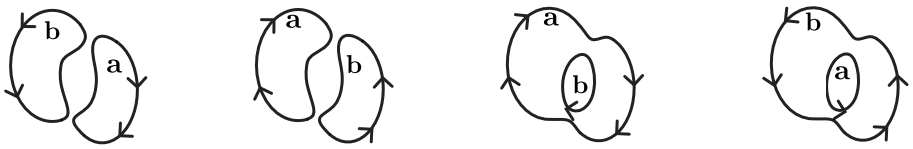

Figure 4.5: *The four generators of the Hopf link Lee homology.*

Consider first the diagram D_O with orientation O. After performing an orientation-preserving resolution, we obtain the corresponding configuration. Assigning the appropriate labels to the circles according to the prescribed rules yields:

$$\mathfrak{s}_O = \mathbf{b} \otimes \mathbf{a} \in \mathcal{H}^i_{Lee}(L),$$

where $i = \sum_{p \in E_O, q \notin E_O} 2 \cdot lk(L_p, L_q)$ with $E_O \subset \{1, 2\}$. Since $E_O = \emptyset$, it follows that $i = 0$.

For the reverse orientation $D_{\bar{O}}$, applying the same procedure gives:

$$\mathfrak{s}_{\bar{O}} = \mathbf{a} \otimes \mathbf{b} \in \mathcal{H}^i_{Lee}(L),$$

where $i = \sum_{p \in E_{\bar{O}}, q \in \complement E_{\bar{O}}} 2 \cdot lk(L_p, L_q)$ and $\complement E_{\bar{O}}$ is the complement in $\{1,2\}$ of $E_{\bar{O}}$. As $\complement E_{\bar{O}} = \emptyset$, we again have $i = 0$.

Next, consider D_o where only the first component is reversed. The orientation-preserving resolution and labeling produce:

$$\mathfrak{s}_o = \mathbf{a} \otimes \mathbf{b} \in \mathcal{H}^i_{Lee}(L),$$

with $i = \sum_{p \in E_o, q \in \complement E_o} 2 \cdot lk(L_p, L_q)$. Since $E_o = \{1\}$, it follows that $i = 2 \cdot \sum lk(L_1, L_2) = 2 \cdot 1 = 2$.

Finally, for $D_{\bar{o}}$, , where only the second component is reversed, we obtain:

$$\mathfrak{s}_{\bar{o}} = \mathbf{b} \otimes \mathbf{a} \in \mathcal{H}^i_{Lee}(L),$$

where $i = \sum_{p \in E_{\bar{o}}, q \in \complement E_{\bar{o}}} 2 \cdot lk(L_p, L_q)$. Given that $E_{\bar{o}} = \{2\}$, we compute $i = 2 \cdot \sum lk(L_2, L_1) = 2 \cdot 1 = 2$.

From these results, we conclude that $\mathcal{H}^0_{Lee}(L)$ is generated by $\mathfrak{s}_O$ and $\mathfrak{s}_{\bar{O}}$, while $\mathcal{H}^2_{Lee}(L)$ is generated by $\mathfrak{s}_o$ and $\mathfrak{s}_{\bar{o}}$. This outcome is consistent with the computations obtained by evaluating the Lee homology directly from the chain complex.

4.1.4 The Frobenius Algebra arising from Lee homology

We have already seen that in the original formulation of Khovanov homology, the underlying *Frobenius algebra* is

$$V = A = \mathbb{Q}[x]/(x^2),$$

Lee's construction replaces this algebra with a filtered Frobenius algebra

$$V = A_{Lee} = \mathbb{Q}[x]/(x^2 - 1),$$

which gives rise to a 2-dimensional Topological Quantum Filed Theory, as for the Khovanov homology.

A natural question may arise: for what Frobenius algebra does this construction (cube resolution and $2d$-TQFT) produce a link invariant?

Mackaay, Turner and Vaz solved this problem in [MTV13]. In this section, we will not see any proof of the theorems since it is not our aim to go into the details of it, but it is interesting to have an idea of these subject.

For $c, h, t \in \mathbb{Q}$ with $c \neq 0$, we define

$$A_{c,h,t} := \mathbb{Q}[x]/(x^2 - hx - t)$$

to be a Frobenius algebra with comultiplication defined by:

$$\Delta(v^+) = \Delta(\mathbf{1}) = \frac{1}{c}(v^- \otimes v^+ + v^+ \otimes v^- - h(v^+ \otimes v^-)),$$

$$\Delta(v^-) = \Delta(\mathbf{x}) = \frac{1}{c}(v^- \otimes v^- + t(v^+ \otimes v^-)),$$

and counit by:

$$\epsilon(v^+) = \epsilon(\mathbf{1}) = 0 \qquad\qquad \epsilon(v^-) = \epsilon(\mathbf{x}) = c$$

Remark 4.17. $A_{1,0,0}$ is the Frobenius algebra that comes from the Khovanov homology theory, on the other hand, for Lee homology theory, the underlying Frobenius algebra is $A_{1,0,1}$.

Theorem 4.18. *If A is a Frobenius algebra producing a link isotopy invariant arising from the cube resolution construction, then A is isomorphic to $A_{c,h,t}$ for some $c, h, t \in \mathbb{Q}$ and $c \neq 0$.*

Peculiarly, the Khovanov and the Lee homologies are essentially the only two link homology theories that one can produce, in the sense of this proposition:

Proposition 4.19 ([MTV13])**.** *The link homology theory produced by the Frobenius Algebra $A_{c,h,t}$ is isomorphic to:*

i. Khovanov homology, if $h^2 + 4t = 0$,

ii. Lee homology otherwise.

4.2 Spectral sequence and Khovanov homology

The algebraic construction carried out in the previous section reveals a fundamental relation between Khovanov homology and Lee homology. The two theories are defined by chain complexes that share the same underlying graded module but differ in their differentials: the Khovanov differential d is homogeneous with respect to the quantum grading j, while the Lee differential $d' = d + \phi$ is not, with the perturbation ϕ raising the quantum grading by 4. As a consequence, the two homology theories have strikingly different characters. Khovanov homology $\mathcal{H}^{*,*}(L)$ is a bigraded invariant of considerable complexity, sensitive to subtle features of the knot type, yet difficult to compute in general. Lee homology $\mathcal{H}_{Lee}(L)$, by contrast, is entirely determined by the number of components of L: it is isomorphic to $\mathbb{Q}^{2^m}$ for any m-component link, spanned by explicit canonical generators whose construction we recalled in the previous section. The former is rich but computationally intractable; the latter is computable but carries no information beyond the number of components.

An appropriate framework for studying the relationship between these two theories is that of *filtered complexes* and their associated *spectral sequences* (see Appendix 5.4). The key observation is that, although d' is not homogeneous with respect to j, it never lowers the quantum grading. The Lee complex therefore admits a natural filtration by quantum degree, and the associated spectral sequence interpolates between the two theories in a precise sense: its E^0-page is the Khovanov chain complex, its E^1-page is Khovanov homology, and it converges to Lee homology.

This interpolation is not merely of theoretical interest. The filtration on the Lee complex induces a filtration on Lee homology through the convergence of the spectral sequence, and it is precisely this filtered structure that underlies the definition of the Rasmussen s-invariant explained in Section 4.3.

We refer the reader to Appendix 5.4, based on [Cho06], for the necessary background on spectral sequences of filtered complexes.

4.2.1 Construction

The Filtration on the Lee Complex

Let D be a diagram of an oriented link L with m components. Recall from the previous section that the Lee differential decomposes as

$$d' = d + \phi,$$

where d is the original Khovanov differential, preserving the quantum grading j, and ϕ raises it by 4:

$$\mathcal{C}_{Lee}^{i,j}(D) \xrightarrow{d'} \mathcal{C}_{Lee}^{i+1,j}(D) \oplus \mathcal{C}_{Lee}^{i+1,j+4}(D),$$

where,

$$d : \mathcal{C}_{Lee}^{i,j}(D) \longrightarrow \mathcal{C}_{Lee}^{i+1,j}(D), \qquad \phi : \mathcal{C}_{Lee}^{i,j}(D) \longrightarrow \mathcal{C}_{Lee}^{i+1,j+4}(D).$$

This decomposition suggests filtering the Lee complex by the quantum grading. For each pair (i, j), define

$$G^{i,j} := \bigcup_{k \geq j} \mathcal{C}_{Lee}^{i,k}(D).$$

Remark 4.20. Since the quantum grading in Lee homology changes by multiples of 2, one have, $G^{i,j} = G^{i,j+1}$ whenever j has the same parity as the number m of components of D, and $G^{i,j} = G^{i,j-1}$ otherwise.

In each homological degree i, this gives a finite nested sequence of subgroups

$$0 =: G^{i,j_M+2} \subseteq G^{i,j_M} \subseteq \ \ldots \ \subseteq G^{i,j_m+2} \subseteq G^{i,j_m} = \mathcal{C}_{Lee}^{i}(D),$$

where j_m and j_M denote respectively the minimum and maximum quantum degrees for which $\mathcal{C}_{Lee}^{i,j}(D)$ is non-trivial.

By construction, the differential d' respects the filtration:

$$d'(G^{i,j}) \subseteq G^{i+1,j} \qquad \forall\, i, j.$$

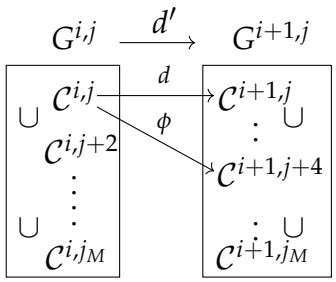

This is the key structural observation: although d' is not homogeneous with respect to j, it never lowers the quantum grading, and therefore $\mathcal{C}_{Lee}(D)$ equipped with $\{G^{i,j}\}$ is a *filtered chain complex*.

4.2.2 The Pages of the Spectral Sequence

The 0-page

The 0-page of the spectral sequence is the associated graded complex of the filtration:

$$E^0_{i,j} := G^{i,j}/G^{i,j+2} = (\cup_{k\geq j}\mathcal{C}^{i,j}(D))/(\cup_{k\geq j+2}\mathcal{C}^{i,j}(D)) \cong \mathcal{C}^{i,j}(D).$$

Remark 4.21. If j does not have the same parity as the number m of components of D, then $E^0_{i,j} = 0$ by the parity consideration above.

Since any finite-dimensional vector space over $\mathbb{Q}$ splits non-canonically over any subspace, we may decompose each homological chain group as

$$\mathcal{C}^i(D) \cong \bigoplus_{j\geq j_m}^{j_M} E^0_{i,j} \cong \bigoplus_{j\geq j_m}^{j_M} \mathcal{C}^{i,j}(D).$$

The Lee differential d', respecting the filtration, induces a boundary map

$$\partial^0 : \bigoplus_{j\geq j_m}^{j_M} E^0_{i,j} \longrightarrow \bigoplus_{j\geq j_m}^{j_M} E^0_{i+1,j},$$

such that $\partial^0(E^0_{i,j}) \subseteq E^0_{i+1,j}$, i.e.,

$$\partial^0 : E^0_{i,j} \longrightarrow E^0_{i+1,j}$$

on each graded piece. To see this, note that two elements of $G^{i,j}$ differing by an element of $G^{i,j+2}$ are mapped by d' to elements of $G^{i+1,j}$ differing by an element of $d'(G^{i,j+2}) \subseteq G^{i+1,j+2}$, so the induced map on the quotient $E^0_{i,j} = G^{i,j}/G^{i,j+2}$ is well defined. Since the only component of $d' = d + \phi$ that preserves the quantum grading is the Khovanov differential d, we conclude $\partial^0 = d$ and therefore

$$(E^0_{*,*}, \partial^0) \cong (\mathcal{C}^{*,*}(D), d).$$

The 0-page of the spectral sequence is thus precisely the Khovanov chain complex of D.

$$\begin{array}{ccccccc}
\cdots & \xrightarrow{\partial^0} & E^0_{i-1,j_m} & \xrightarrow{\partial^0} & E^0_{i,j_m} & \xrightarrow{\partial^0} & E^0_{i+1,j_m} & \xrightarrow{\partial^0} \cdots \\
\cdots & \xrightarrow{\partial^0} & 0 & \xrightarrow{\partial^0} & 0 & \xrightarrow{\partial^0} & 0 & \xrightarrow{\partial^0} \cdots \\
\cdots & \xrightarrow{\partial^0} & E^0_{i-1,j_m+2} & \xrightarrow{\partial^0} & E^0_{i,j_m+2} & \xrightarrow{\partial^0} & E^0_{i+1,j_m+2} & \xrightarrow{\partial^0} \cdots \\
 & & \vdots & & \vdots & & \vdots & \\
 & & \vdots & & \vdots & & \vdots & \\
\cdots & \xrightarrow{\partial^0} & E^0_{i-1,j_M} & \xrightarrow{\partial^0} & E^0_{i,j_M} & \xrightarrow{\partial^0} & E^0_{i+1,j_M} & \xrightarrow{\partial^0} \cdots
\end{array}$$

The E^1-page

Taking homology of the 0-page with respect to $\partial^0 = d$, we obtain

$$E^1_{i,j} := H^i(E^0_{*,j}, \partial^0) \cong \mathcal{H}^{i,j}(L),$$

so the 1-page is naturally identified with the Khovanov homology of L. The Lee differential d' then induces a differential on the 1-page,

$$\partial^1 : E^1_{i,j} \longrightarrow E^1_{i+1,j+1}.$$

However, by the parity remark above, one of the two groups $E^1_{i,j}$ or $E^1_{i+1,j+1}$ is always trivial for any fixed j, since consecutive quantum degrees of different parity cannot be both non-zero. Therefore $\partial^1 = 0$, and the E^1-page coincides with Khovanov homology equipped with the zero differential:

$$(E^1_{*,*}, \partial^1) \cong (\mathcal{H}^{*,*}(L), 0).$$

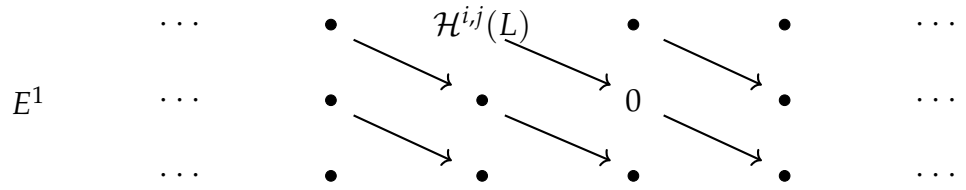

Higher pages

Since $\partial^1 = 0$, the E^2-page coincides with the E^1-page. More generally, since the perturbation ϕ raises the quantum grading by exactly 4, a degree argument shows

that the differential ∂^r on the E^r-page maps $E^r_{i,j}$ to $E^r_{i+1,j+r}$, and can therefore only be non-zero when r is a multiple of 4. In particular, $\partial^2 = \partial^3 = 0$, and the first potentially non-trivial differential appears on the E^4-page:

$$\partial^4 : E^4_{i,j} \longrightarrow E^4_{i+1,j+4}.$$

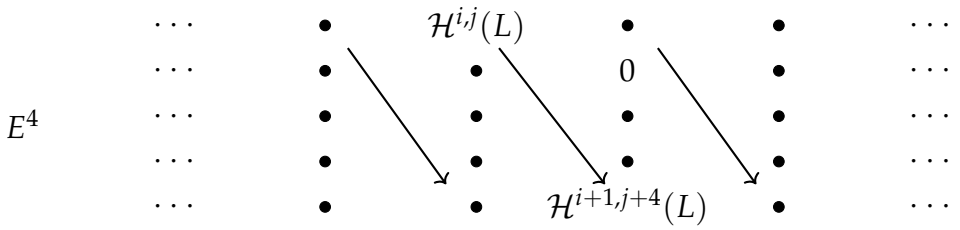

Whether ∂^4 is actually non-zero depends on the specific knot, and its non-triviality is precisely what distinguishes knots whose Khovanov homology does not already coincide with their Lee homology.

4.2.3 Convergence

Applying the standard convergence theorem for spectral sequences of finite filtered complexes (see Appendix 5.4, Theorem 5.48), we obtain the following fundamental result:

Theorem 4.22. *[Ras10] There exists a spectral sequence with E^0-page isomorphic to the Khovanov chain complex $\mathcal{C}^{*,*}(D)$, whose E^1-page is isomorphic to the Khovanov homology $\mathcal{H}^{*,*}(L)$, and which converges to the Lee homology $\mathcal{H}_{Lee}(L)$. Moreover, the E^1-page and all higher pages are invariants of the link L, independent of the choice of diagram D.*

Proof. The existence of the spectral sequence and the identification of its pages follow from the filtration constructed above together with the standard theory of spectral sequences of filtered complexes, as recalled in Appendix 5.4. The invariance of the higher pages is established in [Ras10, Theorem 2.1]. □

Remark 4.23. The spectral sequence does not in general collapse at the E^1-page. For most knots, the higher differentials $\partial^4, \partial^8, \ldots$ are non-trivial, meaning that Khovanov homology genuinely differs from Lee homology and the spectral sequence provides non-trivial information about the relationship between the two. For the unknot and more generally for knots whose Khovanov homology is already as

thin as possible, the spectral sequence collapses at E^2, but this is the exception rather than the rule.

Transition to the Rasmussen s-invariant

The spectral sequence constructed above does more than establish a formal relationship between Khovanov homology and Lee homology. The filtration on the Lee complex induces a filtration on the E^∞-page, and hence on Lee homology itself, and it is precisely this filtered structure that carries the geometric information about the knot. For a knot K, the two canonical generators $\mathfrak{s}_o$ and $\mathfrak{s}_{\bar{o}}$ of Lee homology each sit at a specific filtration level, and the average of these two filtration levels turns out to be a knot invariant. This is the Rasmussen s-invariant, whose definition and properties we develop in Section 4.3.

We conclude this section showing a practical example on the computation of the Lee spectral sequence of the trefoil 3_1.

4.2.4 Example

We illustrate the spectral sequence construction explicitly for the right-handed trefoil knot 3_1 working over $\mathbb{Q}$. Recall that we have already computed the Khovanov complex $\mathcal{C}(3_1)$ in Section 3.3. Since $E^0_{i,j} \cong \mathcal{C}^{i,j}(3_1)$, the E^0-page of the spectral sequence is the Khovanov chain complex equipped with the differential $\partial^0 = d$:

$$
\begin{array}{lccccccccc}
j=1\text{:} & 0 \longrightarrow & \mathbb{Q} & \xrightarrow{d} & 0 & \xrightarrow{d} & 0 & \xrightarrow{d} & \mathbb{Q} & \longrightarrow 0 \\
j=3\text{:} & 0 \longrightarrow & \mathbb{Q} & \xrightarrow{d} & \mathbb{Q}^2 & \xrightarrow{d} & \mathbb{Q}^2 & \xrightarrow{d} & \mathbb{Q} & \longrightarrow 0 \\
j=5\text{:} & 0 \longrightarrow & \mathbb{Q} & \xrightarrow{d} & \mathbb{Q}^2 & \xrightarrow{d} & \mathbb{Q}^2 & \xrightarrow{d} & \mathbb{Q} & \longrightarrow 0 \\
j=7\text{:} & 0 \longrightarrow & 0 & \xrightarrow{d} & 0 & \xrightarrow{d} & \mathbb{Q} & \xrightarrow{d} & \mathbb{Q} & \longrightarrow 0 \\
j=9\text{:} & 0 \longrightarrow & 0 & \xrightarrow{d} & 0 & \xrightarrow{d} & 0 & \xrightarrow{d} & \mathbb{Q} & \longrightarrow 0 \\
 & & i=0 & & i=1 & & i=2 & & i=3 &
\end{array}
$$

Taking homology with respect to $\partial^0 = d$, we obtain the E^1-page, which is the Khovanov homology $\mathcal{H}^{*,*}(3_1)$ over $\mathbb{Q}$:

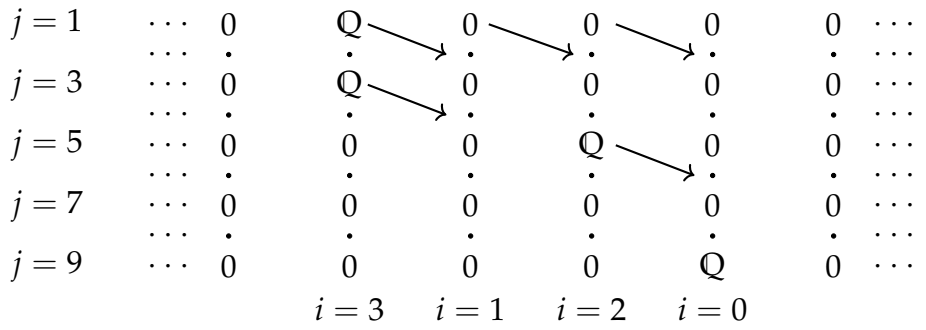

Since the quantum grading changes by 2 for a knot and ∂^1 would map $E^1_{i,j}$ to $E^1_{i+1,j+1}$, which lands in a trivial grading level by parity, we have $\partial^1 = 0$. Similarly, $\partial^2 = \partial^3 = 0$, and therefore $E^1 = E^2 = E^3 = E^4$ as bigraded vector spaces.

The first potentially non-trivial differential appears on the E^4-page, where $\partial^4 : E^4_{i,j} \to E^4_{i+1,j+4}$. In the case of the trefoil, the only non-trivial instance (the one in red in the figure above) of this map is

$$\partial^4 : E^4_{2,5} \longrightarrow E^4_{3,9}, \qquad \mathbb{Q} \longrightarrow \mathbb{Q}.$$

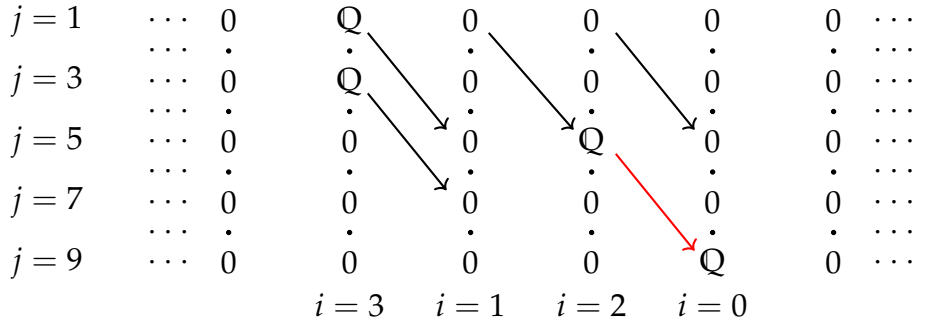

To compute this map explicitly, we return to the level of the Lee complex and recall the differential $(d')^2$ from the resolution at the second crossing:

$$(d')^2 : V_1 \otimes V_2 \oplus V_1 \otimes V_2 \oplus V_1 \otimes V_3\{5\} \longrightarrow V_1 \otimes V_2 \otimes V_3\{6\}$$
$$(v_{1,1} \otimes v_{1,2},\, v_{2,1} \otimes v_{2,2},\, v_{3,1} \otimes v_{3,3}) \longmapsto \Delta'(v_{1,2}) - \Delta'(v_{2,1}) + \Delta'(v_{3,1}).$$

The homology class in $E^4_{2,5} \cong \mathcal{H}^{2,5}(3_1)$ is represented by

$$[(v^- \otimes v^+,\, v^- \otimes v^+,\, -v^- \otimes v^+)].$$

Applying ϕ (the non-Khovanov part of d'), we obtain

$$\partial^4[(v^- \otimes v^+,\, v^- \otimes v^+,\, -v^- \otimes v^+)] = [v^- \otimes \Delta'(v^+) - \Delta'(v^-) \otimes v^+ - v^- \otimes \Delta'(v^+)] =$$

$$= [v^- \otimes (v^+ \otimes v^- + v^- \otimes v^+) - (v^+ \otimes v^+ + v^- \otimes v^+) \otimes v^+ -$$
$$v^- \otimes (v^+ \otimes v^- + v^- \otimes v^+)] = [-v^+ \otimes v^+ \otimes v^+ - v^- \otimes v^+ \otimes v^-] =$$
$$= [-v^+ \otimes v^+ \otimes v^+] \in \mathcal{H}^{3,9}(3_1),$$

where the last equality uses the relation $v^- \otimes v^+ \otimes v^- = 0$ in the Lee complex. This is precisely the generator of $E^4_{3,9} \cong \mathbb{Q}$, and therefore ∂^4 is an isomorphism.

Taking homology with respect to ∂^4, both $E^4_{2,5}$ and $E^4_{3,9}$ are killed, and we obtain

$$E^5_{i,j} = \begin{cases} \mathbb{Q} & \text{if } (i,j) = (0,1), \\ \mathbb{Q} & \text{if } (i,j) = (0,3), \\ 0 & \text{otherwise.} \end{cases}$$

Since all subsequent differentials ∂^r for $r \geq 5$ necessarily vanish by degree considerations (there are no more non-trivial groups to map between), the spectral sequence stabilises at the E^5-page, and therefore $E^5 = E^\infty$.

We conclude that the Lee homology of the trefoil knot is

$$\mathcal{H}_{Lee}(3_1) = \mathbb{Q} \oplus \mathbb{Q},$$

concentrated in homological degree 0, and spanned by the canonical generators

$$\mathfrak{s}_{3_1} = [v^- \otimes v^+ - v^+ \otimes v^-] \quad \text{(quantum degree } j = 3),$$

$$\bar{\mathfrak{s}}_{3_1} = [v^- \otimes v^-] \quad \text{(quantum degree } j = 1).$$

This confirms the general structure theorem for Lee homology of knots (Proposition 4.13, and exhibits explicitly how the spectral sequence interpolates between the four-dimensional Khovanov homology and the two-dimensional Lee homology of the trefoil.

4.3 Rasmussen s-invariant

Building on the spectral sequence from Khovanov homology to Lee homology, Rasmussen introduced a powerful numerical invariant, $s(K) \in 2\mathbb{Z}$ [Ras10], known as the *s-invariant*. This invariant arises from the filtration on Lee homology induced by the quantum grading on the Khovanov complex, and can be extracted from the behavior of the spectral sequence at its terminal page.

Despite its combinatorial origin, the s-invariant encodes deep geometric information on the knot. By providing a sharp lower bound for the smooth sliced

genus, $g_*(K)$, it famously yielded the first purely combinatorial proof of the Milnor Conjecture for torus knots, a result previously accessible only through gauge-theoretic methods.

In this subsection, we formalize the definition of $s(K)$ via the filtered Lee complex and detail its fundamental properties following [Ras10].

4.3.1 Definition

Let K be a knot. To define the s invariant, we first need a quantum grading on $\mathcal{H}_{Lee}(K)$. Since the spectral sequence described above converges to $\mathcal{H}_{Lee}(K)$, it is reasonable to adopt as a grading the quantum grading defined on $\mathcal{C}_{Lee}(D)$ induced by this spectral sequence. We denote this grading by s.

If $x \in \mathcal{H}^0_{Lee}(K)$, then x can be written as a sum of homogeneous components $v_1, ...v_k \in \mathcal{H}^0_{Lee}(K)$: $x = \sum_{i=1...k} v_i$. We then define:

$$s(x) := \min\{\, j(v_i) \mid \; i \in \{1,..,k\}, \;\; x = \sum_{i=1...k} v_i \quad : v_i \in \mathcal{H}_{Lee}(K) \text{ homogeneous}\},$$

where $j(v) := deg(v) + r + n_+ - 2n_-$ is the quantum grading on the Khovanov complex introduced in Chapter 3.

Definition 4.24. Let K be a knot, we define:

$$s_{max}(K) = \max\{s(x) : \; x \in \mathcal{H}_{Lee}(K), \;\; x \neq 0\},$$

$$s_{min}(K) = \min\{s(x) : \; x \in \mathcal{H}_{Lee}(K), \;\; x \neq 0\}.$$

Example 4.25 (Unknot). For the unknot ◯, the Lee homology is given by

$$\mathcal{H}_{Lee}(\bigcirc) =< v^+, v^- >,$$

hence $s_{max}(\bigcirc) = 1$ and $s_{min}(\bigcirc) = -1$.

Example 4.26 (Right-handed trefoil knot). Recall that for the right-handed trefoil knot is given by:

$$\mathcal{H}^0_{Lee}(\text{trefoil}) = \mathbb{Q} \oplus \mathbb{Q},$$

generated by $[v^- \otimes v^+ - v^+ \otimes v^-]$ of degree 3 and $v^- \otimes v^-$ of degree 1. Hence, $s_{max}(\text{trefoil}) = 3$ and $s_{min}(\text{trefoil}) = 1$.

Our aim now is to prove the following fundamental property:

Proposition 4.27. *[Ras10, Proposition 3.3]*

$$s_{max}(K) = s_{min}(K) + 2.$$

This result allows us to define the Rasmussen s-invariant consistently:

Definition 4.28 (Rasmussen s invariant). Let K be a knot, we define the *Rasmussen $s(K)$ invariant* of K as:

$$s(K) = s_{max}(K) - 1 = s_{min}(K) + 1.$$

Example 4.29. From Example 4.25 and Example 4.26 we can easily recover the s-invariant for the unknot U an the right-handed trefoil knot 3_1:

$$s(U) = s_{max}(U) - 1 = 1 - 1 = 0,$$

$$s(3_1) = s_{max}(3_1) - 1 = 3 - 1 = 1.$$

The spectral sequence from Khovanov homology to Lee homology guarantees that $s(K)$ is a knot invariant, independent of the chosen diagram (Theorem 4.22).

Remark 4.30. Since the quantum degrees of the Lee complex of a knot are always odd (see Remark 3.10), $s(K)$ is always an even integer.

To prove Proposition 4.3.1, we first need some preliminary results on the Lee homology of links.

Proposition 4.31. *[Ras10, Lemma 3.5] Let L be an n-component link. There is a direct sum decomposition of $\mathcal{H}_{Lee}(L) \cong \mathcal{H}^{+1}_{Lee}(L) \oplus \mathcal{H}^{-1}_{Lee}(L)$ where $\mathcal{H}^{+1}_{Lee}(L)$ is a subgroup of $\mathcal{H}_{Lee}(L)$ generated by all elements whose quantum grading s is congruent to n mod 4 and $\mathcal{H}^{-1}_{Lee}(L)$ is generated by all elements whose quantum grading is congruent to $2 + n$ mod 4.*

Moreover, for any $o \in Or(L)$ orientation of L, the elements $\mathfrak{s}_o + \mathfrak{s}_{\bar{o}}$ and $\mathfrak{s}_o - \mathfrak{s}_{\bar{o}}$ lie in different summands of this decomposition.

Remark 4.32. The shift by n in the quantum degree mod 4 is necessary to account for the parity of the quantum grading when the number of components n is odd.

The notation $\mathcal{H}^{+1}_{Lee}(L)$ and $\mathcal{H}^{-1}_{Lee}(L)$ reflects the case of the unknot, for which $\mathcal{H}_{Lee}(\bigcirc)$ decomposes into two subgroups of degrees 1 and -1. In the literature, these summands are often denoted by $\mathcal{H}^{o}_{Lee}(L)$ and $\mathcal{H}^{e}_{Lee}(L)$, for odd and even.

Proof. The first part of the statement follows from the fact that the quantum grading jumps in two units together with the observation that m' and Δ' have quantum degree 0 and 4, respectively. Consequently, the Lee differential preserves the quantum grading modulo 4, yielding the claimed decomposition.

For the second statement, if $j(v^-)$ is congruent with $n+2$ mod 2, we construct a linear map $\iota : \mathcal{C}_{Lee}(D) \longrightarrow \mathcal{C}_{Lee}(D)$ that acts as the identity on $\mathcal{C}^{-1}_{Lee}(D)$ and as minus the identity on $\mathcal{C}^{+1}_{Lee}(D)$. Define a linear map

$$\begin{aligned} i : & V \longrightarrow V \\ & v^+ \longmapsto -v^+ \\ & v^- \longmapsto v^- \end{aligned}$$

With respect to the basis$\{\mathbf{a}, \mathbf{b}\}$, this map satisfies $\iota(\mathbf{a}) = \mathbf{b}$, $\iota(\mathbf{b}) = \mathbf{a}$ and we compute $\mathbf{a} + i(\mathbf{a}) = i(\mathbf{b}) + \mathbf{b} = v^- + v^+ + v^- - v^+ = 2v^-$, $\mathbf{a} - i(\mathbf{a}) = i(\mathbf{b}) - \mathbf{b} = v^- + v^+ - v^- + v^+ = 2v^+$. To each state s we consider the associated diagram resolution D_s and we set $k(s)$ the number of its components. We define $i^{\otimes k(s)} : V^{\otimes k(s)} \longrightarrow V^{\otimes k(s)}$ as

$$i^{\otimes k(s)}(v_1 \otimes .... \otimes v_{k(s)}) = i(v_1) \otimes ... \otimes i(v_{k(s)})$$

and we set ι to agree with $i^{\otimes k(s)}$ on each summand $V^{\otimes k(s)}$ of $\mathcal{C}_{Lee}(D)$.

Now, let $o \in Or(L)$ be an orientation of L and $\mathfrak{s}_o$ the corresponding canonical generator. By construction, we get

$$\iota(\mathfrak{s}_o) = \mathfrak{s}_{\bar{o}}.$$

Moreover, for any homogeneous $v \in \mathcal{C}^{+1}(D)$ we have $(id + \iota)(v) = 0$ and $(id - \iota))(v) = 2v$, while for any $w \in \mathcal{C}^{-1}(D)$, $(id + \iota)(w) = 2w$ and $(id - \iota))(w) = 0$.

We observe that $\mathfrak{s}_o$ is not homogeneous with respect to the quantum grading j, moreover it it decomposes uniquely as $\mathfrak{s}_o = \mathfrak{s}_o^+ + \mathfrak{s}_o^-$ where $\mathfrak{s}_o^+, \mathfrak{s}_o^- \neq 0$, $\mathfrak{s}_o^+ \in \mathcal{C}^{+1}(D)$ and $\mathfrak{s}_o^- \in \mathcal{C}^{-1}(D)$. Therefore,

$$\mathfrak{s}_o + \iota(\mathfrak{s}_o) = \mathfrak{s}_o^+ + \mathfrak{s}_o^- + \iota(\mathfrak{s}_o^+ + \mathfrak{s}_o^-) = \mathfrak{s}_o^+ + \mathfrak{s}_o^- - \mathfrak{s}_o^+ + \mathfrak{s}_o^- = 2\mathfrak{s}_o^- \in \mathcal{C}^{-1}(D),$$

$$\mathfrak{s}_o - \iota(\mathfrak{s}_o) = \mathfrak{s}_o^+ + \mathfrak{s}_o^- - \iota(\mathfrak{s}_o^+ + \mathfrak{s}_o^-) = \mathfrak{s}_o^+ + \mathfrak{s}_o^- + \mathfrak{s}_o^+ - \mathfrak{s}_o^- = 2\mathfrak{s}_o^+ \in \mathcal{C}^{+1}(D).$$

If instead the quantum grading of v^- is congruent to n mod 4 the result follows by exchanging the roles of $\mathcal{C}^{-1}_{Lee}(D)$ with $\mathcal{C}^{+1}_{Lee}(D)$, or eventually by replacing $\iota = -i^{\otimes k}$. □

Remark 4.33. Proposition 4.31 implies that for a knot K, it holds:

$$\mathcal{H}_{Lee}(K) \cong < \mathfrak{s}_o - \mathfrak{s}_{\bar{o}} > \oplus < \mathfrak{s}_o + \mathfrak{s}_{\bar{o}} > .$$

Corollary 4.34. *Let K be a knot; then*

$$s(\mathfrak{s}_o) = s(\mathfrak{s}_{\bar{o}}) = s_{min}(K).$$

Proof. Recall that, for all knots K, $dim(\mathcal{H}_{Lee}(K)) = 2$, and $\mathfrak{s}_o$ is not homogeneous. We have $s(\mathfrak{s}_o) = \min\{s(v_i) : s(\mathfrak{s}_o) = \sum v_i,\ v_i \text{ homogeneous}\}$, hence $s(\mathfrak{s}_o), s(\mathfrak{s}_{\bar{o}}) \leq s(\mathfrak{s}_o \pm \mathfrak{s}_{\bar{o}})$. Therefore,

$$s(\mathfrak{s}_o) = s(\mathfrak{s}_o) = s_{min}(K).$$

□

Corollary 4.35. *Given a knot K, $s_{max}(K) > s_{min}(K)$.*

Proof. It is a direct consequence of Proposition 4.31 and the previous remark. □

Lemma 4.36. *[Ras10, Lemma 3.8] Let K_1 and K_2 be two non oriented knots. There exists a homological short exact sequence:*

$$0 \longrightarrow \mathcal{H}_{Lee}(K_1 \#_{\times} K_2) \xrightarrow{\beta*} \mathcal{H}_{Lee}(K_1) \otimes \mathcal{H}_{Lee}(K_2) \xrightarrow{d'_*} \mathcal{H}_{Lee}(K_1 \#_{=} K_2) \longrightarrow 0.$$

where $K_1 \#_{\times} K_2$ and $K_1 \#_{=} K_2$ denote the connected sum of K_1 and K_2 connected in the two possible ways.

Remark 4.37. The connected sum of two knots is only well defined once orientations are chosen. Throughout the statement and proof of this lemma, we slightly abuse notation by referring to both diagrams Figure 4.6 as connecting sum of the K_1 and K_2, even though, without fixed orientations, they may represent different knots. We denote by $K_1 \#_{\times} K_2$ the diagram in which the two knots are joined

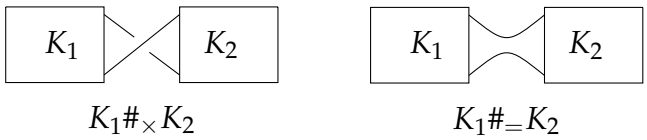

$K_1 \#_{\times} K_2$ $\qquad$ $K_1 \#_{=} K_2$

Figure 4.6: *The two way of connecting two knots.*

through a positive crossing at the connecting point, and by $K_1 \#_{\times} K_2$ the diagram in which the connection is made without introducing a crossing.

Proof. Consider the following diagram for $K_1\#K_2$: $K_1\#_\times K_2$ the diagram obtained by joining K_1 and K_2 as showed in Figure 4.3.1, so that its 0 smoothing is a two component link $K_1 \sqcup K_2$ and its 1 smoothing is $K_1\#_= K_2$:

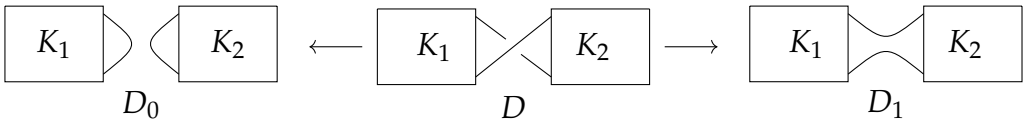

We can now apply the long exact sequence (4.1.2) constructed in the proof of Theorem 4.12. Using the same argument as in case 2), together with the known structure of Lee homology, this long exact sequence reduces to the short exact sequence

$$0 \longrightarrow \mathcal{H}^0_{Lee}(D) \xrightarrow{\beta^*} \mathcal{H}^0_{Lee}(D_0) \xrightarrow{d'^*} \mathcal{H}^0_{Lee}(D_1) \longrightarrow 0$$

The two generators of $\mathcal{H}^0_{Lee}(D)$ map under the two generators of $\mathcal{H}^0_{Lee}(D_0)$ whose orientations are coherent with theirs, while the two remaining generators of $\mathcal{H}^0_{Lee}(D_0)$ map the two generators of $\mathcal{H}^0_{Lee}(D_1)$. Consequently, since $\mathcal{H}_{Lee}(K_1 \sqcup K_2) \cong \mathcal{H}_{Lee}(K_1) \otimes \mathcal{H}_{Lee}(K_2)$ we obtain the required short exact sequence.

By construction, the map β^* has filtered degree -1. To see that d'^* is a filtered map of degree -1 we need to consider the quantum degree s induced by the filtration. Although the differential d' has quantum degree 0, the absence of a quantum degree shift in the associated spectral sequence implies that the induced map d'^* decreases the grading by one. □

Proof of Proposition 4.3.1 . We now specialize the exact sequence of Lemma 4.36 by taking $K_1 = K$ and $K_2 = \bigcirc$ the unknot. Let $\mathfrak{s}_\mathbf{a}$ and $\mathfrak{s}_\mathbf{b}$ be the two canonical generators of K according to the label near the connecting point, and let $\mathbf{a}$ and $\mathbf{b}$ be the corresponding canonical generators of the unknot U. Without loss of generality, we can assume that $s(\mathfrak{s}_\mathbf{a} - \mathfrak{s}_\mathbf{b}) = s_{max}(K)$.

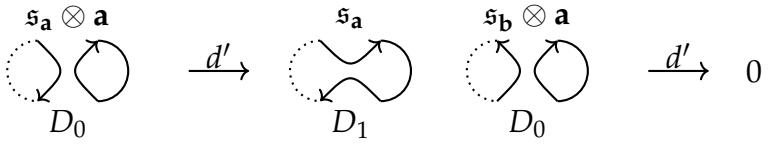

From the above figure, we see that $d'((\mathfrak{s}_\mathbf{a} - \mathfrak{s}_\mathbf{b}) \otimes \mathbf{a}) = \mathfrak{s}_\mathbf{a}$. Moreover, since d'^* is a filtered map of degree -1, it follows that:

$$s((\mathfrak{s}_\mathbf{a} - \mathfrak{s}_\mathbf{b}) \otimes \mathbf{a}) \leq s(\mathfrak{s}_\mathbf{a}) + 1.$$

Using the assumption $s(\mathfrak{s}_\mathbf{a} - \mathfrak{s}_\mathbf{b}) = s_{max}(K)$, this inequality becomes

$$s_{max}(K) - 1 \leq s_{min}(K) + 1.$$

therefore,

$$s_{min}(K) < s_{max}(K) \leq s_{min}(K) + 2.$$

This implies $s_{max}(K) = s_{min}(K) + 2$. which completes the proof. □

Example 4.38. Let us evaluate the s invariant for the trefoil knot  . We recall from the previous example that

$$\mathcal{H}^0_{Lee}(\text{}) = \mathbb{Q} \oplus \mathbb{Q},$$

generated by $[v^- \otimes v^+ - v^+ \otimes v^-]$ of s-degree 3 and $v^- \otimes v^-$ of s-degree 1. Hence, the Proposition 4.3.1 holds and

$$s(\text{}) = s_{max}(3_1) - 1 = 3 - 1 = 2,$$

or equivalently,

$$s(\text{}) = s_{min}(3_1) + 1 = 1 + 1 = 2.$$

4.3.2 Properties

The Rasmussen s invariant behaves well under the connected sum and with respect to the mirror image. In particular, the following holds:

Proposition 4.39. *([Ras10, Proposition 3.9]) Let K^* be the mirror image of a knot K. Then we have:*

$$s_{max}(K^*) = -s_{min}(K),$$
$$s_{min}(K^*) = -s_{max}(K),$$
$$s(K^*) = -s(K).$$

Proof. The proof can be found in [Ras10]. □

Proposition 4.40. *([Ras10, Proposition 3.3]) Let K_1 and K_2 be two oriented knots. Then:*

$$s(K_1 \# K_2) = s(K_1) + s(K_2).$$

Proof. Choose a diagram of the connected sum $K_1 \# K_2$ so that the connected sum point is a positive crossing, as in the Lemma 4.36. For each K_i, we denote the canonical generators of $\mathcal{H}_{Lee}(K_i)$ by $\mathfrak{s}^i_{\mathbf{a}}$ and $\mathfrak{s}^i_{\mathbf{b}}$ according to the label near the connected point.

Consider the short exact sequence of Lemma 4.36. Since the oriented resolution of the diagram $K_1 \#_\times K_2$ coincides with the one of the disjoint union $K_1 \sqcup K_2$, the

map β^* sends one canonical generator $\mathfrak{s}_o$ of $\mathcal{H}_{Lee}(K_1\#K_2)$ to $\mathfrak{s}^1_{\mathbf{a}} \otimes \mathfrak{s}^2_{\mathbf{b}}$, and the other to $\mathfrak{s}^1_{\mathbf{b}} \otimes \mathfrak{s}^2_{\mathbf{a}}$. Since β^* is a filtered map of degree -1, we obtain

$$s(\mathfrak{s}_o) - 1 \leq s(\mathfrak{s}_{\mathbf{a}} \otimes \mathfrak{s}_{\mathbf{b}}),$$

$$s_{min}(K_1\#K_2) - 1 \leq s_{min}(K_1) + s_{min}(K_2).$$

Applying the same argument to the mirror knots K_1^* and K_2^* and using the identity $s_{min}(K^*) = -s_{max}(K)$, we get

$$s_{max}(K_1\#K_2) + 1 \geq s_{max}(K_1) + s_{max}(K_2).$$

Since $s_{max}(K) = s_{min}(K) + 2$, the latter inequality implies

$$s_{min}(K_1\#K_2) + 3 \geq s_{min}(K_1) + s_{min}(K_2) + 4,$$

and hence

$$s_{min}(K_1\#K_2) \leq s_{min}(K_1) + s_{min}(K_2) + 1.$$

Combining these inequalities, we conclude that

$$s_{max}(K_1\#K_2) = s_{max}(K_1) + s_{max}(K_2) - 1$$

Which prove the proposition. □

4.4 A bound for the slice genus

Before explaining how the Rasmussen s invariant provides a bound for the slice genus of a knot, we first need to introduce the definition of *slice genus*. The notion of knot genus was introduced in Section 1.2.3. The slice genus, however, concerns surfaces embedded in the four-dimensional ball D^4, whose boundary is a knot in S^3. Hence:

Definition 4.41 (Slice genus). The slice genus $g_*(K)$ of a knot K is defined as the minimum genus of a compact, connected, oriented surface in D^4, whose boundary is $K \subset S^3$, that is,

$$g_*(K) = \min\{g(S) : S \subset D^4 \text{ is a surface and } \partial S = K\}$$

Remark 4.42. Since any Seifert surface embedded in S^3 can also be viewed as a surface in D^4, it immediately follows that:

$$g_*(K) \leq g(K).$$

As in the case of the knot genus, the slice genus can be difficult to compute. This difficulty arises from the fact that even when a surface of a given genus spanning a knot is found, it is often unclear whether such a surface of strictly smaller genus exists. For this reason, effective lower bounds for the slice genus are particularly valuable. The Rasmussen s-invariant provides such a bound. Indeed, Rasmussen in [Ras10] proved that for every knot K, it holds:

$$|s(K)| \leq 2g_*(K).$$

We devote this section to the proof of this result.

Example 4.43 (Stevedore's knot). A classical example of a knot whose slice genus differs from its Seifert genus is the Stevedore's knot $K_{6,1}$ which has genus 1 and slice genus 0; in fact, it is a slice knot,meaning that it bounds a smoothed embedded disk in D^4 [BM+05].

The genus of $K_{6,1}$ can be calculated from a Seifert surface obtained from the minimal diagram taken from Rolfsen knot table [Rol76].

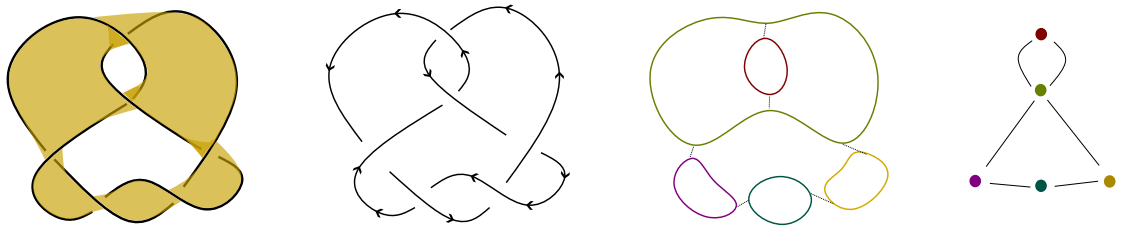

Figure 4.7: *Stevedore Seifert surface and its Seifert graph.*

Thanks to its Seifert graph we can use the formula introduced in Section 1.2.3, we can compute the genus of the Seifert surface obtained by applying the Seifert algorithm to the diagram of $K_{6,1}$ shown in Figure 4.7:

$$g(S) = \frac{E - V + 1}{2} = \frac{6 - 5 + 1}{2} = 1,$$

From [BM+05], we know that the Rasmussen s invariant of the Stevedore's knot is $s(K_{6,1}) = 0$. Consequently, the s invariant alone does not obstruct the existence of a slice surface of genus zero in D^4 bounding it. Indeed, in this case such a surface does exist: $K_{6,1}$ is a slice knot.

We now illustrate this fact by exhibiting sequence of equivalent knots from the standard diagram of $K_{6,1}$ to a slice diagram of $K_{6,1}$ (Figure 4.8). Such a sequence, referred to as a ribbon sequence, demonstrates that the knot bounds a ribbon disk in B^4:

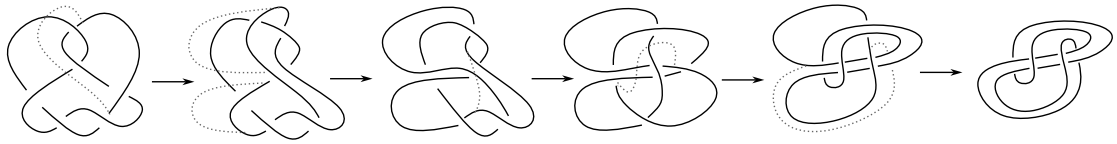

Figure 4.8: *A ribbon sequence for the Stevedore knot.*

With this representation, it is easy to see that the knot $K_{6,1}$ bounds a disk in D^4. See Figure 4.9

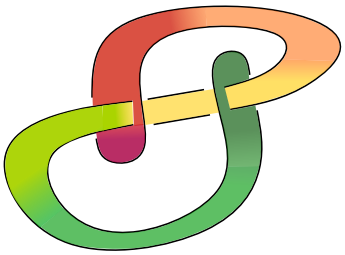

Figure 4.9: *The disk bounding the Stevedore's knot, the colors represent the fourth dimension.*

The proof of this important theorem is long and technical, and requires some notions on oriented cobordism between knot which can be found in [CS93]. For this reason, we will only outline the idea of the proof given by Rasmussen in [Ras10].

Given two links L_0 and L_1 in $\mathbb{R}^3$, there is an oriented cobordism $S \subset \mathbb{R}^3 \times [0,1]$ from L_0 to L_1. The key idea is to define a map $\phi_S : \mathcal{H}_{Lee}(L_0) \longrightarrow \mathcal{H}_{Lee}(L_1)$ induced by the cobordism S; moreover, we want this assignment to be functorial, in the sense that if S is the composition of two cobordisms S_0 and S_1, then ϕ_S is the composition of ϕ_{S_0} and ϕ_{S_1}.

This morphism can be construct as filtered map of degree equal to the Euler characteristic of S, $\chi(S)$, and behave well with respect to the canonical generators $\mathfrak{s}_o$.

Lemma 4.44. *Suppose S is an oriented cobordism from L_0 to L_1 which is weakly connected, in the sense that every component of S has a boundary component in L_0. Then $\phi_S([\mathfrak{s}_{o_0}])$ is a nonzero multiple of $[\mathfrak{s}_{o_1}]$.*

Lemma 4.45. *If S is a connected cobordism between knots K_0 and K_1, then ϕ_S is an isomorphism.*

Theorem 4.46. *[Ras10, Theorem 1] Let K be knot, then the following holds:*

$$|s(K)| \leq 2g_*(K).$$

Proof. Suppose $K \subset S^3$ bounds an oriented surface S of genus g in B^4. Removing a small disk from S gives a cobordism $S' = S - B^2$ from K to the unknot U, with Euler characteristic $\chi(S') = 1 - 2g - 1 = -2g$. Up to isotopy, we may take $K = S \cap \{0\}$ and $U = S \cap \{1\}$.

Let $x \in \mathcal{H}_{Lee}(K) - \{0\}$ be such that $s(x) = s_{max}(K)$. By Lemma 4.45, $\phi_S(x)$ is a nonzero element of $\mathcal{H}_{Lee}(U)$. Since ϕ_S is a filtered map of degree $-2g$, we have

$$s(\phi_s(x)) \geq s(x) - 2g.$$

On the other hand, the Lee homology of the unknot satisfies $s_{max}(U) = 1$, so

$$s(\phi_S(x)) \leq 1.$$

Combing these inequalities gives $s(x) \leq 2g + 1$, so $s_{max}(K) \leq 2g + 1$ and

$$s(K) \leq 2g.$$

To obtain the lower bound, we apply the same argument to the mirror knot K^*, which bounds a surface S^* of the same genus g. Using the fact that $s(K) = -s(K^*)$ we conclude.

$$-2g \leq s(K) \leq 2g.$$

Thus

$$|s(K)| \leq 2g_*(K).$$

□

For the family of positive knots (see Definition 1.39, the Rasmussen invariant gives a stronger and sharper result:

Theorem 4.47. *([Ras10, Theorem 1]) If K is a positive knot then:*

$$|s(K)| = s(K) = 2g_*(K) = 2g(K).$$

Proof. Since K is positive, we can compute $s(K)$ directly from any positive diagrams D. In such a diagram, the oriented resolution corresponds to the extreme corner of the cube resolution. Therefore, $\mathfrak{s}_o$ has homological degree 0 and $\mathcal{H}^{-1}_{Lee}(K) = 0$. Recall that the minimal quantum degree of the canonical generator

is $s(\mathfrak{s}_0) = s_{min}(K)$. If D has $n = n_+$ crossings and its oriented resolution D_o has k components, then:

$$s_{min}(K) = -k + n_+ = n - k.$$

This follows from the fact that $s(\mathfrak{s}_o) = deg((v^-)^{\otimes k})$. Therefore, by the definition of the Rasmussen invariant,

$$s(K) = n - k + 1.$$

On the other hand, applying the Seifert algorithm on D and the formula in (1.2.3), we deduce: $2g(K) \leq 2g(S) = n - k + 1 = s(K) \leq 2g_*(K)$. But, since $g_*(K) \leq g(K)$, we conclude:

$$|s(K)| = s(K) = 2g_*(K) = 2g(K),$$

as claimed. □

As an immediate corollary, Rasmussen [Ras10] obtain a purely Khovanov homology proof of the Milnor Conjecture, which was first proved using gauge theory by Kronheimer and Mrowka [KM93].

Corollary 4.48 (The Milnor Conjecture). *The slice genus of $T(p,q)$ torus knot is*

$$g_*(T(p,q)) = \frac{(p-1)(q-1)}{2}.$$

Proof. It is well-known that every torus knot $T(p,q)$ is positive. This property can be easily verified by inspecting its standard diagram (see Section 1.3), which contains $(p-1)q$ crossings all of them positive. Consequently, the Rasmussen invariant satisfies:

$$|s(K)| = s(K) = 2g_*(K) = 2g(K).$$

Applying Seifert's algorithm to this standard diagram, we obtain $k = p$ Seifert circles. Since the diagram has $n = (p-1)q$ crossings, and as in the previous proof we have that $s(K) = n - k + 1$, it follows that:

$$g_*(T(p,q)) = \frac{(p-1)q - p + 1}{2} = \frac{pq - q - p + 1}{2} = \frac{(p-1)(q-1)}{2}.$$

□

Chapter 5

Appendix

5.1 Graded Vector Spaces

The theory of Khovanov homology is built upon the framework of graded vector spaces, which provides the algebraic foundation for organizing homological information according to multiple degrees. We recall here the essential definitions and constructions based on [Wei94] and [Kho00].

Definition 5.1 (Graded vector space). A *graded vector space* over a field $\mathbb{F}$ is a vector space V together with a direct sum decomposition

$$V = \bigoplus_{i \in \mathbb{Z}} V^i,$$

where each V^i is a vector space over $\mathbb{F}$. The integer i is called the *degree* or *grading*, and elements of V^i are said to be *homogeneous of degree* i.

Example 5.2. The polynomial ring $\mathbb{F}[x]$ is a graded vector space with grading given by degree: $\mathbb{F}[x]^i$ consists of all polynomials of degree i, together with the zero polynomial.

Definition 5.3 (Morphism of graded vector spaces). A linear map $f : V \to W$ between graded vector spaces is a *morphism of degree* d (or a *homogeneous map of degree* d) if $f(V^i) \subseteq W^{i+d}$ for all $i \in \mathbb{Z}$. A morphism of degree 0 is called a *graded morphism* or simply a *morphism of graded vector spaces*.

Definition 5.4 (Grading shift). Let V be a graded vector space and $k \in \mathbb{Z}$. The *grading shift* $V\{k\}$ is the graded vector space defined by

$$V^i\{k\} = V^{i-k}.$$

Equivalently, if $v \in V$ is homogeneous of degree i, then v viewed as an element of $V\{k\}$ has degree $i + k$.

Notation 5.5. The shift notation varies in the literature. Some authors use $V[k]$ or $V(k)$ instead of $V\{k\}$. In Chapter 3, we adopt the curly bracket notation $V\{k\}$ for quantum grading shifts, reserving square brackets $V[k]$ for homological degree shifts, following the conventions of [Bar02].

Definition 5.6 (Bigraded vector space). A *bigraded vector space* is a vector space V equipped with a direct sum decomposition

$$V = \bigoplus_{i,j \in \mathbb{Z}} V^{i,j},$$

indexed by pairs of integers (i, j). Elements of $V^{i,j}$ are said to have *bidegree* (i, j).

Bigraded vector spaces arise naturally in Khovanov homology, where the first grading records homological information and the second records a quantum grading.

Definition 5.7 (Tensor product of graded spaces). Let V and W be graded vector spaces. Their *tensor product* $V \otimes W$ is the graded vector space with

$$(V \otimes W)^k = \bigoplus_{i+j=k} V^i \otimes W^j.$$

Proposition 5.8. *The grading shift satisfies the following properties:*

1. $(V\{k\})\{l\} = V\{k + l\}$,
2. $(V \oplus W)\{k\} = V\{k\} \oplus W\{k\}$,
3. $(V \otimes W)\{k\} \cong V\{k\} \otimes W \cong V \otimes W\{k\}$.

These formal properties ensure that grading shifts behave functorially and are compatible with the standard algebraic operations on vector spaces, as shown in [Bar02; Tur17].

5.2 Chain complexes and homology

We now introduce the notion of a chain complex of graded vector spaces, which forms the foundation for defining Khovanov homology. In this section we follow [Hat02] and [Wei94].

Definition 5.9 (Chain complex). A *chain complex* (C, d) of graded vector spaces is a sequence of graded vector spaces and morphisms

$$\cdots \xrightarrow{d_{i-2}} C^{i-1} \xrightarrow{d_{i-1}} C^i \xrightarrow{d_i} C^{i+1} \xrightarrow{d_{i+1}} \cdots$$

such that $d^2 = 0$, i.e., $d_i \circ d_{i-1} = 0$. The maps $d_i : C^i \to C^{i+1}$ are called *differentials* or *boundary maps*.

When the vector spaces in a chain complex are themselves graded, we obtain a bigraded structure.

Definition 5.10 (Bigraded chain complex). A *bigraded chain complex* is a chain complex $(C^{*,*}, d)$ where each C^i is a graded vector space, so that

$$C^i = \bigoplus_{j \in \mathbb{Z}} C^{i,j}.$$

The differential $d_i : C^{i,j} \to C^{i+1,j+k}$ has bidegree $(1, k)$ for some fixed integer k. When $k = 0$, the differential preserves the internal degree, which is the case for the Khovanov differential introduced in Section 3.1.

Remark 5.11. The condition $d^2 = 0$ ensures that the image of $d_{i-1} : C^{i-1} \to C^i$ is contained in the kernel of $d_i : C^i \to C^{i+1}$, i.e.,

$$Im(\, d_{i-1}\,) \subseteq Ker(\, d_i\,),$$

making it possible to define homology as a quotient.

Definition 5.12 (Homology). Let (C^*, d) be a chain complex. The *homology* of C^* is the graded vector space

$$H^i(C) = \frac{Ker(\, d_i : C^i \to C^{i+1})}{Im(\, d_{i-1} : C^{i-1} \to C^i)}.$$

Elements of $Ker(d)$ are called *cycles*, and elements of $Im(d)$ are called *boundaries*. Two cycles that differ by a boundary are said to be *homologous*.

For a bigraded chain complex, the homology inherits a bigrading:

Definition 5.13 (Bigraded homology). Let $(C^{*,*}, d)$ be a bigraded chain complex with differential of bidegree $(1, k)$. The *bigraded homology* is

$$H^{i,j}(C) = \frac{Ker(\, d_i : C^{i,j} \to C^{i+1,j+k}\,)}{Im(\, d_{i-1} : C^{i-1,j-k} \to C^{i,j}\,)}.$$

Definition 5.14 (Exact sequence). A chain complex (C^*, d) is called *exact* at C^i if $H^i(C) = 0$, i.e., if

$$Ker(\, d_i : C^i \to C^{i+1}) = Im(\, d_{i-1} : C^{i-1} \to C^i).$$

A complex that is exact everywhere is called an *exact sequence*.

Definition 5.15 (Short exact sequence). A *short exact sequence* is an exact sequence of the form

$$0 \longrightarrow A \xrightarrow{f} B \xrightarrow{g} C \longrightarrow 0.$$

Exactness at A means f is injective, exactness at C means g is surjective, and exactness at B means $Im(f) = Ker(g)$.

Proposition 5.16 (Splitting lemma). *Let $0 \to A \xrightarrow{f} B \xrightarrow{g} C \to 0$ be a short exact sequence of vector spaces. Then the sequence splits, i.e., $B \cong A \oplus C$.*

Proof. Over a field, every short exact sequence of vector spaces splits by choosing a basis. Specifically, since g is surjective, we can choose a section $s : C \to B$ (not necessarily a chain map) such that $g \circ s = \mathrm{id}_C$. Then the map $A \oplus C \to B$ given by $(a, c) \mapsto f(a) + s(c)$ is an isomorphism. □

Definition 5.17 (Chain map). A *chain map* $f : C \to D$ between two chain complexes (C, d_C) and (D, d_D) is a collection of linear maps $f^i : C^i \to D^i$ such that the following diagram commutes for all i:

$$\begin{array}{ccc} C^i & \xrightarrow{d_C} & C^{i+1} \\ {\scriptstyle f}\downarrow & & \downarrow{\scriptstyle f} \\ D^i & \xrightarrow{d_D} & D^{i+1} \end{array}$$

That is, $d_D \circ f = f \circ d_C$.

Remark 5.18. The commutativity condition ensures that chain maps preserve the structure of cycles and boundaries: if c is a cycle in C^*, then $f(c)$ is a cycle in D^*, and if c is a boundary, then $f(c)$ is a boundary.

Proposition 5.19. *A chain map $f : C^* \to D^*$ induces a map on homology*

$$f^* : H(C) \longrightarrow H(D).$$

Moreover, this construction satisfies:

1. *$id^* = id$ (identity maps induce identity on homology),*
2. *if $f : C^* \to D^*$ and $g : D^* \to E^*$ are two chain maps so that $g \circ f : C^* \to E^*$ is a chin map, then $(g \circ f)^* = g^* \circ f^*$ (composition is preserved).*

Proof. If $[c] \in H^i(C)$ is represented by a cycle $c \in Ker(d_C)$, then $f(c) \in Ker(d_D)$ since $d_D \circ f = f \circ d_C$. Moreover, if $c = d_C(b)$ is a boundary, then $f(c) = f(d_C(b)) = d_D(f(b))$ is also a boundary. Therefore f induces a well-defined map $f^* : [c] \mapsto [f(c)]$. □

Corollary 5.20. *If $f : C^* \to D^*$ is a chain map that is an isomorphism (i.e., each $f^i : C^i \to D^i$ is an isomorphism), then the induced map $(f^i)^* : H(C^i) \to H(D^i)$ is also an isomorphism.*

Proof. Since f is an isomorphism, it has an inverse $g : D \to C$ which is also a chain map. By functoriality, $g^* \circ f^* = (g \circ f)^* = \mathrm{id}^* = \mathrm{id}$, and similarly $f^* \circ g^* = \mathrm{id}$. Therefore f^* is an isomorphism. □

5.3 Frobenius Algebra and $2D$ TQFT

In this Section we will introduce the concepts of commutative Frobenius Algebra, and 2-dimension Topological Quantum Field Theory TQFT. The aim is to establish the connection between this to equivalent categories, which will illuminate the algebraic structure underlying the cobordism-based formulation of Khovanov homology in Section 3.5 of Chapter 3. For this Section we follow [Koc04] and [Abr97].

5.3.1 Cobordism

We first introduce the definition of cobordism, which provides the geometric foundation for Topological Quantum Field Theory.

Definition 5.21 (Unoriented cobordism). Let Σ_1 and Σ_2 two closed manifolds of dimension $n-1$. An *unoriented cobordism* between Σ_1 and Σ_2 is a compact manifold M of dimension n, whose boundary is $\Sigma_1 \cup \Sigma_2$. If there exist a cobordism between two manifolds, they are said to be *cobordant*.

Example 5.22. When $n = 2$, cobordisms are surfaces with boundary. For instance, a cylinder $S^1 \times [0,1]$ is a cobordism between two circles S^1 and S^1. A pair of pants

(a sphere with three boundary circles removed) provides a cobordism from one circle to two circles.

For the purposes of TQFT, we require oriented cobordisms, where we distinguish between "incoming" and "outgoing" boundaries, corresponding to past and future time.

Definition 5.23 (Oriented cobordism). Let Σ_0 and Σ_1 be two $n-1$ manifolds. An *oriented cobordism* between them is a oriented manifold M whose *in-boundary* is Σ_0 and *out-boundary* is Σ_1. We write:

$$\Sigma_0 \xRightarrow{M} \Sigma_1$$

Remark 5.24. The orientation-reversing convention for the in-boundary ensures that the induced orientation on ∂M from M matches the given orientations on both boundary components when viewed from inside M [Koc04].

Example 5.25. Consider $(1+1)$-dimensional cobordisms (surfaces with boundary between circles):

(a) The cylinder $[0,1] \times S^1$ is a cobordism from S^1 to S^1, representing the identity.
(b) A disk D^2 is a cobordism from the empty manifold $\emptyset$ to S^1, representing "creation".
(c) A disk (with reversed orientation on the boundary) is a cobordism from S^1 to $\emptyset$, representing "annihilation".
(d) A pair of pants is a cobordism from S^1 to $S^1 \sqcup S^1$, representing "splitting" or "comultiplication".
(e) A pair of pants (upside down) is a cobordism from $S^1 \sqcup S^1$ to S^1, representing "merging" or "multiplication".

See Figure 5.1.

Definition 5.26 (Composition of cobordisms). If $M_1 : \Sigma_0 \to \Sigma_1$ and $M_2 : \Sigma_1 \to \Sigma_2$ are oriented cobordisms, their *composition* is the cobordism $M_2 \circ M_1 : \Sigma_0 \to \Sigma_2$ obtained by gluing M_1 and M_2 along their common boundary Σ_1.

Example 5.27 (Composition of cobordisms). We illustrate composition in the category of $(1+1)$-dimensional cobordisms.

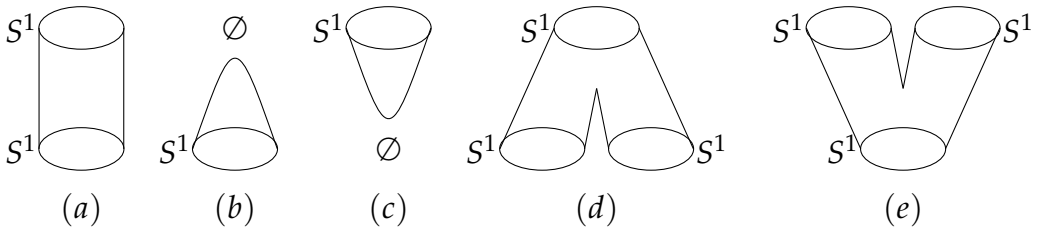

Figure 5.1: *The* $(1+1)$*-dimentional cobordisms described in Example 5.25*

(a) **Composing cylinders:** Let $M_1 : S^1 \to S^1$ be the cylinder $S^1 \times [0,1]$ and $M_2 : S^1 \to S^1$ be another cylinder $S^1 \times [1,2]$. Their composition $M_2 \circ M_1$ is obtained by gluing along the common boundary S^1, resulting in the longer cylinder $S^1 \times [0,2]$, which is diffeomorphic to $S^1 \times [0,1]$ by rescaling. This illustrates that the cylinder acts as an identity morphism.

(b) **Creation followed by annihilation:** Let $M_1 : \emptyset \to S^1$ be a disk D^2 (creation) and $M_2 : S^1 \to \emptyset$ be a disk with reversed boundary orientation (annihilation). Their composition $M_2 \circ M_1 : \emptyset \to \emptyset$ is obtained by gluing the two disks along their common boundary circle. The result is a closed surface. specifically, a 2-sphere S^2, which represents a cobordism from the empty set to itself.

(c) **Multiplication followed by comultiplication:** Consider $M_1 : S^1 \sqcup S^1 \to S^1$ given by a pair of pants (merging two circles into one) and $M_2 : S^1 \to S^1 \sqcup S^1$ given by an inverted pair of pants (splitting one circle into two). The composition $M_2 \circ M_1 : S^1 \sqcup S^1 \to S^1 \sqcup S^1$ is obtained by gluing the single-circle boundaries.

After gluing, we obtain a surface with two boundary circles at the bottom and two at the top. This surface is homeomorphic to a cylinder with two tubes attached, representing the composition $\delta \circ \mu : S^1 \sqcup S^1 \to S^1 \sqcup S^1$ in the Frobenius algebra which will be defined in Section 5.3.3.

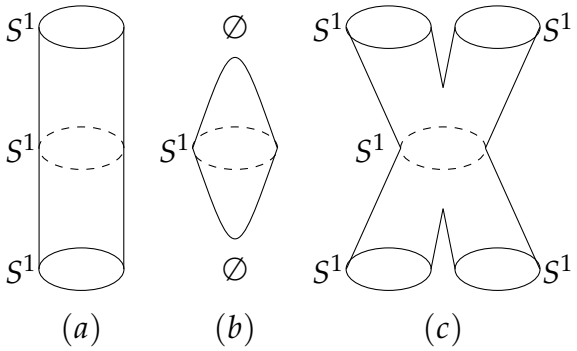

Figure 5.2: *Composition of cobordism showed in Example 5.27*

Remark 5.28. Composition of cobordisms is associative up to diffeomorphism, and the cylinder $\Sigma \times [0,1]$ acts as an identity. This makes oriented cobordisms into a category, denoted $\mathbf{Cob}_n$, where objects are closed oriented $(n-1)$-manifolds and morphisms are oriented n-dimensional cobordisms [Koc04].

5.3.2 Topological Quantum Field theory

For what we need, we can think about quantum field theory as a "function" that takes in input spaces and space times and associates to them state spaces and time evolution operators. The space is represented as an closed oriented $n-1$ manifold while the space time as an oriented n manifold whose in-boundary represents time 0 and out-boundary time 1.

Definition 5.29 (n-dimensional TQFT). An n-dimensional *topological quantum field theory* over a field $\mathbb{F}$ is a symmetric monoidal functor

$$Z : \mathbf{Cob}_n \to \mathbf{Vect}_{\mathbb{F}}$$

from the category of n-dimensional oriented cobordisms to the category of finite-dimensional $\mathbb{F}$-vector spaces. Specifically:

- To each closed oriented $(n-1)$-manifold Σ, Z assigns a finite-dimensional vector space $Z(\Sigma)$,
- To each oriented cobordism $M : \Sigma_0 \to \Sigma_1$, Z assigns a linear map $Z(M) : Z(\Sigma_0) \to Z(\Sigma_1)$,
- $Z(\Sigma_0 \sqcup \Sigma_1) = Z(\Sigma_0) \otimes Z(\Sigma_1)$ (monoidal structure),
- $Z(M_2 \circ M_1) = Z(M_2) \circ Z(M_1)$ (functoriality).

Example 5.30. For a $(1+1)$-dimensional TQFT, the basic building blocks are:

- $Z(\emptyset) = \mathbb{F}$,
- $Z(S^1) = V$ for some vector space V,
- $Z(\text{disk with 0 in, 1 out}) = \iota : \mathbb{F} \to V$ (unit),
- $Z(\text{disk with 1 in, 0 out}) = \epsilon : V \to \mathbb{F}$ (counit),
- $Z(\text{pants, 2 in 1 out}) = \mu : V \otimes V \to V$ (multiplication),

- $Z(\text{pants, 1 in 2 out}) = \delta : V \to V \otimes V$ (comultiplication).

The fundamental theorem, due to Dijkgraaf [Dij92] (see also [Koc04; Abr97]), states that $(1+1)$-dimensional TQFTs are completely classified by commutative Frobenius algebras, see Section 5.3.4, Theorem 5.36.

5.3.3 Frobenius Algebra

A Frobenius algebra $\mathcal{A}$ is a vector space equipped with compatible algebra and coalgebra structures. There are several equivalent definitions emphasizing different aspects of its structure. We present the definition most suited to the TQFT connection [Koc04]

Definition 5.31 ($\mathbb{F}$**-algebra).** Let $\mathbb{F}$ be a field. A $\mathbb{F}$-*algebra* is a $\mathbb{F}$-vector space A equipped with two $\mathbb{F}$-linear maps

$$\mu : A \otimes A \to A \quad \text{(multiplication)}, \qquad \iota : \mathbb{F} \to A \quad \text{(unit)},$$

such that the following diagrams commute:

Associativity:

$$\begin{array}{ccc} A \otimes A \otimes A & \xrightarrow{\mathrm{id}_A \otimes \mu} & A \otimes A \\ \downarrow{\scriptstyle \mu \otimes \mathrm{id}_A} & & \downarrow{\scriptstyle \mu} \\ A \otimes A & \xrightarrow{\mu} & A \end{array}$$

Unit conditions:

$$\begin{array}{ccc} \mathbb{F} \otimes A & \xrightarrow{\iota \otimes \mathrm{id}_A} & A \otimes A \\ & \searrow^{\cong} & \downarrow{\scriptstyle \mu} \\ & & A \end{array} \qquad \begin{array}{ccc} A \otimes \mathbb{F} & \xrightarrow{\mathrm{id}_A \otimes \iota} & A \otimes A \\ & \searrow^{\cong} & \downarrow{\scriptstyle \mu} \\ & & A \end{array}$$

where the diagonal maps are the canonical isomorphisms $\mathbb{F} \otimes A \cong A \cong A \otimes \mathbb{F}$ and $id_A : A \longrightarrow A$ is the identity map.

Definition 5.32 (Coalgebra over $\mathbb{F}$). A coalgebra over a field $\mathbb{F}$ is a $\mathbb{F}$-vector space together with two linear maps

$$\delta : A \to A \otimes A \quad \text{(comultiplication)}, \qquad \epsilon : A \to \mathbb{F} \quad \text{(counit)},$$

such that the following diagrams commute:

Coassociativity:

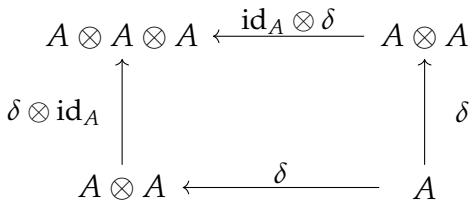

Counit conditions:

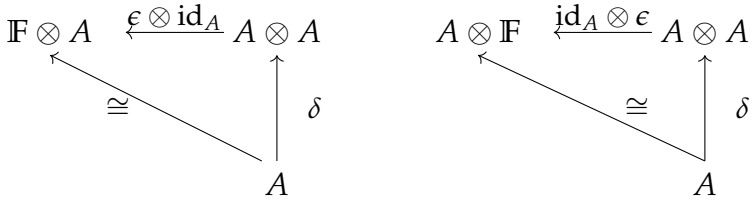

Remark 5.33. The coalgebra axioms are precisely the duals of the algebra axioms: they are obtained by reversing all arrows in the commutative diagrams.

Definition 5.34 (Frobenius condition). Let (A, μ, ι) be an algebra and (A, δ, ϵ) a coalgebra on the same vector space A. The *Frobenius condition* (or *Frobenius compatibility*) is the requirement that the following diagram commutes:

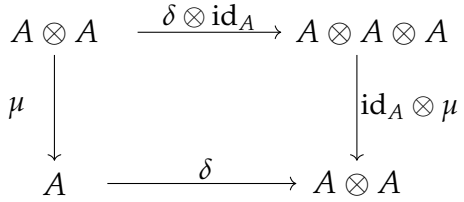

Equivalently: $(\mathrm{id}_A \otimes \mu) \circ (\delta \otimes \mathrm{id}_A) = \delta \circ \mu$.

Definition 5.35 (Frobenius algebra). A *Frobenius algebra* $\mathcal{A}$ is a quintuple $\mathcal{A} = (A, \mu, \iota, \delta, \epsilon)$ where:

- (A, μ, ι) is an algebra,
- (A, δ, ϵ) is a coalgebra,
- The Frobenius condition holds: $(\mathrm{id}_A \otimes \mu) \circ (\delta \otimes \mathrm{id}_A) = \delta \circ \mu$.

A Frobenius algebra is *commutative* if $\mu(a \otimes b) = \mu(b \otimes a)$ for all $a, b \in A$.

5.3.4 The TQFT-Frobenius Correspondence

The fundamental theorem connecting TQFTs and Frobenius algebras is the following:

Theorem 5.36. *[Koc04] There is an equivalence of categories between:*

- $(1+1)$*-dimensional topological quantum field theories over* $\mathbb{F}$*, and*
- *Commutative Frobenius algebras over* $\mathbb{F}$*.*

More precisely, given a $(1+1)$*-TQFT* Z*, the vector space* $A = Z(S^1)$ *inherits a commutative Frobenius algebra structure from the basic cobordisms. Conversely, given a commutative Frobenius algebra* A*, one can construct a* $(1+1)$*-TQFT* Z *by setting* $Z(S^1) = A$ *and defining* Z *on cobordisms via the algebra and coalgebra operations.*

Proof sketch. Given a $(1+1)$-TQFT Z, define $A = Z(S^1)$. The basic cobordisms provide the Frobenius structure:

- Multiplication $\mu : A \otimes A \to A$ comes from $Z(\text{pair of pants, 2 in 1 out})$,
- Unit $\iota : \mathbb{F} \to A$ from $Z(\text{disk, 0 in 1 out})$,
- Comultiplication $\delta : A \to A \otimes A$ from $Z(\text{pair of pants, 1 in 2 out})$,
- Counit $\epsilon : A \to \mathbb{F}$ from $Z(\text{disk, 1 in 0 out})$.

The associativity, unit, coassociativity, counit, and Frobenius conditions follow from functoriality applied to appropriate gluings of cobordisms. For complete details, see [Koc04, Theorem 2.4.10] or [Abr97, Chapter 3]. □

Remark 5.37. This correspondence is one of the most beautiful results in topological field theory. It shows that the purely topological notion of gluing surfaces corresponds precisely to algebraic operations in a Frobenius algebra.

5.4 Spectral sequences

This appendix provides a self-contained introduction to spectral sequences, following the intuitive approach of Chow [Cho06] and adjusting the indexes to be coherent with the notation in Section 4.2.

Spectral sequences are powerful algebraic tools that allow us to compute the homology of a complex object by successive approximations. Rather than presenting the general abstract theory, we focus on the specific framework needed for understanding the Lee spectral sequence in Chapter 4.

Spectral sequences address a fundamental challenge in homological algebra: computing the homology of a complicated chain complex. Given a chain complex (C, ∂):

$$\cdots \xrightarrow{\partial_{d-2}} C^{d-1} \xrightarrow{\partial_{d-1}} C^{d} \xrightarrow{\partial_{d}} C^{d+1} \xrightarrow{\partial_{d+1}} \cdots$$

where $\partial_d : C^d \to C^{d+1}$ satisfies $\partial_*^2 = 0$, we seek to compute the homology $H^d(C) = Ker(\partial_d)/Im(\partial_{d-1})$. When the complex is large or has intricate structure, this direct computation may be intractable. Spectral sequences provide a systematic method to compute this homology through successive approximations, exploiting additional structure on the complex in the form of a filtration.

We will omit subindex ∂_* in the rest of this section to avoid cumbersome notation.

5.4.1 Filtered chain Complexes

Definition 5.38 (Filtration). A *filtration* on a chain complex (C, ∂) is a nested sequence of subcomplexe of C

$$\cdots \subseteq G^{*,p+1} \subseteq G^{*,p} \subseteq G^{*,p-1} \subseteq \cdots \subseteq C^*$$

such that $\partial(G^{d,p}) \subseteq G^{d+1,p}$ for all p and d.

Remark 5.39. In literature the filtration is often noted as:

$$\cdots \subseteq F^{p+1}C^* \subseteq F^pC^* \subseteq F^{p-1}C^* \subseteq \cdots \subseteq C^*,$$

to emphasize the associated chain complex C.

The condition that ∂ respects the filtration ensures that each $G^{*,p}$ is itself a chain complex.

Example 5.40. Consider a chain complex $C = C^0 \oplus C^1 \oplus C^2$ with a filtration defined by

$$G^{*,0} = C^0 \oplus C^1 \oplus C^2, \quad G^{*,1} = C^1 \oplus C^2, \quad G^{*,2} = C^2, \quad G^{*,3} = 0.$$

If the differential respects this decomposition, this defines a valid filtration.

Given a filtration, we construct the *associated graded complex*, which treats each filtration level independently.

Definition 5.41 (**Associated graded complex**)**.** The associated graded complex of $(C^*, G^{*,p})$ is defined as

$$E^0_{p,d} = G^{d,p} / G^{d,p+1}$$

with differential $\partial^0 : E^0_{p,d} \to E^0_{p,d+1}$ induced from ∂.

Proposition 5.42. *The differential ∂^0 is well-defined.*

Proof. If $x, x' \in G^{p,d}$ differ by an element $y \in G^{d,p+1}$, then

$$\partial(x) - \partial(x') = \partial(y) \in \partial(G^{d,p+1}) \subseteq G^{d+1,p+1},$$

so $\partial(x)$ and $\partial(x')$ represent the same class in $E^0_{p,d+1} = G^{d+1,p} / G^{d+1,p+1}$. □

The E^0-page consists of the layers of the filtration, treated independently. We have discarded information about how these layers interact through the original differential.

5.4.2 Construction of the Spectral Sequence

We now construct a sequence of pages $E^1, E^2, E^3, \ldots$ pages by repeatedly taking homology.

Definition 5.43 (**The E^1-page**)**.** The E^1-page is obtained by taking the homology of E^0 with respect to ∂^0:

$$E^1_{p,d} = H^d(E^0_{p,*}, \partial^0) = \frac{ker(\partial^0 : E^0_{p,d} \to E^0_{p,d+1})}{Im(\partial^0 : E^0_{p,d-1} \to E^0_{p,d})}.$$

At the E^1-page, we have computed the homology of each filtered piece independently. This provides a first approximation to the homology of the full complex. However, in forming the associated graded E^0, we discarded information about cross-filtration interactions components of ∂ that map $G^{d,p}$ into $G^{d+1,p+r}$ for $r > 0$. These interactions reappear as higher differentials.

Definition 5.44 (**The E^r-page**). For $r \geq 1$, the E^r-page has a differential

$$\partial^r : E^r_{p,d} \to E^r_{p+r,d+1}$$

of bidegree $(r, 1)$, and the next page is defined by taking cohomology:

$$E^{r+1}_{p,d} = \frac{ker(\partial^r : E^r_{p,d} \to E^r_{p+r,d+1})}{Im(\partial^r : E^r_{p-r,d-1} \to E^r_{p,d})}.$$

The crucial feature is that ∂^r shifts the filtration index p by exactly r. This reflects a fundamental principle: the differential ∂^r detects interactions between filtration levels that are r steps apart. At E^0 and E^1, we only see what happens within each filtration level. At E^2, we see how adjacent levels interact. As r increases, we detect progressively more subtle long-range interactions in the filtration.

Remark 5.45. Elements of $E^r_{p,d}$ have *bidegree* (p, d), where p is the filtration degree and d is the internal degree. The differential ∂^r has bidegree $(r, 1)$: it increases the filtration degree by r and increases the internal degree by 1.

5.4.3 Convergence

Under suitable finiteness conditions, the spectral sequence stabilizes.

Definition 5.46 (**Convergence**). A spectral sequence converges if for each (p, d), there exists $R = R(p, d)$ such that

$$E^r_{p,d} = E^{r+1}_{p,d} = \cdots \qquad \text{for all } r \geq R.$$

We denote the stable value by $E^\infty_{p,d}$.

Theorem 5.47 (**Convergence for finite filtrations**). *Let $(C^*, \partial, G^{*,p})$ be a filtered chain complex satisfying:*

1. *Each C^d is finite-dimensional over a field $\mathbb{F}$,*
2. *The filtration is finite: there exist integers $p_0 < p_1$ such that*

$$G^{*,p_0} = C^* \quad \textit{and} \quad G^{*,p_1} = 0.$$

Then the spectral sequence converges: for each (p, d), there exists R such that $E^r_{p,d} = E^{r+1}_{p,d}$ for all $r \geq R$.

Proof. For fixed (p, d), the sequence

$$E^1_{p,d},\ E^2_{p,d},\ E^3_{p,d},\ \dots$$

is a sequence of subquotients of a finite-dimensional vector space, obtained by repeatedly taking kernels and cokernels. Each page $E^{r+1}_{p,d}$ is obtained from $E^r_{p,d}$ by taking $Ker(\partial^r)/Im(\partial^r)$, which is either equal to $E^r_{p,d}$ (if $\partial^r = 0$ at that position) or strictly smaller in dimension. Since dimension is a non-negative integer that can only decrease, and we start with finite dimension $\dim(E^0_{p,d}) < \infty$, the sequence must eventually stabilize.

More precisely, for sufficiently large r, the differential $\partial^r : E^r_{p,d} \to E^r_{p+r,d+1}$ has source or target outside the range $[p_0, p_1]$ of the filtration, in which case it is automatically zero. □

The key question is: what does E^∞ compute?

Theorem 5.48 (Convergence to homology). *Under the hypotheses of Theorem 5.47, the filtration on C^* induces a filtration on homology:*

$$F^pH^d(C) = Im(H^d(G^{*,p}) \to H^d(C^*)),$$

and the E^∞-page computes the associated graded:

$$E^\infty_{p,d} \cong \frac{F^pH^d(C)}{F^{p+1}H^d(C)}.$$

This theorem is fundamental: the spectral sequence computes the homology of C, but presents it as the associated graded of a filtered vector space rather than directly. If the filtration on $H^d(C)$ splits (which is automatic over a field when the filtration is finite), then we can recover $H^d(C)$ itself:

$$H^d(C) \cong \bigoplus_p E^\infty_{p,d}.$$

Bibliography

[Abr97] Lowell Edward Abrams. *Frobenius algebra structures in topological quantum field theory and quantum cohomology*. Thesis (Ph.D.)–The Johns Hopkins University. ProQuest LLC, Ann Arbor, MI, 1997, p. 92.

[Ale28] J. W. Alexander. "Topological invariants of knots and links". In: *Trans. Amer. Math. Soc.* 30.2 (1928), pp. 275–306.

[Bar02] Dror Bar-Natan. "On Khovanov's categorification of the Jones polynomial". In: *Algebr. Geom. Topol.* 2 (2002), pp. 337–370.

[Bar05] Dror Bar-Natan. "Khovanov's homology for tangles and cobordisms". In: *Geom. Topol.* 9 (2005), pp. 1443–1499.

[BM+05] Dror Bar-Natan, Scott Morrison, et al. *The Knot Atlas*. Online knot database. 2005. URL: `http://katlas.org`.

[BZH14] Gerhard Burde, Heiner Zieschang, and Michael Heusener. *Knots*. extended. Vol. 5. De Gruyter Studies in Mathematics. De Gruyter, Berlin, 2014, pp. xiv+417.

[Cho06] Timothy Y. Chow. "You could have invented spectral sequences". In: *Notices Amer. Math. Soc.* 53.1 (2006), pp. 15–19.

[Cro04] Peter R. Cromwell. *Knots and links*. Cambridge University Press, Cambridge, 2004, pp. xviii+328.

[CS93] J. Scott Carter and Masahico Saito. "Reidemeister moves for surface isotopies and their interpretation as moves to movies". In: *J. Knot Theory Ramifications* 2.3 (1993), pp. 251–284.

[Deh14] M. Dehn. "Die beiden Kleeblattschlingen". In: *Math. Ann.* 75.3 (1914), pp. 402–413.

[Dij92] Robbert Dijkgraaf. "Intersection theory, integrable hierarchies and topological field theory". In: *New symmetry principles in quantum field theory (Cargèse, 1991)*. Vol. 295. NATO Adv. Sci. Inst. Ser. B: Phys. Plenum, New York, 1992, pp. 95–158.

[Fra30] Lev Semenovich Frankl F.; Pontrjagin. "Ein Knotensatz mit Anwendung auf die Dimensionstheorie". In: *Math. Ann.* 102 (1930), pp. 785–789.

[Hat02] Allen Hatcher. *Algebraic topology*. Cambridge University Press, Cambridge, 2002, pp. xii+544.

[Jon85] Vaughan F. R. Jones. "A polynomial invariant for knots via von Neumann algebras". In: *Bull. Amer. Math. Soc. (N.S.)* 12.1 (1985), pp. 103–111.

[Kau87] Louis H. Kauffman. "State models and the Jones polynomial". In: *Topology* 26.3 (1987), pp. 395–407.

[Kaw96] Akio Kawauchi. *A survey of knot theory*. Translated and revised from the 1990 Japanese original by the author. Birkhäuser Verlag, Basel, 1996, pp. xxii+420.

[Kho00] Mikhail Khovanov. "A categorification of the Jones polynomial". In: *Duke Math. J.* 101.3 (2000), pp. 359–426.

[KM11] P. B. Kronheimer and T. S. Mrowka. "Khovanov homology is an unknot-detector". In: *Publ. Math. Inst. Hautes Études Sci.* 113 (2011), pp. 97–208.

[KM93] P. B. Kronheimer and T. S. Mrowka. "Gauge theory for embedded surfaces. I". In: *Topology* 32.4 (1993), pp. 773–826.

[Koc04] Joachim Kock. *Frobenius algebras and 2D topological quantum field theories*. Vol. 59. London Mathematical Society Student Texts. Cambridge University Press, Cambridge, 2004, pp. xiv+240.

[KT57] Shin'ichi Kinoshita and Hidetaka Terasaka. "On unions of knots". In: *Osaka Math. J.* 9 (1957), pp. 131–153.

[Lee05] Eun Soo Lee. "An endomorphism of the Khovanov invariant". In: *Adv. Math.* 197.2 (2005), pp. 554–586.

[Lic97] W. B. Raymond Lickorish. *An introduction to knot theory*. Vol. 175. Graduate Texts in Mathematics. Springer-Verlag, New York, 1997, pp. x+201.

[Mon23] Gabriel Montoya-Vega. "A glimpse of the Khovanov homology of $T(2,n)$ via long exact sequence". In: (2023). URL: arXiv:2308.08452.

[MTV13] M. Mackaay, P. Turner, and P. Vaz. "Erratum: A remark on Rasmussen's invariant of knots [MR2320159]". In: *J. Knot Theory Ramifications* 22.1 (2013), pp. 1392001, 1.

[Muk+18] Sujoy Mukherjee et al. "Search for torsion in Khovanov homology". In: *Exp. Math.* 27.4 (2018), pp. 488–497.

[Mur08] Kunio Murasugi. *Knot theory & its applications*. Modern Birkhäuser Classics. Translated from the 1993 Japanese original by Bohdan Kurpita, Reprint of the 1996 translation [MR1391727]. Birkhäuser Boston, Inc., Boston, MA, 2008, pp. x+341.

[Mur87] Kunio Murasugi. "Jones polynomials and classical conjectures in knot theory". In: *Topology* 26.2 (1987), pp. 187–194.

[PPS09] Milena D. Pabiniak, Józef H. Przytycki, and Radmila Sazdanović. "On the first group of the chromatic cohomology of graphs". In: *Geom. Dedicata* 140 (2009), pp. 19–48.

[Ras10] Jacob Rasmussen. "Khovanov homology and the slice genus". In: *Invent. Math.* 182.2 (2010), pp. 419–447.

[Rei74] K. Reidemeister. *Knotentheorie*. Reprint. Springer-Verlag, Berlin-New York, 1974, pp. vi+74.

[Rol76] Dale Rolfsen. *Knots and links*. Vol. No. 7. Mathematics Lecture Series. Publish or Perish, Inc., Berkeley, CA, 1976, pp. ix+439.

[Sch49] Horst Schubert. "Die eindeutige Zerlegbarkeit eines Knotens in Primknoten". In: *S.-B. Heidelberger Akad. Wiss. Math.-Nat. Kl.* 1949.3 (1949), pp. 57–104.

[Sei34] H. Seifert. "Über das Geschlecht von Knoten". In: *Math. Ann.* 110 (1934), pp. 571–592.

[Thi87] Morwen B. Thistlethwaite. "A spanning tree expansion of the Jones polynomial". In: *Topology* 26.3 (1987), pp. 297–309.

[Tur17] Paul Turner. "Five lectures on Khovanov homology". In: *J. Knot Theory Ramifications* 26.3 (2017), pp. 1741009, 41.

[Vir04] Oleg Viro. "Khovanov homology, its definitions and ramifications". In: *Fund. Math.* 184 (2004), pp. 317–342.

[Wat07] Liam Watson. “Knots with identical Khovanov homology”. In: *Algebr. Geom. Topol.* 7 (2007), pp. 1389–1407.

[Wei94] Charles A. Weibel. *An introduction to homological algebra*. Vol. 38. Cambridge Studies in Advanced Mathematics. Cambridge University Press, Cambridge, 1994, pp. xiv+450.

Acknowledgments

I would like to express my sincere gratitude to my co-supervisor, Professor Marithania Silvero, for their guidance, patience, and constant support throughout the writing of this thesis. Their careful reading of the manuscript and their detailed and thoughtful feedback have been invaluable. I am also grateful to my supervisor, Professor Alessia Cattabriga, for her helpful suggestions on several parts of this work.

I would like to thank my family for their unwavering encouragement and support throughout my studies. Finally, I wish to thank my friends and colleagues for the stimulating conversations and the good times shared during these years.